Universidade de Lisboa

Faculdade de Ciências

Departamento de Biologia Animal

Coupling of atherosclerosis progression and bone disturbances in a mouse model

Renata Inês Proença Casimiro

Orientada por:

Maria José Parreira Santos, MD PhD
Unidade de Investigação em Reumatologia, JEFonseca Lab, Instituto de Medicina Molecular, Faculdade de Medicina de Lisboa, Universidade de Lisboa
Deodália Dias, PhD
Departamento de Biologia Animal da Faculdade de Ciências, Universidade de Lisboa

Dissertação

Mestrado em Biologia Humana e Ambiente

2015

Todas as afirmações efectuadas no presente documento são de exclusiva responsabilidade do seu autor, não cabendo qualquer responsabilidade à Faculdade de Ciências da Universidade de Lisboa pelos conteúdos nele apresentados.

As referências desta dissertação encontram-se formatadas de acordo com as regras da revista Nature.

Index

Figures Index

Tables Index

Agradecimentos

Gostaria de começar por agradecer às minhas orientadoras, Professora Maria José Santos e Professora Deodália Dias, pelo apoio e orientação que me deram no decorrer deste ano. Quero agradecer ao Professor João Eurico Fonseca e à Professora Helena Canhão, por me terem aceitado na Unidade de Investigação em Reumatologia e me terem deixado fazer parte desta equipa, como também pelo contributo que deram a este projecto.

Quero fazer um agradecimento muito especial à Diana Fernandes, que no decorrer deste ano, foi muito mais que uma colega e mentora, foi uma amiga que deu sempre 200% de si para me ajudar neste percurso. Ajudou-me a crescer como pessoa e tornou esta experiência em algo inesquecível, incluindo os *brainstormings* feitos face a algumas dificuldades encontradas, que intensificaram a minha vontade de seguir investigação e "herdar" a sua capacidade implacável de superar obstáculos.

Tenho um agradecimento muito especial também à minha companheira de laboratório Natacha Leonardo, que ao longo deste ano fomos inseparáveis e que também tornou, toda esta experiência ainda mais inesquecível e gratificante.

A todas as pessoas da Unidade, que de alguma forma me ajudaram neste percurso, em especial à Inês Perpétuo, Soraia Silva, Ana Pereira e Vítor Proa pelo apoio e pela boa disposição incomparável.

Por último, tenho de agradecer à minha família, em especial aos meus pais, pelo apoio incansável e pela confiança que sempre tiveram em mim, e também ao Fábio por puxar por mim para dar sempre o meu melhor, sem todos eles esta experiência não teria a mesma importância.

Abbreviations

ApoE	Apolipoprotein E
BV/TV	Bone Volume / Total Volume
cDNA	complementary Deoxyribonucleic Acid
CRP	C-reactive protein
CTX-I	C-terminal cross-link telopeptide of type I collagen
CV	Cardiovascular
DC	Dendritic cells
ECs	Endothelial cells
ELISA	Enzyme-Linked Immunosorbent Assay
FD	Fat Diet
GPI	Glycose-6-Phosphatase Isomerase
HSC	Hematopoietic Stem Cells
ICAM-1	Intercellular Adhesion Molecule 1
IL	Interleukin
LDL	Low Density Lipoprotein
M-CSF	Macrophage Colony-Stimulating Factor
MHC	Major Histocompatibility Complex
MSC	Mesenchymal Stem cell
OB	Osteoblast
OC	Osteoclast
OCY	Osteocyte
OP	Osteoporosis
OPG	Osteoprotegerin
P1NP	N-propeptide of type I collagen
RA	Rheumatoid Arthritis
RANK	Receptor Activator of Nuclear factor Kappa-B
RANKL	Receptor Activator of Nuclear factor Kappa-B Ligand
RNA	Ribonucleic Acid

rRNA	ribossomal RNA
RT-qPCR	Real-Time Quantitative Polymerase Chain Reaction
SLE	Systemic Lupus Erythematosus
SPF	Specific- Pathogen- Free
Tb.Th	Trabecular Thickess
Tb.Sp	Trabecular Separation
TCR	T-cell receptor
TNF	Tumor Necrosis Factor
VCAM-1	Vascular cell adhesion Molecule 1
VLDL	Very Low Density Lipoprotein
VSMCs	Vascular smooth muscle celss

Abstract

Several epidemiological studies have revealed a link between atherosclerosis and osteoporosis, suggesting the existence of common underlying mechanisms. This relationship maybe due to the inflammatory processes that underlies both diseases. Thus, mechanisms regulating inflammation and also bone remodeling could represent potential links between these two diseases.

Therefore this work focused on the evaluation of the alterations in bone and vessel of an animal model of atherosclerosis (ApoE $^{-/-}$). Using different time-points, we measured the serum levels of CTX-I and P1NP to evaluate the systemic repercussions of bone remodeling, and performed histomorphometric analysis to evaluate bone behavior. We have also evaluated the relative gene expression, in bones and aortas, of genes associated with inflammation (IL-1β, IL-6, IL-17A and TNF) and also RANKL and OPG, associated with bone remodeling. The histomorphometric analysis and bone turnover proteins determination in serum shown concordant results, pointing towards bone loss, with the decrease levels of bone volume, trabecular thickness, and P1NP levels in serum coupled with an increase in trabecular separation, and CTX-I in serum. The expression of the genes associated with inflammation in ApoE $^{-/-}$ mice has, in general, lower levels, even in the later time-points, when compared to C57BL/6 mice.

Additionally, a mouse model of inflammation (K/BxA^{g7}) was used to evaluate the progression of both diseases in the same organism, these mice did not developed visible atherosclerotic lesions in the aorta and no significant differences were found comparing to a healthy group (C57BL/6 mice), despite the K/BxA^{g7} displayed a general increase in the expression of the inflammation related genes, in both aorta and bone. Our finding suggests that ApoE $^{-/-}$ mice suffer from bone alterations, and that could be associated with the atherosclerosis development although we did not find any correlation with inflammatory genes in the tissues affected.

To complement this project it will be interesting to increase de number of animals in the study and also to include another group composed by B6 mice but without the fat diet. As for the model of inflammation, it will be interesting to house this animals in a

conventional animal facility, with a more challenging environment, to see if any visible atherosclerotic lesion appear.

Key words: Atherosclerosis, ApoE $^{-/-}$, Bone remodeling, Inflammation, Osteoporosis.

Sumário

As doenças que afectam o sistema cardiovascular e o osso estão entre as doenças que causam maior morbilidade e mortalidade na população, em especial a aterosclerose e a osteoporose. Vários estudos epidemiológicos têm demonstrado que estas duas doenças podem estar relacionadas de alguma forma, uma vez que ambas as patologias estão normalmente presentes no mesmo doente. Doentes com patologia cardiovascular apresentam um risco 1.2 a 6.7 vezes maior de sofrer de fraturas de fragilidade comparando com a população em geral, e esta associação também foi demonstrada em doentes com uma massa óssea reduzida que têm um risco aumentado de desenvolver doenças ao nível cardiovascular, em especial doentes com doenças autoimunes como lúpus eritematoso sistémico ou a artrite reumatoide.

A aterosclerose é caracterizada pela acumulação de partículas lipídicas e células do sistema imunitário que levam ao estreitamento do lúmen das artérias, e numa fase mais avançada do processo pode ocorrer ruptura destas placas ateroscleróticas com possível formação de trombos. Estudos recentes têm demostrado o envolvimento do sistema imune na patogénese da aterosclerose. Este processo é iniciado pelos monócitos que posteriormente se diferenciam em macrófagos com capacidade de acumular lípidos no citoplasma formando as conhecidas *foam cells*, ou células espumosas, com capacidade de produzir citocinas pro-inflamatórias. Estas citocinas desempenham diversas funções no organismo, mas estão maioritariamente associadas a processos inflamatórios, processos estes que levam à progressão da aterosclerose, mas também estão associados a outras patologias como a osteoporose.

A osteoporose é uma doença resultante de um desequilíbrio no *turnover* ósseo, caracterizada pela perda de massa óssea, com alteração da microarquitectura do osso, diminuição da densidade mineral óssea e consequente aumento das fraturas de fragilidade.

A associação entre estas duas patologias tem ganho robustez especialmente com o paradoxo da calcificação das placas com a baixa densidade óssea e também com a

presença, no vaso, de várias proteínas associadas à remodelação óssea, como RANKL (Receptor Activator of Nuclear factor Kappa-B Ligand), OPG (Osteoprotegerin) e colagénio tipo 1. Estudos em modelos animais têm reforçado estes dados. Ratinhos *knock-out* para OPG, para além de apresentarem uma osteoporose generalizada, exibiram também um aumento da calcificação ao nível vascular.

Este estudo centrou-se na hipótese da existência de mecanismos fisiopatológicos comuns aos dois sistemas. Pretendemos avaliar ao longo do tempo, utilizando um modelo animal (ApoE $^{-/-}$) que é geneticamente propenso ao desenvolvimento de aterosclerose (por delecção do gene da apolipoproteína E), o efeito da inflamação sobre os ossos e os vasos. Os objectivos deste trabalho foram a avaliação dos níveis séricos de CTX-I (C-terminal cross-link telopeptide of type I collagen) e P1NP (N-propeptide of type I collagen), duas proteínas resultantes do processo de *turnover* ósseo (marcadores de reabsorção e de formação óssea, respectivamente), como também a microarquitectura óssea das vértebras lombares por histomorfometria, para compreender possíveis efeitos ao nível do osso trabecular. Pretendemos ainda avaliar a progressão das lesões ateroscleróticas e avaliar a relação entre a aorta e o osso pela determinação dos níveis de expressão de genes associados com a inflamação (interleucina (IL-) 1β; IL-6; IL-17A e TNF (Tumor Necrosis Factor)) e com a remodelação óssea (RANKL e OPG).

Adicionalmente, como objectivo secundário deste estudo, pretendeu-se avaliar as variações no osso e no vaso, especialmente o desenvolvimento de lesões ateroscleróticas ao nível da aorta, num modelo animal inflamatório (K/BxA^{g7}), que desenvolve uma artrite espontânea (com consequente desenvolvimento de uma osteoporose secundária) e que foi descrito como estando predisposto para o desenvolvimento de aterosclerose.

Para cumprir com os objectivos foram formados 5 grupos correspondendo aos diferentes *time-points* (8, 16, 20, 24 e 28 semanas de idade) para as duas estirpes de ratinhos usados (ApoE $^{-/-}$, como modelo de aterosclerose, e C57BL/6, como controlo saudável), com 10 animais em cada grupo, dos quais 5 foram destinados para os testes de expressão génica (osso e aorta) e histomorfometria, e os outros 5 para avaliação das lesões na aorta. Todos os ratinhos estiveram sob uma dieta gorda desde as 10 semanas.

Para o objectivo secundário foram usados ratinhos K/BxA^{g7} divididos em dois grupos, num foi introduzida a dieta gorda às 10 semanas de idade (N=4) e noutro manteve-se com a dieta normal durante toda a experiência (N=5). Estes animais foram avaliados às 24 semanas de idade, com doseamento dos níveis séricos de CTX-I e P1NP, avaliação da expressão génica (osso e aorta) e da presença de lesões na aorta.

A todos os animais, no momento da eutanásia foi recolhido sangue por punção cardíaca e posteriormente centrifugado para a obtenção do plasma. Após perfusão, as aortas foram recolhidas e conservadas em PBS (até serem congeladas com azoto líquido para posteriormente se proceder à extração de RNA) ou em paraformaldeído para a quantificação das lesões por marcação dos lípidos com Oil Red O. Foram ainda recolhidos e imediatamente congelados diversos ossos, incluindo um fémur (após remoção da medula) para extracção de RNA e as vértebras lombares para a histomorfometria. Os níveis séricos de CTX-I e P1NP foram determinados por ELISA (Enzyme-Linked Immunosorbent Assay) e as vértebras lombares (L3-L4) foram analisadas por histomorfometria para a determinação do volume de osso trabecular, espessura trabecular e também a separação entre trabéculas. Os fémures e aortas destinados à extração de RNA foram reduzidos a um pó fino, a extração foi efectuada com TRIzol®/clorofórmio e posteriormente foi realizada a síntese de cDNA para a análise da expressão génica utilizando SYBR®Green e primers desenhados especificamente para cada gene a avaliar. A quantificação foi feita por PCR (Polymerase Chain Reaction) quantitativo em tempo real e na análise final todos os genes foram normalizados para o rRNA 18S utilizado como *housekeeping gene* (gene de referência).

Todos os animais utilizados neste estudo foram avaliados semanalmente e o seu peso registado. Adicionalmente, ao modelo de artrite, e como forma de avaliar a progressão da doença, foi aplicado um *score* clínico avaliado pela observação semanal dos animais.

Pela avaliação dos dados histomorfométricos e dos níveis séricos dos marcadores de remodelação óssea verifica-se uma concordância entre os resultados obtidos, com uma diminuição significativa no volume ósseo, na espessura trabecular e níveis de P1NP ao longo do tempo, e um aumento na separação inter-trabecular e nos níveis séricos de

CTX –I, sugerindo que ambos os grupos experimentais foram sofrendo de uma perda de massa óssea, com especial ênfase no grupo ApoE $^{-/-}$, onde se verificaram algumas diferenças estatisticamente significativas em comparação com o grupo B6.

Os resultados obtidos na expressão génica mostraram algumas diferenças estatisticamente significativas entre B6 e ApoE $^{-/-}$, contudo, de uma maneira geral, foi o grupo dos ratinhos B6 que apresentou maiores níveis de expressão das citocinas, tanto na aorta como no osso. Não se encontrou uma associação com significância estatística na correlação da expressão das citocinas entre os dois tecidos. No entanto verificámos a existência de uma relação entre IL-1β e IL-6, e entre TNF e OPG no osso dos ApoE $^{-/-}$ às 16 semanas e no grupo dos B6 às 28 semanas apenas entre TNF e OPG, mas estas correlações foram pontuais, cingindo-se a apenas um ponto de avaliação, e não se verificou a continuidade destas correlações nos *time-points* seguintes. A falta de um forte suporte estatístico nestes resultados pode dever-se ao facto de a expressão dos genes avaliados, principalmente na aorta, apresentar valores muito dispersos, além de serem muito diferentes dos valores obtidos no osso. Esta discrepância poderá dever-se ao facto de a aorta ser um tecido menos robusto e que poderá estar mais susceptível à degradação do RNA durante o processamento da amostra.

Procedeu-se posteriormente à comparação dos dados obtidos nas diversas análises efectuadas, medição de marcadores séricos, histomorfometria e expressão génica. Observou-se uma correlação negativa entre a espessura trabecular e os níveis de expressão da OPG no osso dos ratinhos ApoE $^{-/-}$ com 16 semanas, e também entre o volume ósseo e a separação trabecular no grupo B6 às 28 semanas, mas mais uma vez estas correlações foram pontuais, sem grande significado biológico.

Estes resultados estão de acordo com o esperado face aos dados epidemiológicos e de estudos em modelo animal que reforçam a associação entre a progressão da aterosclerose e a perda de massa óssea com possível desenvolvimento de uma osteoporose. Contudo os dados de expressão génica não apoiam esta conclusão (chegando a ser discordantes), apesar de existirem alguns estudos com este modelo animal que reportam um aumento da formação óssea em ratinhos ApoE $^{-/-}$, pelo que os dados com este modelo são ainda um pouco contraditórios.

É importante ter em conta que o grupo controlo (B6) estava também sujeito a dieta gorda, uma vez que esta dieta potencia e acelera o desenvolvimento das lesões ateroscleróticas nos ratinhos ApoE $^{-/-}$. A dieta gorda foi introduzida em ambos os grupos, a fim de uniformizar qualquer alteração introduzida pela dieta, pois um estudo prévio de Hirasawa *et al.* reportou que a dieta gorda induz uma redução da mineralização óssea. No entanto face aos resultados obtidos, este trabalho poderia beneficiar de uma análise dos parâmetros estudados, num grupo controlo (B6) sem dieta gorda de forma a verificar os níveis normais de todas as proteínas estudadas.

Quanto ao objectivo secundário e ao modelo de inflamação (K/BxA^{g7}), não foram encontradas lesões ateroscleróticas visíveis na aorta, contrariamente ao que foi reportado por Rose *et al.*. Este resultado poderá ter duas justificações: as condições de alojamento dos animais, visto que se encontravam num biotério de roedores SPF (specific pathogen-free), e o tempo de avaliação deste estudo. Relativamente às condições de alojamento, estas podem ter influência na microbiota o que, por sua vez, poderá ter um importante papel no desenvolvimento das lesões (foi já descrito como tendo uma elevada relevância no desenvolvimento de diversas doenças inflamatórias). Os dados preliminares obtidos não mostram nenhuma diferença estatisticamente significativa, contudo, de uma forma geral, ambos os grupos de K/BxA^{g7} mostraram níveis elevados da expressão dos genes analisados. No entanto, os níveis séricos apontam para uma remodelação óssea alterada no sentido da formação (aumento dos níveis de P1NP, e do ratio CTX-I/P1NP), contrariamente ao esperado, não só pela descrição do modelo, como pelo aumento do *score* clínico verificado nestas animais ao longo do tempo.

Conclui-se com este trabalho que o modelo animal de aterosclerose apresenta algumas alterações ao nível do osso, ao longo do tempo, apesar dos resultados obtidos necessitarem ser confirmados para melhor compreensão do seu significado biológico. De forma a melhorar este trabalho seria interessante aumentar o número de animais em estudo (B6, ApoE $^{-/-}$ e K/BxA^{g7}) para reforçar o poder estatístico dos resultados, como também para verificar se as tendências observadas se mantêm. Relativamente ao modelo animal de inflamação, em específico, seria importante fazer uma análise

histomorfométrica para avaliar as alterações na microarquitectura do osso, num modelo caracterizado pelas conhecidas alterações ósseas, e uma vez que não se observaram lesões visíveis nos vasos destes ratinhos, e sabendo a importância do ambiente em que os animais estão alojados, seria importante testar os efeitos sobre os vasos deste modelo num ambiente menos limpo, colocando-os por exemplo, num biotério convencional. Será também interessante, se os ratinhos apresentarem lesões em ambos os tecidos (ossos e vasos), avaliar a progressão estudando os mesmos *time-points* definidos para os outros modelos experimentais.

Palavras-chave: Aterosclerose, ApoE $^{-/-}$, Remodelação óssea, Inflamação, Osteoporose.

Introduction

Cardiovascular diseases (CV) and osteoporosis (OP) are among the most prevalent health problems and contribute significantly to increased morbidity and mortality of the population. According to the World Health Organization, CV diseases are the first cause of death worldwide [1], and atherosclerosis is the major cause of CV events [2]. Osteoporosis is the most common human bone disease, characterized by decreased bone mineral density and increased fracture risk due to low bone mass and structural deterioration of bone [3,4]. The incidence of these conditions increases with age and they frequently coexist in the same patient. Epidemiological studies have clearly demonstrated that in patients with CV diseases, the risk for osteoporotic fracture is 1.2 to 6.7 times higher than in general population [5]. This relationship is also observed in patients with low bone mass who have an increased risk for CV events, vascular calcification and atherosclerosis progression [6,7]. This association is particularly relevant in patients with chronic autoimmune diseases like Systemic Lupus Erythematosus (SLE) and Rheumatoid Arthritis (RA) that have increased rates of subclinical atherosclerosis [8] with respectively, an 5-8 and 2-3 fold higher risk of CV events [9].

Atherosclerosis

Atherosclerosis is the most common pathologic process that underlies cardiovascular diseases [2,10,11]. It affects arterial walls, and is characterized by the accumulation of lipid particles and cells of the immune system in sub-endothelial regions, leading to narrowing of the arterial lumen (stenosis), which can evolve to plaque formation, plaque rupture and thrombosis. It begins with a disruption and activation of endothelial cells (ECs) with increased surface adhesion molecules (including ICAM-1 and VCAM-1) leading to augmented vascular permeability that allows the attachment and infiltration of lipids and inflammatory cells into the sub-endothelial space. These inflammatory cells, specifically monocytes will then differentiate into macrophages which will for one hand

accumulate lipids forming the foam cells, and for the other hand produce and release pro-inflammatory cytokines (e.g. Interleukin (IL-)1, IL-6) creating an inflammatory environment and perpetuating this cycle. In early lesions, VSMCs (vascular smooth muscle cells) proliferate/migrate and form a fibrous cap that encloses the growing lipid core, forming a more stabilized plaque. However, with the gradual loss of VSMCs by apoptosis and increase activity of matrix-degrading enzymes in the cap it can result in plaque rupture, with subsequent platelet aggregation (that come in circulation and attach to the plaque) and thrombosis [12] (Figure 1). So it is stated to be more complex process than just a passive accumulation of cholesterol in the vessel, as previously thought [13,14].

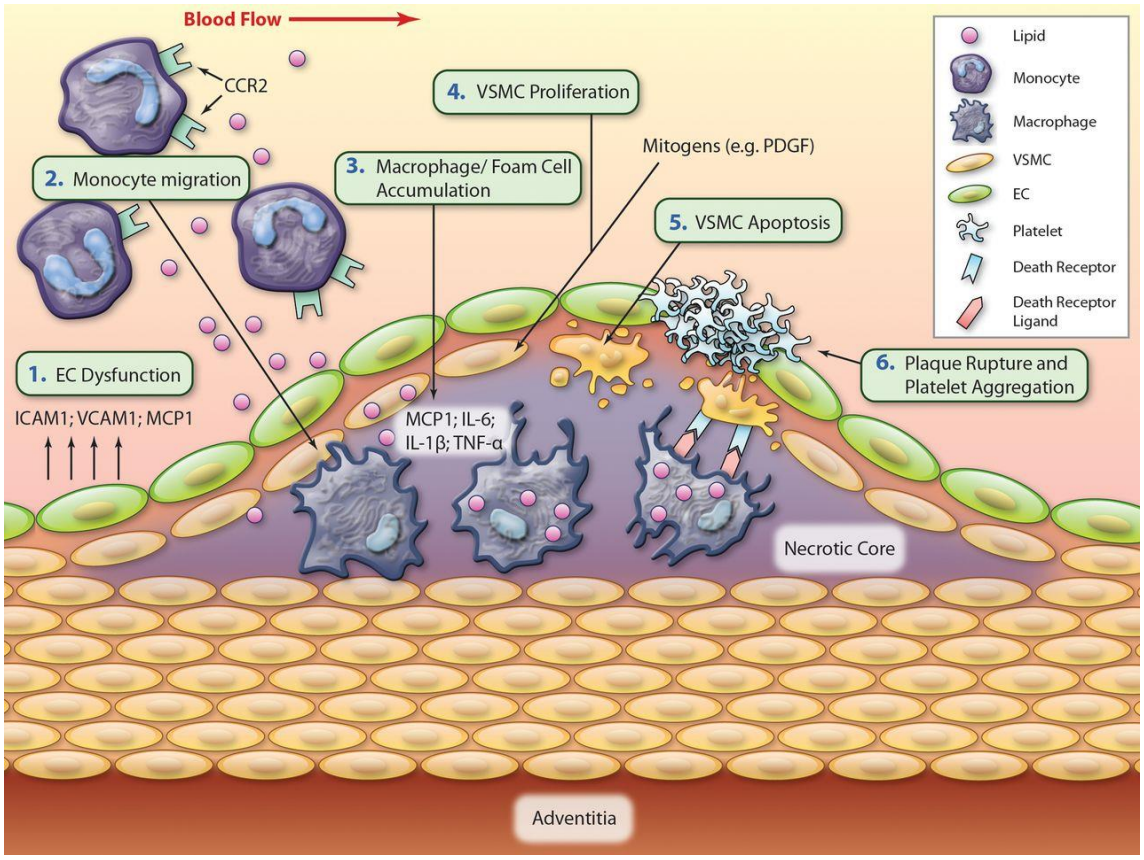

Figure 1 - Representation of atherogenesis and an unstable atherosclerotic plaque.

Plaque formation involving a series of events: (1) EC (endothelial cells) dysfunction and activation. (2) Attachment and infiltration of lipids and inflammatory cells into the sub-endothelial space. (3) Formation of foam cells and release of pro-inflammatory cytokines (e.g. IL-1, IL-6. (4) Formation of a fibrous cap that encloses the growing lipid core. (5) Gradual degradation of the fibrous cap. (6) Plaque rupture, with subsequent platelet attachment and thrombosis. (Adapted from Bennet J., 2012) [12].

Therefore the development of cardiovascular diseases involves not only the genetic factors but also other acquired and modifiable risk factors such as smoking, hypercholesterolemia, *diabetes mellitus* and hypertension [15,16].

This relation with conditions like type 2 diabetes and obesity comes from the interactions between inflammatory and immunity components, and molecules altered in these diseases [17]. The adipose tissue is responsible for the secretion of several hormone-like molecules called adipokines. These molecules are associated with a low-grade inflammation and have pro-inflammatory and atherogenic functions (e.g. Leptin, resistin and grelin). However, adiponectin described to have a pro-inflammatory action, has been recently associated with a vascular protective effect, showing an anti-inflammatory and anti-atherosclerotic action [11], in cases of chronic inflammatory/autoimmune diseases (SLE and AR, for example) [18], demonstrating that are still a lot to discover about the mechanisms behind adipokines action.

Recent studies showed the involvement of the immune system in the pathogenesis of atherosclerosis, with innate and adaptive immune responses. The immune response is initiated through monocyte-derived macrophages developing into foam cells and subsequently occur a presentation of antigens to T cells leading to its activation and production of numerous soluble pro-inflammatory cytokines, such as Interleukin (IL)-1 β, IL-6, TNF (tumor necrosis factor), among others [16,19], contributing to lesion aggravation [13]. These cytokines have a variety of roles in the organism and act in multiple sites, but are mostly associated with the inflammatory processes. IL-1β is expressed by activated macrophages and is a cytokine implicated in several diseases, such as diabetes and leukemia but also in diseases with a strong inflammatory component like inflammatory bowel disease, RA [20] and also, atherosclerosis [21]. This cytokine often acts together with IL-6, which has also the responsibility of promoting immune responses, particularly plasma cells and macrophages differentiation. The activation of the inflammatory process leads to an interaction with other molecules that modulate various mechanisms in other tissues, e.g. adipose tissue and blood vessels, leading to the activation and increase of plasma levels of inflammatory mediators like TNF and C-

reactive protein (CRP) among others [22,23]. These are believed to play an important role in development of atherosclerotic plaques and perpetuation of the inflammatory status. These cytokines can be up-regulated by the nuclear transcription factor (NF)-$_k$B which is activated under oxidative stress, creating a vicious cycle, resulting in a perpetuation of the high levels of these cytokines, thus maintaining a chronic low-grade inflammation with consequences for the organism due to mediation of pathophysiology of diseases like atherosclerosis and osteoporosis [13,24,25].

Osteoporosis

Osteoporosis (OP) is a skeletal condition characterized by an imbalance in bone turnover with loss of bone mass and deterioration of bone microarchitecture resulting in decreased bone mineral density (BMD) and increased bone fragility. OP is a major risk for fragility fractures, causing substantial morbidity mainly amongst the elderly [26,27].

This disease can be divided in two distinct pathological conditions:

Primary OP is the most common type of osteoporosis with a relatively unknown origin although it's mainly defined as an age-related condition, characterized by bone mass loss increasing with age leading to weakening of bones and fractures [28,29]. It is also associated with menopause, mainly due to estrogen deficiency that causes an impairment in bone turnover cycle, causing this disease to be more frequent in women that in men [29 30].

Secondary OP on the other hand has a direct cause. It is essentially associated with endocrine, metabolic or inflammatory diseases such as RA [31], SLE [32] and ankylosing spondylitis [33], or medications that cause bone metabolism imbalance [34]. Its complexity is due to its heterogeneous character, attributed to various endocrine, metabolic, and mechanical factors along with the usual risk factors such as age, menopause and certain lifestyle behaviors [27]. Rising molecular evidence suggests that inflammatory conditions with release of inflammatory cytokines like IL-1, IL-6, IL-17 and TNF can modulate by

promoting (in the case of IL-1, IL-6, IL-17 and TNF) or inhibiting (IL-12, IL-33 and also the IL-6 which has this double function) osteoclastogenesis [35] as well as leading to alternative pathways within bone remodeling [25,35,36].

Bone remodeling

Bone is a dynamic tissue that undergoes constant adjustments throughout life in order to preserve the structural integrity but also has the function of support and allowing body movement as well as acting as a mineral reservoir (responsible for regulation of mineral homeostasis) and harbors bone marrow (where hematopoiesis occur) [37].

Bone is composed by a cortical and a trabecular portion. The **cortical bone** represents 80% of skeletal bone and gives rigidity and strength to the skeleton. It is dense and compact and forms the hard outer layer of bones providing the mechanical strength and protection. The **trabecular bone**, also known as cancellous bone, only composes 20% of whole skeleton and is a spongy-like tissue present in the interior of the bone, highly vascularized and is formed by a porous network called trabeculae which confers a more flexible characteristic hence the resistance to compression [38] .

Bone remodeling is a dynamic and continuous process that occurs throughout life, in which old bone is replaced by new one through the action of osteoblasts, osteoclasts and osteocytes [39,40]. These cells have a central role in the maintenance of the skeleton mechanical integrity and repair of fractures [39] (Figure 2).

Osteoblasts (OB) are cells derived from the mesenchymal lineage [41] and are responsible in one hand, for the formation of new bone, and on the other for the production of both stimulatory and inhibitory factors such as macrophage colony-stimulating factor (M-CSF), receptor activator of nuclear factor kappa-B ligand (RANKL), required for the proliferation of osteoclast progenitors, and osteoprotegerin (OPG) responsible for

regulating osteoclasts formation and activity by inhibiting its differentiation and activation [42,43].

Osteoclasts (OC) are derived from hematopoietic lineage [41] and are responsible for the destruction and resorption of the old bone maintaining mineral homeostasis in addition to shape, size and integrity of bones [41,43,44].

The molecular cross-talk between osteoblasts and osteoclasts is essential for these cells to differentiate into mature osteoclasts in order to be active and resorb bone, in a process known as osteoclastogenesis [45]. In this process osteoclast differentiation is mediated by the receptor activator of nuclear factor kappa-B (RANK), RANKL and OPG triad [22,46,47]. The binding of RANKL (released by activated osteoblasts) to its receptor RANK at the surface of osteoclasts precursors [43] triggers the formation of multinucleated osteoclasts [45]. The activity of these mature osteoclasts is orchestrated by a molecular machinery and is also regulated by systemic hormones, e.g. estrogen, and cytokines, such as TNF allowing the regulation of bone resorption process. TNF is an inflammatory cytokine that can promote osteoclastogenesis in a direct form by engagement of osteoclast precursor cells or in a more indirect way via induction of M-CSF and RANKL expression on mesenchymal cells [48]. It has been suggested to play an important role in the osteoclast development and function, and appears to potentiate the effect of RANKL signaling [49,50], thus contributing to bone loss in chronic inflammatory disorders [51]. Another cytokine that is shown to be elevated at sites of inflammation is IL-1β, that apart of being expressed by activated macrophages and responsible for direct induction of osteoclast formation, is believed to play a critical role in mediating TNF effects [36,52].

There are two main proteins released during this process that are usually used as markers for the remodeling process, being the N-propeptide of type I collagen (P1NP) one of the enzymes used as bone formation marker (since it is released to circulation as a product of enzyme cleavage of procollagen type I during bone matrix formation), while C-terminal cross-link telopeptide of type I collagen (CTX-I) is the most commonly used as bone resorption marker (as a product released into circulation from type I collagen degradation, through cathepsin K activity, during osteoclastic bone resorption) [53].

The regulation of osteoclastogenesis is mediated by these cytokines but also by RANKL/ OPG ratio, in which changes in this ratio inhibits or favors the process of bone resorption. In the specific case of inflammatory diseases up-regulation of RANKL expression and down-regulation of OPG expression normally occurs, favoring osteoclastogenesis [36]. But when this process is no longer needed, is released more OPG, a soluble glycoprotein, member of the tumor necrosis factor receptor superfamily and expressed by osteoblasts, that acts like a soluble decoy receptor for RANKL, inhibiting the bond with its proper receptor (RANK), thus preventing the interaction of RANKL with RANK [54]. The change in this interaction leads to the inhibition of osteoclasts differentiation and activation of specific pro-inflammatory cytokines, as well as signaling pathways, preventing excessive bone resorption [47]. Animal models demonstrated the role of OPG in this process, in which OPG $^{-/-}$ mice develop severe osteoporosis [55] contrary to OPG overexpression that causes severe osteopetrosis in mice [56].

Osteocytes (OCY) are terminally differentiated osteoblasts that become entrapped in lacunae on the newly mineralized bone matrix and have a specialized morphology and a molecular signature that allow to serve as a bone response mechanism for mechanical stress and occurrence of microfractures [57,58]. These cells are able to communicate with each other and with cells on the bone surface through dendritic processes, but also this process allows them to be in contact with the bone marrow giving them the capability to recruit osteoblasts and osteoclasts precursors involved in bone remodeling [59].

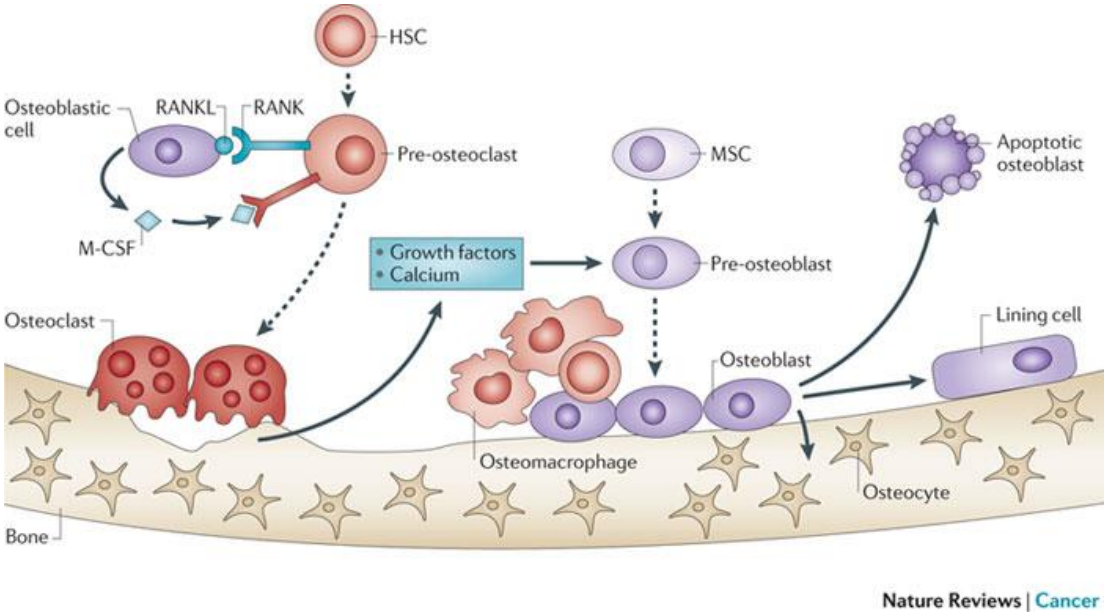

Figure 2 - Representation of bone remodeling process.

Osteoclasts, derived from hematopoietic stem cells (HSCs), become activated by stimuli from RANK-RANKL (receptor activator of NF-kB and RANK ligand) binding and M-CSF (macrophage colony stimulating factor), gaining the ability to resorb bone and releasing growth factors and calcium that will allow the differentiation of mesenchymal stem cell (MSC) into osteoblasts, that will replace the voids with new bone. Osteocytes are terminally differentiated osteoblasts that are embedded in bone and are responsible for signaling osteoclasts and osteoblasts after mechanical changes. (Adapted from Weilbaecher K. et al. 2011) [60].

The association between vascular and skeletal system has gain prominence over the years, especially the paradox between vascular calcification and low bone density, supported by several studies in mice and humans.

Vascular calcification is a well-accepted marker of increased cardiovascular risk [61] and has been pointed as a possible predictor of CV events [5,15]. It is shown to be an active, cell-regulated process characterized by an ectopic mineral deposition in blood vessels, predominantly aortas. This mineralization can occur either in the tunica intima, associated with atherosclerosis (related with lipid accumulation and inflammation with focal plaque calcification) or in the tunica media of the vessel, a more generalized stiffening, known as arteriosclerosis or Monckeberg's medial calcific sclerosis (associated mostly with ageing, osteoporosis and other conditions like hypertension or *diabetes mellitus)* [62,63]. It was thought to be a passive, inevitable, natural process of

ageing, but this deposition of minerals in the vessels was shown to be more complex and in an organized manner. It is not a mere calcification, but an ossification-like process with deposition of mineral hydroxyapatite produced by calcifying vascular cells that has the ability to recapitulate the osteoblastic differentiation leading to the expression of several proteins implicated in this process causing a bone-like formation in the vascular system [64].

The presence of ossified bone within plaques and expression of several proteins implicated in normal bone development suggests shared mechanisms that recapitulate bone formation. Among these proteins believed to mediate arterial wall calcification stands OPG, RANKL, Ostepontin, Collagen type I and also pro-inflammatory cytokines [65], implicated in modulating adaptive immunity and considered as potential regulators of atherosclerotic lesions development and calcification. Furthermore, both RANKL and OPG are known to be expressed not only by bone-related cells but also by many components of the cardiovascular system, such as endothelial cells, platelets, and VSMCs being the last one in particular also pointed as possible responsible for this calcification due to its multi-potential capability to transform into osteo/chondrocytic-like cells [61,66,67].

Although there is a strong association between these proteins and lesion alterations, the mechanism by which calcification process is regulated is still unknown [68–70].

Animal model studies have demonstrated that OPG $^{-/-}$ mice apart of osteoporosis also shown an unexpected increase in vascular calcification [65], raising the evidence that OPG it is a key regulator not only in pathogenesis of osteoporosis but also in vascular calcification [5,42]. In humans this association was also demonstrated in several epidemiological studies and was shown to be more generalized that solely in cases of severe bone loss, characteristic of osteoporosis [71,72].

Several epidemiologic studies associated bone disturbances, especially low bone mineral density, with cardiovascular diseases (CV) as well as subclinical atherosclerosis, (two of the most common conditions associated with the elderly) [9], suggesting that the relationship between low bone mineral density and increased CV risk it is not only a result of ageing and traditional risk factors, but that a direct association and shared pathogenic mechanisms exist. [5,72,73].

The relation between these two conditions seems to be due to the inflammatory state through increase of monocytes/macrophages leading to the production of several pro-inflammatory cytokines being IL-17 one of them. IL-17A is a pleiotropic cytokine produced by Th17 T-helper cell subset (CD4+ activated T cells) and also by other inflammatory cells like mast cells [74]. This pro-inflammatory cytokine promotes and amplifies inflammation by enhancing the production of other cytokines like IL-1, TNF, IL-6 as well as chemokines, specially IL-8, in various types of cells including macrophages [75], initiating the recruitment and activation of immune system, and leading to local inflammation and tissue damage [49,76]. In addition, it can also induce RANKL leading to enhanced osteoclastogenesis and subsequent bone destruction [74]. It has been involved in a variety of autoimmune and inflammatory diseases, especially inflammatory arthritic disease like RA, psoriasis and ankylosing spondylitis [74,77] and its concentration has been found to be elevated in peripheral blood and synovial fluid of RA patients compared to healthy controls [48,78].

Animal Models

The ApoE knockout mice is a very well established model to study atherosclerosis progression. The loss of the gene encoding apolipoprotein E (ApoE), a glycoprotein synthesized mainly in the liver and brain that serves as a structural component of very low density lipoprotein (VLDL) particles, loses their function as a ligand for LDL-receptors, predisposing mice to develop atherosclerotic lesions resembling those seen in humans [79].

Apolipoprotein E (ApoE) deficient mice are generated by targeting and inactivating the apoE gene, which is essential for the transport and metabolism of lipids, leading to lipid accumulation and atherosclerotic plaque formation.

These ApoE knockout mice tend to develop spontaneously and in a short time [80] a full range of atherosclerotic lesions distributed throughout the arterial tree, with progression from fatty streaks to fibrous plaques [81]. Although mice do not experience plaque rupture, contrary to humans where this is a very common complication of atherosclerosis, they are hypercholesterolemic due to probable delayed clearance of large atherogenic particles from the circulation.

Because this pathology can be exacerbated with a diet rich in fat and cholesterol, with appearance of fatty streaks in the proximal aorta at 3 months of age [82] makes them a good study group for atherosclerosis progression studies [83].

To understand bone disturbances related to systemic inflammation, the K/BxA^{g7} mice have been used due to their spontaneous development of a chronic and severely destructive arthritis with 100% penetrance, that recapitulates many of the clinical, histological, and immunological features of human RA [84,85]. RA is a chronic autoimmune inflammatory disease characterized by inflammation of the synovial tissues and disruption in bone remodeling balance with generalized osteoporosis attributed to the effects of chronic inflammation, especially the changes in innate and adaptive immune systems including the increment of B and T cells with increase of inflammatory cytokines in circulation [31].

Arthritis appears when these mice expressing KRN T-cell receptor (TCR) transgene are crossed into mice carrying the H-2^{g7} haplotype present in the major histocompatibility complex (MHC), due to the TCR recognition of a peptide derived from the glycolytic enzyme glycose-6-phosphatase isomerase (GPI) presented by the MHC class II molecule H2-A^{g7}, which results in production of high titers of autoantibodies to GPI, that are essential for the arthritogenic effect [86,87] leading to a development of spontaneous and erosive arthritis as described previously [88].

As in humans, in mice the disease is progressive and symmetrical, and exhibits the classical histological features such as leukocyte invasion, synovitis, pannus formation, cartilage, and bone destruction [89,90]. The arthritis appears at around 3 to 4 weeks old, it is predominantly distal, affecting ankles, wrists, associated tendon sheaths and digits, with less involvement of the knee and no involvement of hips and shoulders [86], and there are no gender differences reported [91]. Additionally this murine model is also susceptible to atherosclerosis with develop of dyslipidaemia, cardiac valvulitis and increased serum levels of pro-inflammatory cytokines and chemokines [85].

We hypothesize that bone and vascular disturbances share common pathophysiological mechanisms and common factors may underlie the pathogenesis of these two conditions. With the use of animal models we expect to be able to evaluate changes over-time and accompany the disease evolution since its initial stage until a more advanced stage in a short period of time.

Aims

The present work aims to address the interactions between bones and arteries, using animal models.

The specific aims to this work are to evaluate

1) In an animal model of atherosclerosis:

- Changes in serum levels of bone turnover markers throughout disease progression;
- The morphology of vessels and the bone structure through disease progression;
- The gene expression levels of inflammation and bone remodeling markers in bones and arteries.

2) In an animal model that develops spontaneous arthritis:

- Describe the kinetics of atherosclerosis and bone alterations.

Materials and Methods

Mice models and diets

Apolipoprotein E (ApoE) deficient mice were purchased from Charles River Laboratories International [92]. These mice have C57BL/6 strain as genetic background and were divided in 5 groups (1 group per time-point) with 10 female mice in each group (N=5 for lesions quantification, and N=5 for gene expression analysis). To evaluate if there are atherosclerotic lesions differences between genders, were also evaluated male mice (2 to 3 per group) for this parameter.

Starting at 10 weeks old, all groups were fed a fat diet (atherogenic diet), specifically the ssniff® SM R/M High Fat (standard) with 15.2 % fat and 12.5 mg/kg Cholesterol (see Annex I).

As control group for the role of the diet were used C57BL/6 strain female mice, from the same genetic background of the experimental groups. The atherogenic diet was also introduced at 10 weeks of age.

The KRN mice (C57BL/6 background) were a gift from Drs. Christophe Benoist and Diane Mathis. These mice were intercrossed with B6.H-2^{g7} (available from The Jackson Laboratory) [93] to generate the K/BxA^{g7} mice. In order to confirm the predisposition to atherogenesis, were used a small group of animals, divided in two groups, one fed chow diet (regular diet) to serve as control group for arthritis progression (N=19), and the other fed with the same fat diet (atherogenic diet) described above (N=10), predisposing them to development of atherosclerotic lesions [82]. In each group, the mice were led until the 24 weeks to evaluate atherosclerosis progression in a relatively advance stage.

Genotypes were confirmed by polymerase chain reaction (PCR) in which was expected to obtain negative homozygoty for the ApoE (ApoE $^{-/-}$) and heterozygoty for the K/BxN (KRN $^{+/-}$) mice.

Mice were maintained in temperature controlled room on a 12-hour light cycle and under specific- pathogen- free (SPF) conditions. *

This study were guided by the law and ethical regulations related to the use of animals for research (86/609/CEE), reviewed by the IMM Animal Ethics Committee, and licensed by the Direcção-Geral de Alimentação e Veterinária (DGAV).

Therefore we have two experimental groups:

ApoE $^{-/-}$ mice	Fat diet	Develops atherosclerotic lesions
C57BL/6J mice	Fat diet	Control group for the diet effect

To address the second objective, we have two groups of arthritic mice in different conditions (normal and fat diet) to evaluate the atherosclerosis and bone kinetics:

K/BxA^{g7} mice	Fat diet	Develops inflammatory arthritis with secondary osteoporosis, and is predispose to atherosclerotic lesions
K/BxA^{g7} mice	Normal diet	Develops inflammatory arthritis with secondary osteoporosis

* SPF mice are mice which are demonstrated to be free of a specific list of pathogens (that can vary between mouse rooms depending on their barrier level) typically includes disease-causing pathogens that can affect mouse health and research outcomes) as well as opportunistic and commensal organisms [107].

Tissues collection and storage

Mice from the each experimental group were euthanized with CO_2 (N=10 per group) at different time-points: 8, 16, 20, 24 and 28 weeks old (Figure 3) and then the mice abdomen was open until the heart is exposed.

Blood was collected by cardiac puncture, centrifuged and the serum collected and stored at -80º C for later analysis. Then the heart was perfused with 5 mL of Phosphate Buffered Saline (PBS) solution directly in the left ventricle and, only in the aortas that were intended for lesion quantification (N=5 per group), this was followed by perfusion with 1 mL of paraformaldehyde (PFA) 3.7% (VWR, Leicestershire, UK), to fix the vessels.

The aortas were removed and isolated from the heart until the iliac bifurcation and then the fat tissue was removed under the stereoscope. After cleaning the aortas, they were immediately snap-frozen, when intended for RNA extraction, or placed at 4ºC in PFA 3.7% overnight when intended for lesions quantification. The liver and heart were also harvested, fixed in PFA 3.7% overnight and embedded in paraffin, and then stored for posterior studies.

At the time of sacrifice were also harvested bones from mice, and after fat tissue removed they were immediately frozen individually. We collected both femurs and L1-L5 vertebras to perform the intended assays and the right humerus and left and right tibias (stored at -80ºC) for posterior studies. To the femurs intended for RNA extraction, the bone marrow was flushed out with PBS before snap-frozen.

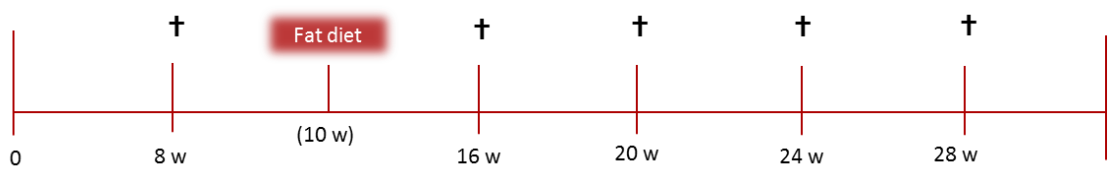

Figure 3 – Experimental timeline

Scheme of the mice euthanasia time-points and the time of introduction of the fat diet. w – weeks.

Lesions quantification

After overnight fixation, the aortas intended for lesions quantification were incubated with Oil Red O solution at 0.2% (Sigma-Aldrich, St. Lois, MO, USA) for 50 minutes. Then they were opened longitudinally. Because this solution has specificity to lipids is expected to stain lesions present in the vessel wall. The aortas were split lengthwise and pinned on a flat surface. Photographs were taken under the stereoscope and reconstituted using Adobe® Photoshop® CC software (version 6.1) to carry out quantification of lesions in relation to the total area of the aorta (from aortic root to the iliac bifurcation) using ImageJ software (version 1.50a). After the quantification, the aortas were embedded in paraffin for posterior histological studies.

RNA extraction

The aortas and femurs intended for gene expression assays were reduced to a fine powder using a porcelain pestle and mortar without thawing with help of liquid nitrogen to keep the sample at a lower temperature and to make it easier to grind. The RNA were then extracted with TRIzol® reagent (Invitrogen. Life Technologies, Paisley, UK) according to a modified version of the protocol described by Hughes *et al.* [94]. Briefly, the bone powder was placed in TRIzol® and homogenized. Then was added chloroform to solubilize the lipids. A digestion with proteinase K (Sigma-Aldrich, St. Lois, MO, USA) was performed at 55ºC, allowing the improvement of RNA quality [95] and next it was treated with isopropyl alcohol (VWR, Leicestershire, UK) in order to precipitate de RNA. The RNA pellet was cleaned with ethanol and then dissolved in Gibco® RNase/DNase-free water (Invitrogen. Life Technologies, Paisley, UK) (see full protocol in Annex II).

The RNA quantification and quality was obtained by absorbance measure using the NanoDrop® ND- 1000 Spectrophotometer (NanoDrop Technologies, Inc., Wilmington, USA) taking into account the 260/280 and 260/230 ratios which gives an idea of the RNA purity (260/280 ratio indicate the presence of protein, phenol or other contaminants

that absorb strongly at or near 280 nm, and the 260/230 ratio is used as a secondary measure of the nucleic acid purity and indicate the presence of contaminants which absorb at 230 nm like EDTA and TRIzol®) [96]. These ratios should be within the 1.8 to 2 range and 2.0 to 2.2 range, respectively [94].

Gene expression

The extracted RNA was reverse transcribed into complementary DNA (cDNA) using DyNAmo cDNA Synthesis Kit (Thermo Fisher Scientific Inc., Waltham, MA, USA) and Random Hexamer Primers (Thermo Fisher Scientific Inc., Waltham, MA, USA) according to manufacturer's instructions. The reverse transcription reaction was performed on a Piko™ Termal cycler (Thermo Fisher Scientific Inc., Waltham, MA, USA) at 37ºC for 30 minutes (for cDNA synthesis) followed by 85ºC for 5 minutes (for enzyme inactivation) and cDNA template were stored at -20ºC for later analysis (see Annex III).

The expression analysis of IL-1β, IL-6, IL-17A, TNF, RANKL, and OPG genes was performed using 3ng/µl of each cDNA template amplified in duplicate by quantitative real time polymerase chain reaction (RT-qPCR) using DyNAmo Flash SYBR® Green qPCR Kit (Thermo Fisher Scientific Inc., Waltham, MA, USA) and designed primers taking into account the GC content, amplicon size, melting temperature and span exon-exon junctions, among others (see Table 1). The expression of these genes was normalized with the housekeeping gene rRNA18S.

Table 1 - Housekeeping and target genes primer sequences

Gene	Foward primer sequence	Reverse primer sequence
IL-1β	5' TGC CAC CTT TTG ACA GTG ATG 3'	5' ATG TGC TGC TGC GAG ATT TG 3'
IL-6	5' GCC TTC TTG GGA CTG ATG CT 3'	5' TGC CAT TGC ACA ACT CTT TTC 3'
IL-17A	5' CCT GGA CTC TCC ACC GCA A 3'	5' TTC CCT CCG CAT TGA CAC AG 3'
TNF	5' AGC CCA CGT CGT AGC AAA C 3'	5' GTG AGG AGC ACG TAG TCG G 3'
RANKL	5' TCC CAT CGG GTT CCC ATA AAG 3'	5' AGG TAC GCT TCC CGA TGT TT 3'
OPG	5' GTG TGG AAT AGA TGT CAC CCT GT 3'	5' CTT GTG AGC TGT GTC TCC GT 3'
rRNA 18S	5' TGT GAT GCC CTT AG 3'	5' CTT ATG ACC CGC AC 3'

The reactions were performed on the Applied Biosystems® 7500 Fast Real-Time PCR system (Life Technologies, Paisley, UK) according to the manufacturer's instructions.

Briefly, the reactions started at 50ºC for 2 minutes and then 95ºC for 7 minutes (to activate the DNA polymerase) followed by 95ºC for 10 seconds (to denature the template DNA) and 60ºC for 10 seconds for 50 cycles, for the annealing/extension step. The reactions were validated by the presence of a single peak in the melt curve analysis.

The data obtained were analyzed using the standard curves analysis. This standard curves were made using cDNA template synthetized with known RNA concentration obtained from healthy mice (C57BL/6), both genders (N=2 from each gender), with 18 weeks of age (approximate bone mass peak for mice).

The cycle threshold (C_T) is defined as a number of cycles required for the fluorescent signal to cross the threshold and exceed the background level. The efficiency of the PCR should be between 90-100%, which means for each cycle the amount of product doubles. For a reaction with efficiency between this limits the slope obtained will be between -3.5 and -3.20 [97]. The conversion of the C_T value in relative expression levels was performed using slope and Y intersect obtained from the standard curve and applying the equation $10^{(CT\text{-}Y\ intersect/slope)}$ [98]. The values obtained with RT-qPCR were normalized with rRNA18S used as housekeeping gene.

Bone turnover markers measurements

Bone turnover markers are biochemical products usually measured in blood or urine that allows the quantification of the bone's metabolic activity.

The levels of P1NP (marker of bone formation) and CTX-I (marker of bone resorption) were determined by Enzyme-Linked Immunosorbent Assay (ELISA) kits (Immunodiagnostic Systems Limited, Tyne & Wear, UK) specific for each one (kit references AC-33F1 and AC-06F1, respectively), performed according to the manufacturer's instructions. Briefly, this technique is based on a double-antibody sandwich assay where each antibody is specific for a different epitope of the antigen molecule. The plates were pre-coated with a monoclonal antibody specific for the antigen to determine, then the sample is added, followed by a second antibody that is conjugated to an enzyme to form an immune complex, responsible for detection. This steps of the ELISA result in a colored end product which correlates to the amount of analyte present in the sample.

Bone micro-architectural properties

The L3-L4 vertebras harvested at each time-point were isolated to perform histomorphometry technique in order to evaluate bone fragility.

Histomorphometry is a technique used to study in a quantitative manner the microarchitecture, remodeling and metabolism of a tissue, such as bone [99].

By histomorphometry, the bone microarchitecture can be assessed by static parameters, such as trabecular thickness (Tb.Th; µm) that gives the medium distance across individual trabeculae, and trabecular separation (Tb.Sp; µm) that gives the medium distance between trabeculae of our region of interest. These architectural parameters are related to the bone volume fraction (BV/TV; %) value that is determined by the percentage of area occupied by calcified bone in relation to the total sample area [99].

Briefly, the samples were fixated with ethanol at 70% (VWR, Leicestershire, UK) for 7 days and then were dehydrated using ethanol at 96% (Proclínica, Lisboa, Portugal) for 24h and ethanol at 100% (VWR, Leicestershire, UK) for 12h. The next step was the clearing in which the samples where embedded in Xylene (Klinipath, Duiven, Holland) for 1h and then the solution was replaced for Methyl methacrylate (MMA) (Sigma-Aldrich, St. Lois, MO, USA) for 3 days. To allow the bone samples to polymerize, a mix solution of MMA solution mixed with Dimethylaniline 2% (Merck, Kenilworth, NJ, USA) were poured over the samples and was leaved to polymerize. All steps were performed at 4ºC. After the resin was already solidified, the samples were cut in sections with 5µm thickness in a Leica RM2145 microtome (Leica, Wetzlar, Germany) with a tungsten blade (Leica, Wetzlar, Germany). Each cut were placed on glass slides previously coated with gelatin chrome alum (Panreac AppliChem, Barcelona, Spain) together with 70% ethanol to keep the samples attached. All sections were stained using aniline blue (VWR, Leicestershire, UK) (see detailed protocol in Annex IV).

For the analysis of the different parameters, the slides were visualized in a Leica DM2500 microscope (Leica, Wetzlar, Germany) equipped with a camera (Leica, Wetzlar, Germany). The images were analyzed using the ImageJ software (version 1.50a) with the BoneJ plugin.

Clinical Evaluation of Arthritis

The severity of arthritis was scored weekly based on an established scoring system through monitoring the swelling of each paw: 0=normal with no observable swelling; 1 = one involved digit or mild swelling of foot and ankle, but foot maintains its original V shape with no deformation; 2= long edges of foot are parallel with each other, with disappearance of the normal V shape and appear to have paw deformation but no visible difficulty of mobility; 3= inversion of the V shape by expansion of the ankle and hindfoot to greater than the width of forefoot with great loss of mobility. (Maximum score of 12) [86] (See Figure 4).

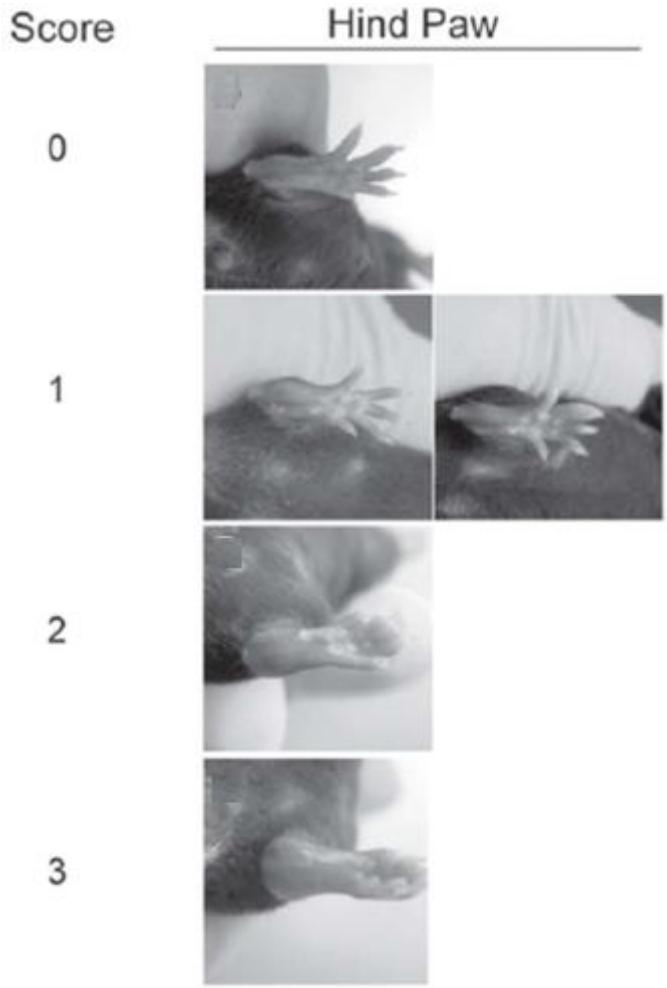

Figure 4 – Clinical Score system

Score (0-3) for each paw with a maximum score of 12 per animal (adapted from Monach et al., 2007) [86].

Statistical analysis

Data obtained are shown as means with standard deviations and medians with IQR (interquartile range - 75% to 25%). The normality of distribution for continuous variables was tested by performing Kolmogorov-Smirnov test, and a Levene's test was performed to evaluate the samples homoscedasticity. Since the N <30 in every groups and the *p* value obtained in both tests was ≤0.05, non-normality was assumed for all statistical tests.

Differences between groups were assessed by Kruskal-Wallis one-way analysis of variance or the Mann-Whitney *U* test when comparing just two independent groups.

Correlations were investigated using the Sperman's rank correlation.

Statistical significance was established as a two-tailed *p* value ≤0.05 to indicate a statistically significance between groups, and the confidence interval for all statistical operations was 95%.

All statistical analyses were performed using the Statistical Package for Social Sciences manager software version 20 (IBM® SPSS V20 software, Inc., Chicago, IL, USA). All graphics were created using GraphPad Prism® software, version 6 (GraphPad software, Inc., La Jolla, CA, USA).

Results

Body weight evaluation

Ten animals from each experimental group, C57BL/6 (B6) and ApoE $^{-/-}$, were used in each time-point. The body weight was measured weekly during the time of the experiment (Table 2 and Figure 5), although the comparisons between groups, and within the same group, was only made at the points of evaluation, e.g. the time-points defined previously (see Figure 3).

Table 2 – Body weight measurements for the experimental groups (B6 and ApoE $^{-/-}$) at different time-points.

Groups	Time-points (age in weeks)	number of animals (N)	Weight (grams)	
			mean with SD	median with IQR
C57BL/6 (B6)	8	50	18,27 ± 1,20	18,35 [19,10 - 17,55]
	16	20	22,16 ± 0,71	22,25 [22,59 - 21,86]
	20	15	22,79 ± 2,02	23,35 [23,78 - 22,30]
	24	15	27,04 ± 3,48	25,60 [29,83 - 25,26]
	28	5	26,17 ± 1,48	26,55 [26,95 - 25,00]
ApoE $^{-/-}$	8	23	18,34 ± 3,18	17,85 [19,45 - 16,85]
	16	40	25,45 ± 3,27	24,38 [26,00 - 23,28]
	20	27	27,04 ± 3,02	25,55 [28,58 - 24,98]
	24	21	27,78 ± 2,81	27,35 [28,50 - 26,35]
	28	13	29,89 ± 3,24	28,85 [30,60 - 27,85]

Values are represented as mean ± standard deviation (SD) and median with IQR (Interquartile range) [75% - 25%].

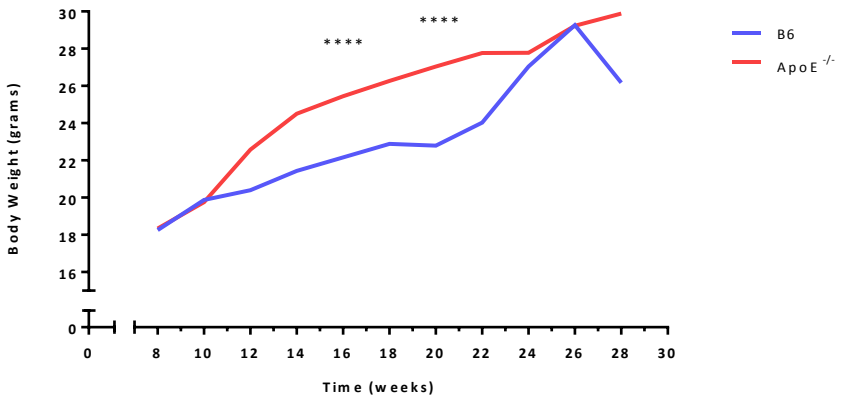

Figure 5 - Representation of Body weight for B6 and ApoE $^{-/-}$ over the time of experiment (8-28w).

The values used are medians. **** represents the statistical significant difference between body weight of B6 and ApoE $^{-/-}$ at 16 weeks (*p*-value <0.0001); and the statistical significant difference between body weight of B6 and ApoE $^{-/-}$ at 20 weeks (*p*-value =0.0003). The values are represented in grams.

Over the time of the experiment both groups increased significantly their body weight at each time-point (see Figure 6). Although this increase occurred in both groups there were body weight differences starting after the introduction of the fat diet (at 10 weeks of age), with statistical significance at 16 weeks (*p*-value <0.0001) and at 20 weeks (*p*-value = 0.0003).

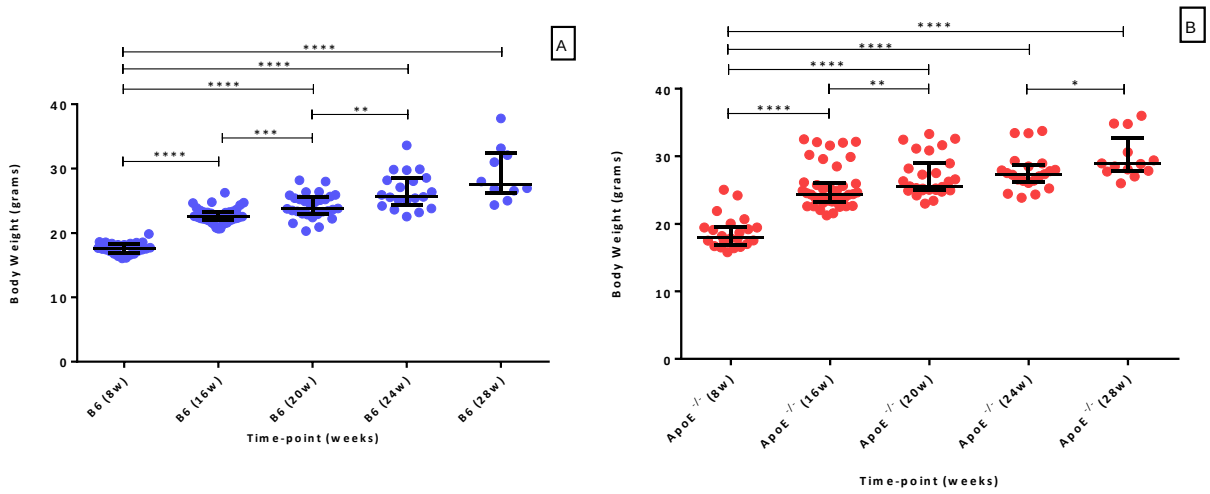

Figure 6 - Body weight assessment for B6 (A) and ApoE $^{-/-}$ (B) at each time-point.

The results are shown as dot plots displaying medians and IQR (interquartile range) [75%-25%].

(A) **** (*p*-value <0.0001) and ** (*p*-value =0.0026) representing the statistical significant increase between B6 body weight medians at different time-points. (B) **** (*p*-value <0.0001), ** (*p*-value =0.0046) and * (*p*-value =0.026) representing the statistical significant body weight increase between ApoE $^{-/-}$ body weight medians at different time-points. The values are represented in grams.

Atherosclerotic lesions

To evaluate the progression of atherosclerosis, the relative area affected with atherosclerotic lesions was quantified. The B6 group did not developed lesions throughout the time of the experiment contrary to ApoE $^{-/-}$ mice that shown signs of atherosclerotic lesions starting as early as 8 weeks (first time-point of evaluation), progressing until the end-point (28 weeks).

Table 3 – Atherosclerotic lesion area measurements for B6 and ApoE $^{-/-}$ mice in each time-point.

Groups	Time-points (age in weeks)	number of animals (N)	Gender (F/M)	Aterosclerotic Lesions	
				mean with SD	median with IQR
C57BL/6 (B6)	8	5	F	0	0
	16	5	F	0	0
	20	5	F	0	0
	24	5	F	0	0
	28	5	F	0	0
ApoE $^{-/-}$	8	5	F	0,16 ± 0,14	0,09 [0,20 - 0,08]
		3	M	0,12 ± 0,14	0,08 [0,18 - 0,04]
	16	5	F	2,14 ± 0,95	1,85 [2,53 - 1,62]
		2	M	4,47 ± 0,30	4,47 [4,57 - 1,62]
	20	5	F	6,62 ± 2,46	7,60 [8,51 - 4,00]
		2	M	8,19 ± 4,41	8,19 [9,75 - 6,63]
	24	5	F	11,09 ± 2,09	11,06 [11,60 - 9,32]
		2	M	16,08 ± 1,46	16,08 [16,59 - 15,56]
	28	5	F	22,48 ± 5,82	21,43 [25,81 - 20,60]
		3	M	28,97 ± 3,42	30,76 [30,94 - 27,90]

The experimental groups are represented by female (F) and/or male (M) mice and the values are represented as means ± standard deviation (SD) and medians with IQR (Interquartile range) [75% - 25%] for each group. The values for atherosclerotic lesions are represented as the area occupied by these lesions in relation to total area of the aorta.

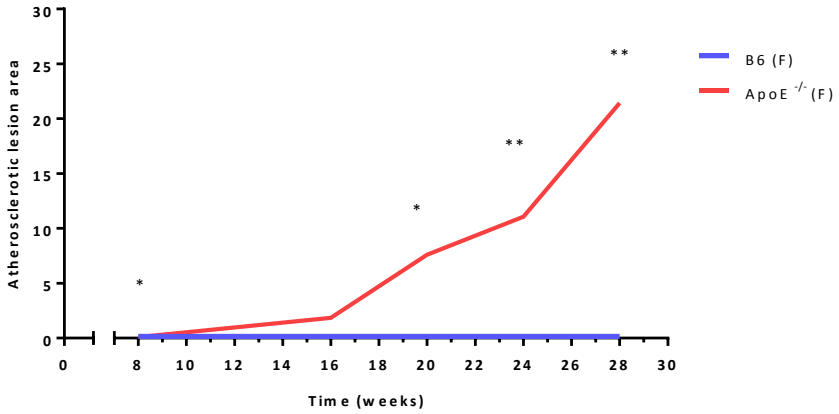

Figure 7 - Representation of atherosclerotic lesions area between B6 and ApoE $^{-/-}$ female (F) mice over the time of experiment (8-28w).

The values represent medians of the area occupied by the atherosclerotic lesions in relation to total area of the aorta. There is a progression of atherosclerotic lesions in ApoE $^{-/-}$ mice but not in B6 mice (the blue line representing this group appears as flat line at zero) with significant differences at 8 and 20 weeks (* *p*-value =0.0286 and * *p*-value = 0.0357, respectively); and 24 and 28 weeks (** *p*-value = 0.0079).

The atherosclerotic lesions only appeared in ApoE $^{-/-}$ mice, without significant differences between genders (data not shown). Although B6 mice did not shown any signs of atherosclerotic lesions throughout the experiment, as expected, the differences reported in Figure 7 between these two groups became more significant after 24 weeks, representing the time when the atherosclerotic lesions in ApoE $^{-/-}$ mice progressed more significantly, this development can be seen in representative images at each time-point (Figure 8).

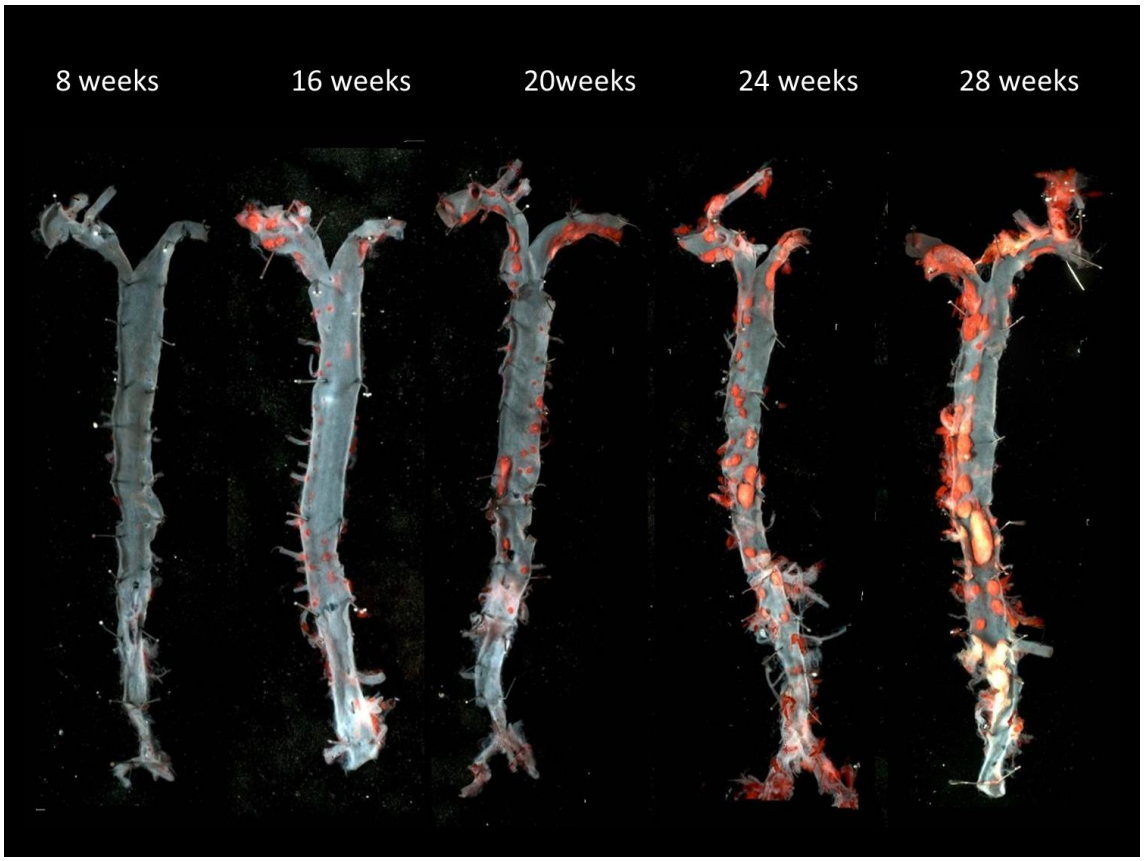

Figure 8 - Oil Red O staining of representative aortic specimens of ApoE $^{-/-}$ groups at each time-point.

Bone turnover markers

To assess bone turnover, the levels of CTX-I and P1NP in serum samples were determined.

Serum levels of CTX-I are presented in Table 4.

Table 4 - Measurements of serum CTX-I levels for B6 and ApoE $^{-/-}$ mice at different time-points.

Groups	Time-points (age in weeks)	number of animals (N)	CTX-I (ng/mL)	
			mean with SD	median with IQR
C57BL/6 (B6)	8	6	39,46 ± 25,10	45,60 [60,50 - 20,24]
	16	5	27,33 ± 7,77	25,68 [31,09 - 23,31]
	20	7	38,01 ± 8,49	38,01 [41,97 - 29,73]
	24	7	21,99 ± 8,30	19,85 [27,38 - 15,11]
	28	7	22,66 ± 8,83	24,44 [27,56 - 15,48]
ApoE $^{-/-}$	8	7	19,93 ± 8,44	15,75 [24,84 - 13,57]
	16	7	22,22 ± 18,66	16,73 [17,09 - 13,65]
	20	7	30,88 ± 17,91	32,97 [41,60 - 15,05]
	24	7	27,86 ± 8,04	26,02 [33,92 - 20,99]
	28	7	31,05 ± 8,70	33,16 [36,05 - 26,15]

Values are represented in nanograms per mL and are shown as means ± standard deviation (SD) and medians with IQR (Interquartile range) [75% - 25%]. CTX-I - C-terminal cross-link telopeptide of type I collagen.

In Figure 9 we can see the alterations in CTX-I serum levels over time. The B6 group presents higher levels of this protein until 20 weeks, and then the levels continue to decrease until levels lower that those determined in ApoE $^{-/-}$ mice. Despite the major difference noticeable at 8 weeks the only statistically significant difference between both groups was at 16 weeks (p-value = 0.0043), this difference is justified when comparing the values dispersion and medians at 8 weeks reported in Figure 10A.

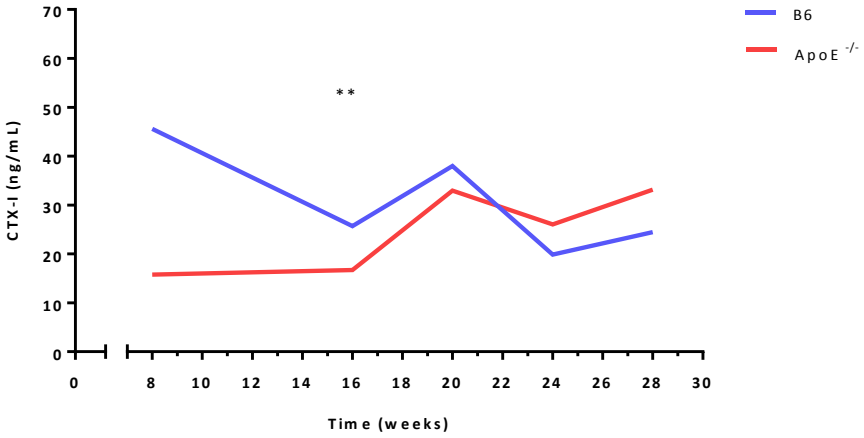

Figure 9 - Representation of CTX-I serum levels for B6 and ApoE $^{-/-}$ along the experimental time.

Values are represented in nanograms per mL and are shown as medians. ** represents the statistical significant difference between B6 and ApoE $^{-/-}$ at 16 weeks (*p*-value = 0.0043). The values used was the median for each time-point. CTX-I - C-terminal cross-link telopeptide of type I collagen.

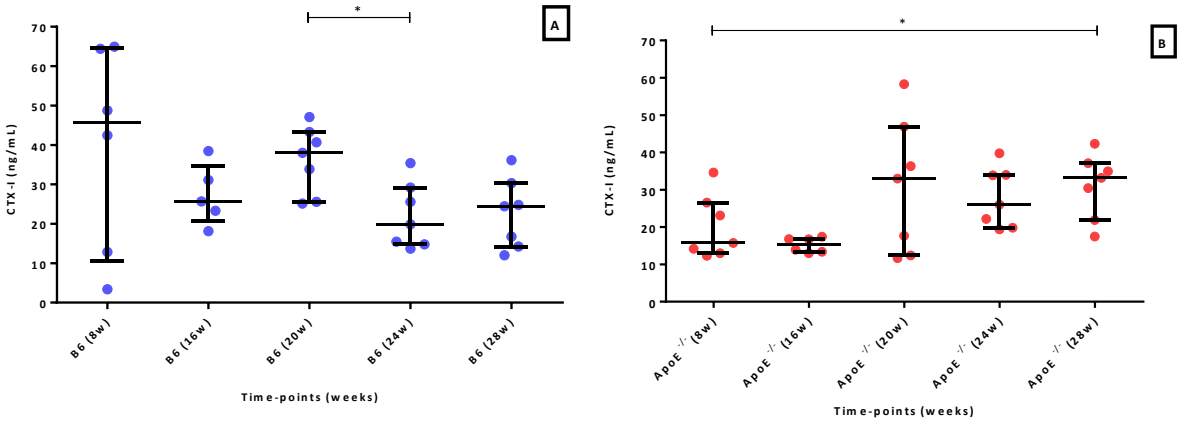

Figure 10 - CTX-I serum levels for B6 (A) and ApoE $^{-/-}$ (B) groups for each time-point.

The results are represented in nanograms per mL and are shown as dot plots displaying medians and IQR (interquartile range) [75-25%] in each time-point. (A) B6 group where * represents the statistically significant decreased levels at 20 to 24 weeks old (*p*-value =0.0262). (B) ApoE $^{-/-}$ group where * represents the statistically significant increased levels between 8 and 28 weeks (*p*-value =0.0262). CTX-I - C-terminal cross-link telopeptide of type I collagen.

Looking more closely at each group (Figure 10) the CTX-I levels tendency is markedly different, i.e. the B6 group shown a slight tendency of decreased CTX-I levels along the different time-points, with statistical differences only from 20 to 24 weeks where this decrease was more marked (*p*-value = 0.0262) and in the ApoE $^{-/-}$ group the tendency

was the opposite, i.e. along the time-points it was observable an increase in this protein levels although not statistically significant except when comparing the start (8 weeks) to the end point (28 weeks) (*p*-value = 0.0379).

For the levels of P1NP in serum, the results are presented in Table 5.

Table 5 - Measurements of P1NP levels in serum of B6 and ApoE $^{-/-}$ mice along the experimental time.

Groups	Time-points (age in weeks)	number of animals (N)	P1NP (ng/mL)	
			mean with SD	median with IQR
C57BL/6 (B6)	8	6	196,45 ± 48,32	213,25 [223,30 - 160,08]
	16	4	81,55 ± 12,64	82,37 [90,86 - 73,07]
	20	7	76,18 ± 26,31	69,34 [86,71 - 60,28]
	24	6	42,01 ± 6,53	43,27 [46,14 - 38,43]
	28	6	39,18 ± 7,64	37,12 [44,50 - 33,17]
ApoE $^{-/-}$	8	7	158,39 ± 61,98	131,00 [210,50 - 127,00]
	16	6	58,68 ± 12,62	58,87 [66,53 - 53,41]
	20	7	73,30 ± 16,76	16,76 [85,33 - 61,25]
	24	7	59,89 ± 19,05	51,19 [76,20 -46,81]
	28	7	60,24 ± 17,75	59,81 [67,78 - 46,45]

Values are represented in nanograms per mL and are shown as means ± standard deviation (SD) and medians with IQR (Interquartile range) [75% - 25%]. P1NP - N-propeptide of type I collagen.

Regarding the P1NP, another protein associated with bone turnover, its levels shown to be more similar between the two experimental groups (Figure 11), meaning the levels decreased over time for both groups until 20 weeks; after this time only ApoE $^{-/-}$ group had a slight increase, but not statistically significant (Figure 12B). Although the differences between both groups seems higher in the beginning, only had statistical significance at 16 weeks (*p*-value =0.0173) and in the last time-point (28w) (*p*-value =0.0221).

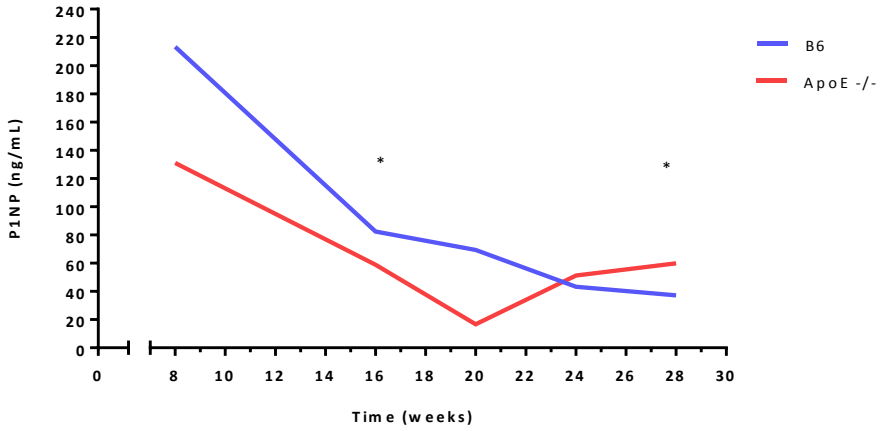

Figure 11 - Representation of P1NP levels in serum from B6 and ApoE $^{-/-}$ mice along the experimental time.

The results are represented in nanograms per mL and are shown as medians. * represents the statistical significant differences between B6 and ApoE $^{-/-}$ at 16 weeks (*p*-value = 0.0173) and at 28 weeks (*p*-value = 0.0221). P1NP - N-propeptide of type I collagen.

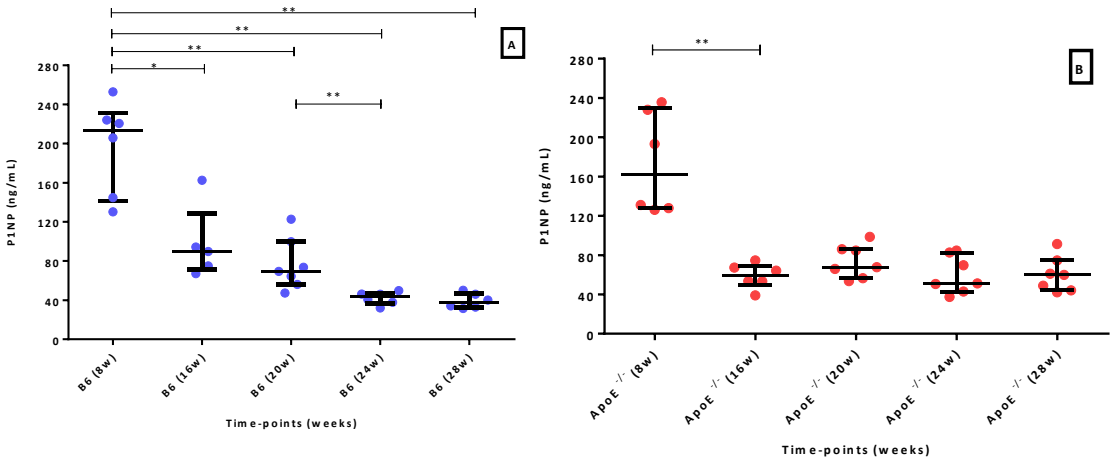

Figure 12 - P1NP serum levels for B6 (A) and ApoE $^{-/-}$ (B) groups at each time-point.

The results are represented in nanograms per mL and are shown as dot plots displaying medians and IQR (interquartile range) [75-25%] in each time-point. (A) B6 group with * representing the statistical significant decreased levels from 8 weeks to 16 weeks old (*p*-value = 0.0173), ** representing the statistical significant decreased levels between 20 and 24 weeks (*p*-value = 0.0023), and the difference between the levels in the beginning (8w) with the other time-points: 8w vs 20w (*p*-value = 0.0012), 8w vs 24w (*p* value = 0.0022) and 8 vs 28w (*p* value = 0.0022). (B) ApoE $^{-/-}$ group with ** representing the statistical significant decreased levels between 8 and 16 weeks (*p*-value = 0.0022). P1NP - N-propeptide of type I collagen.

Although it was visible a decreased in the levels of P1NP in both groups since the beginning (first time-point), the B6 group seemed to experience a more continued reduction of this protein levels, with these levels dropping along the time of the experiment (Figure 12A), while the ApoE $^{-/-}$ group has more stable values of P1NP between 16w and 28w time-points (Figure 12B).

Since CTX-I and P1NP proteins are related to bone resorption and formation, respectively, to evaluate if bone turnover is impaired we looked at CTX-I/ P1NP ratio (Table 6).

Table 6 - CTX/P1NP ratio determination for B6 and ApoE $^{-/-}$ groups for each time-point.

Groups	Time-points (age in weeks)	number of animals (N)	CTX/ P1NP ratio	
			mean with SD	median with IQR
C57BL/6 (B6)	8	3	0,29 ± 0,18	0,21 [0,41 - 0,18]
	16	4	0,31 ± 0,08	0,32 [0,36 - 0,26]
	20	7	0,50 ± 0,12	0,54 [0,58 - 0,41]
	24	6	0,47 ± 0,11	0,46 [0,54 - 0,40]
	28	6	0,59 ± 0,24	0,51 [0,80 - 0,45]
ApoE $^{-/-}$	8	7	0,13 ± 0,03	0,12 [0,13 - 0,11]
	16	6	0,27 ± 0,06	0,26 [0,30 - 0,25]
	20	7	0,41 ± 0,19	0,39 [0,58 - 0,24]
	24	7	0,50 ± 0,19	0,49 [0,52 - 0,43]
	28	7	0,54 ± 0,18	0,52 [0,30 - 0,41]

Values represent means ± standard deviation (SD) and medians with IQR (Interquartile range) [75% - 25%]. CTX-I - C-terminal cross-link telopeptide of type I collagen; P1NP - N-propeptide of type I collagen.

Analyzing the CTX-I/ P1NP ratio throughout time (Figure 13) there was no statistical significant difference between the experimental groups.

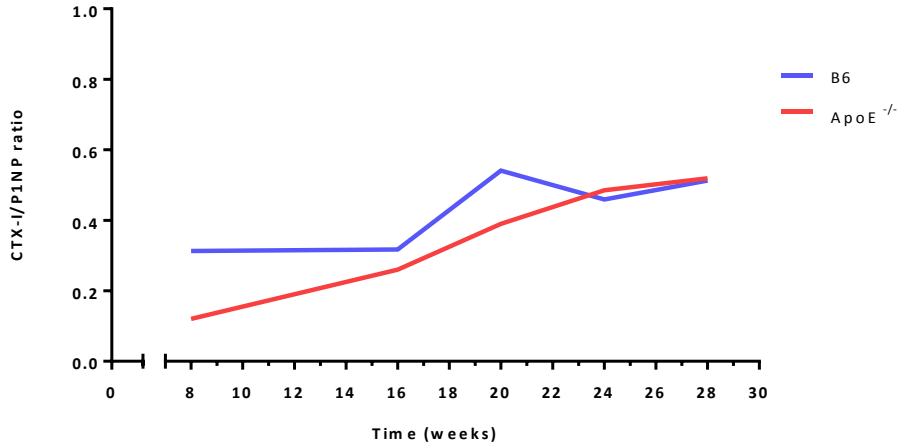

Figure 13 - Representation of CTX-I/P1NP ratio for B6 (A) and ApoE -/- (B) groups at each time-point.

The values represent medians. CTX-I - C-terminal cross-link telopeptide of type I collagen; P1NP - N-propeptide of type I collagen.

But looking to the CTX-I/P1NP ratio alterations over time for each group we can see that contrary to B6 group that increased CTX/P1NP ratio from 16 to 20 weeks old (*p*-value = 0.0424) but then started to stabilized (Figure 14A), the ApoE $^{-/-}$ group presents a more sticking increase over time, even though was only statistically significant compared to levels at baseline (8 weeks) (Figure 14B).

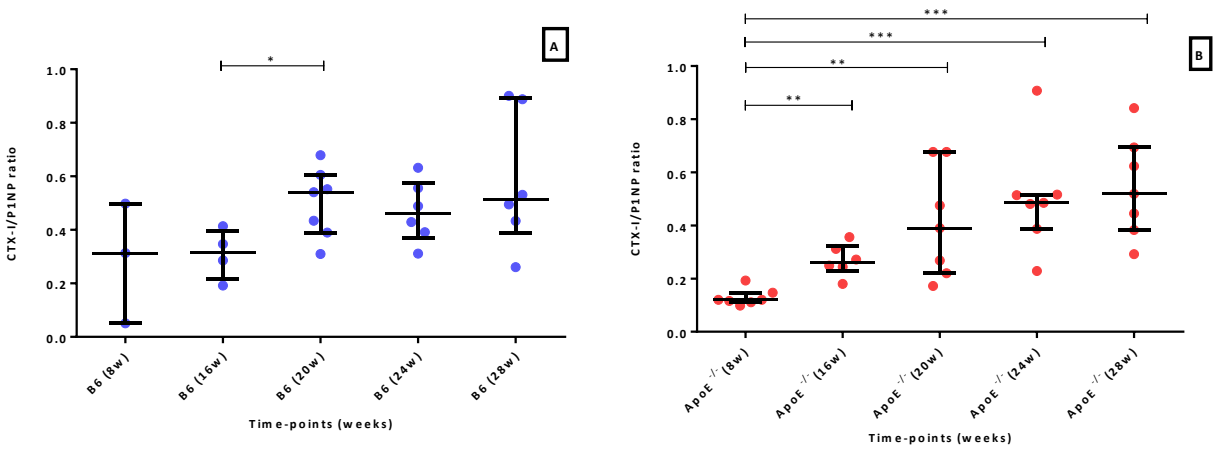

Figure 14 - CTX/P1NP ratio for B6 (A) and ApoE $^{-/-}$ (B) at each time-point.

The results are shown as dot plots displaying medians and IQR (interquartile range) [75-25%] in each time-point. (A) B6 group with * representing the statistical significant increase levels between 16 weeks and 20 weeks old (*p*-value = 0.0424). (B) ApoE $^{-/-}$ group with ** representing the statistical significant increase levels between 8 weeks old group and 16 weeks (*p*-value = 0.0022), 8w *vs* 20 weeks (*p*-value = 0.0022), and *** representing the statistical significant increased levels between 8w *vs* 24 weeks (*p*-value = 0.0006) and 8w *vs* 28 weeks (*p*-value = 0.0006). CTX-I - C-terminal cross-link telopeptide of type I collagen; P1NP - N-propeptide of type I collagen.

Histomorphometry

To address the possible alterations in bone microarquitecture and organization, the 3rd and 4th lumbar vertebras, from each groups at the different time-points, were analyzed by histomorphometric analysis, evaluating several parameters: Bone volume (BV/TV; %), trabecular thickness (Tb.Th; µm) and intra-trabecular separation (Tb.Sp; µm) (Figure 15).

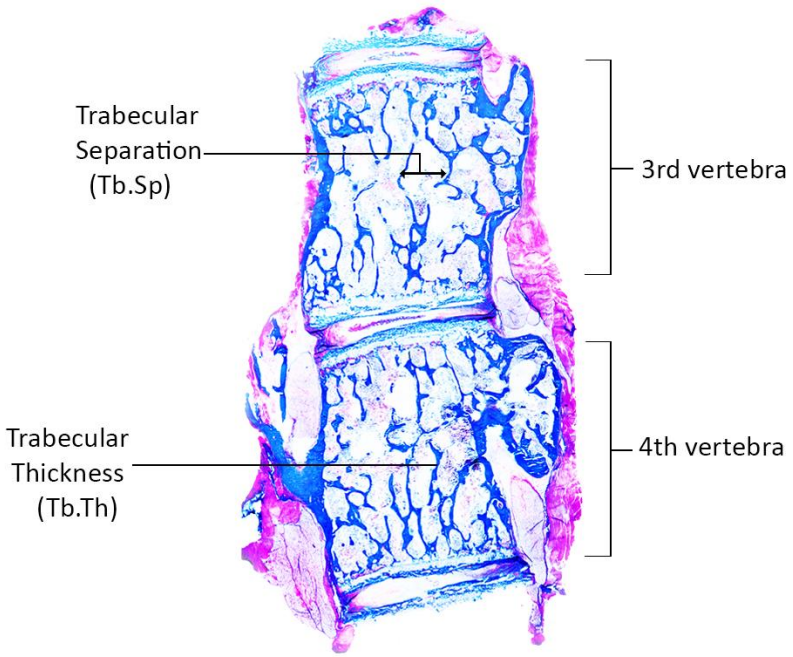

Figure 15 – Aniline blue staining of 3rd and 4th vertebras specimen.

Represents one B6 mice at 8 weeks old. The images were obtained using 5X objective. The distance between two trabeculae is defined by trabecular separation (Tb.Sp) and the thickness of each trabecular are defined by trabecular thickness (Tb.Th), the Bone Volume (not represented) is measured delimiting each vertebra and calculate the area occupied by trabecular bone in relation with total area (BV/TV).

Table 7 - Measurements of bone volume for B6 and ApoE $^{-/-}$ along the experimental time.

Groups	Time-points (age in weeks)	number of animals (N)	BV/TV (%) mean with SD	BV/TV (%) median with IQR
C57BL/6 (B6)	8	5	21,50 ± 3,68	21,75 [23,90 - 19,25]
	16	5	23,36 ± 5,27	21,30 [26,10 - 19,60]
	20	5	20,89 ± 2,20	21,25 [21,55 - 20,80]
	24	5	20,87 ± 6,67	23,30 [24,80 - 16,15]
	28	5	15,64 ± 1,97	15,00 [15,20 - 14,70]
ApoE $^{-/-}$	8	5	22,14 ± 3,24	21,00 [22,55 - 20,05]
	16	5	21,13 ± 3,24	22,00 [23,75 - 18,00]
	20	5	20,23 ± 2,05	20,00 [20,50 - 18,70]
	24	5	17,90 ± 1,10	17,75 [18,90 - 17,25]
	28	5	13,28 ± 2,86	13,90 [15,35 - 12,70]

Values are represented in percentage and are shown as means ± standard deviation (SD) and medians with IQR (Interquartile range) [75% - 25%]. BV/TV - Bone Volume / Total Volume.

The graphic representation of the median values reported in Table 7 (Figure 16), shown a decreased in bone volume in both groups, particularly after 24 weeks and despite the ApoE $^{-/-}$ group had lower percentage of bone volume there were no statistically significant differences between both groups.

The increase at 24 weeks for B6 group was only in 2%, and despite it seems more representative, in Figure 17A we can see that bone volume did not suffer a big change.

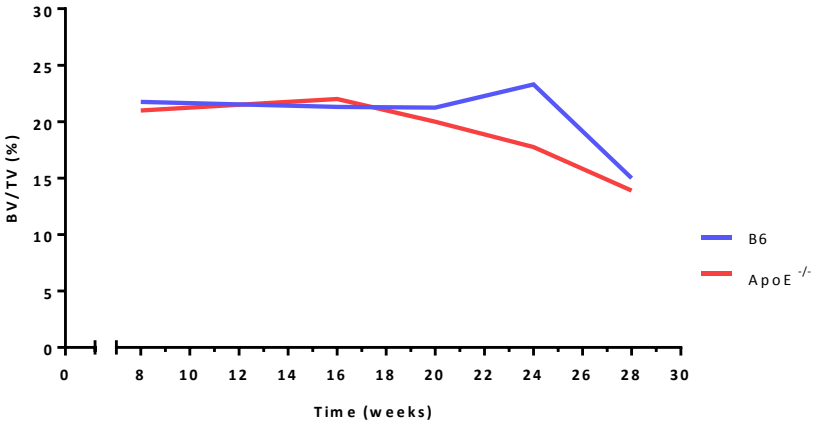

Figure 16 - Representation of bone volume for B6 and ApoE $^{-/-}$ groups along the experimental time.

The values used are medians, represented in percentage. BV/TV - Bone Volume / Total Volume.

Despite the lack of differences between groups, the decrease in bone volume was significant in both, but if on one hand, this decrease was only significant (*p*-value = 0.0159) at the end-point (comparing with the first measurement) for the B6 group (Figure 17A), for the ApoE $^{-/-}$ group, on the other hand, the alterations in bone volume were more significant in an earlier stage (24 weeks) with a reduction of 4% since the beginning (*p*-value = 0.0079), continuing to decrease at 28 weeks (*p*-value = 0.0079, when compared to 8 weeks) (Figure 17B).

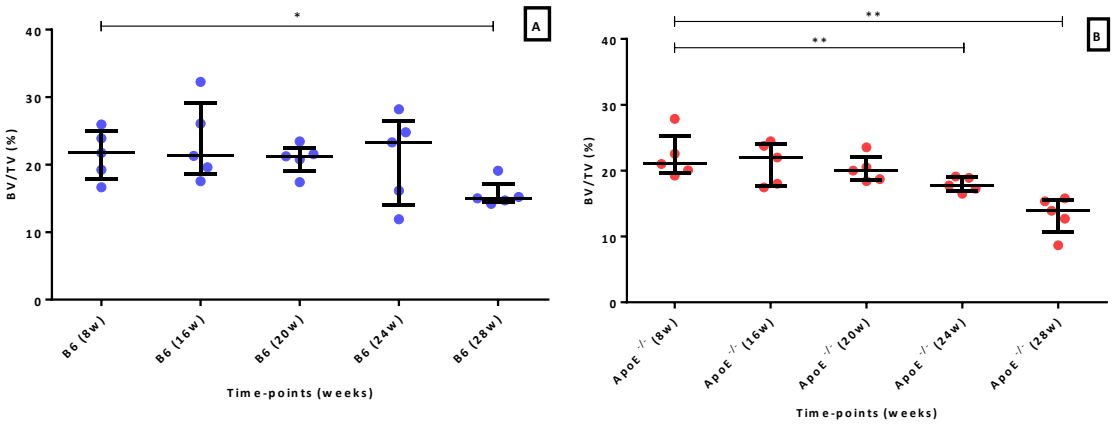

Figure 17 – Bone volume for B6 (A) and ApoE $^{-/-}$ (B) group at each time-point.

The results are represented in percentage and shown as dot plots displaying medians and IQR (interquartile range) [75-25%] in each time-point. (A) B6 group with * representing the statistical significant decrease in bone volume at the beginning and end of experiment (8w *vs* 28 weeks old) (*p*-value = 0.0159). (B) ApoE $^{-/-}$ group with ** representing the statistical significant decrease in bone volume of ApoE $^{-/-}$ group at the beginning and last time-points (24 and 28 weeks old) (*p* value = 0.0079, for both). BV/TV - Bone Volume / Total Volume.

To evaluate the changes in microarquitecture, were used the trabecular thickness (Tb.Th) and trabecular separation (Tb.Sp) parameters to access the quality of bone.

In Table 8 are reported the results of trabecular thickness (Tb.Th), where was possible to see that the values are relatively constant throughout time with a slight decrease at the last time-point.

Table 8 - Measurements of trabecular thickness for B6 and ApoE $^{-/-}$ groups along the experimental time.

Groups	Time-points (age in weeks)	number of animals (N)	Tb. Th (μm)	
			mean with SD	median with IQR
C57BL/6 (B6)	8	5	2,36 ± 0,33	2,34 [2,70 - 2,13]
	16	5	3,28 ± 0,39	3,25 [3,68 - 3,14]
	20	5	3,58 ± 0,36	3,59 [3,82 - 3,23]
	24	5	3,74 ± 0,75	3,79 [4,38 - 3,33]
	28	5	3,45 ± 0,28	3,57 [3,58 - 3,17]
ApoE $^{-/-}$	8	5	3,00 ± 0,32	3,20 [3,26 - 2,73]
	16	5	3,32 ± 0,36	3,16 [3,33 - 3,11]
	20	5	3,40 ± 0,18	3,44 [3,48 - 3,32]
	24	5	3,28 ± 0,27	3,16 [3,56 - 3,06]
	28	5	2,71 ± 0,09	2,76 [2,77 - 2,70]

Values are represented in micrometers and are shown as means ± standard deviation (SD) and medians with IQR (Interquartile range) [75% - 25%]. Tb.Th – Trabecular Thickness.

Looking at the graphic representation of these median values (Figure 18) it is possible to see that the tendency for trabecular thickening along the time, in B6 group (blue line) has a slight decrease in the last time-point. This decline in more striking in ApoE $^{-/-}$ group and starts at 20 weeks old, becoming significantly lower in the ApoE $^{-/-}$ group comparing to B6 group (*p*-value = 0.0079).

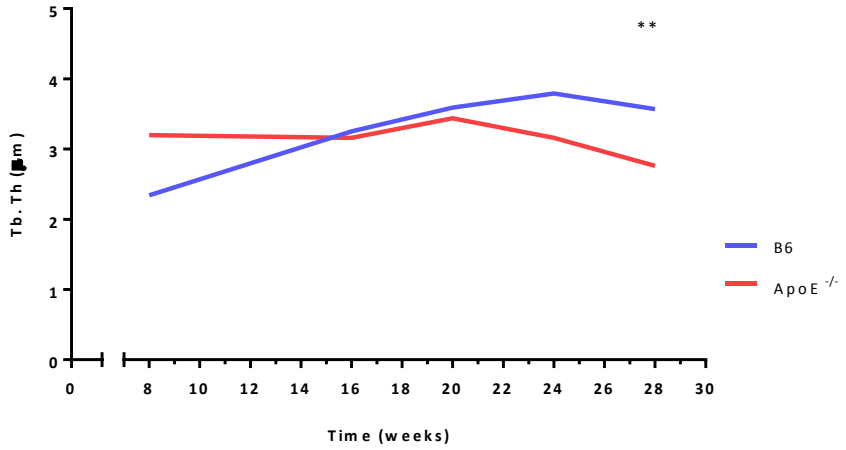

Figure 18 - Representation of trabecular thickness for B6 and ApoE $^{-/-}$ along the time of experiment.

The values are medians, in micrometers. Tb.Th – Trabecular Thickness.

Regarding each group separately, it is possible to see a rapid increase in thickening for B6 group just after the 8 weeks (*p* value = 0.0317) continuing to increase, although not significantly, throughout time and then decrease slightly at 28 weeks (Figure 19A). For the ApoE $^{-/-}$ group these changes are more discrete, i.e. the trabeculae did not appear to suffer big changes through time, showing only a noticeable decrease at 28 weeks (*p*-value = 0.0079) (Figure 19B).

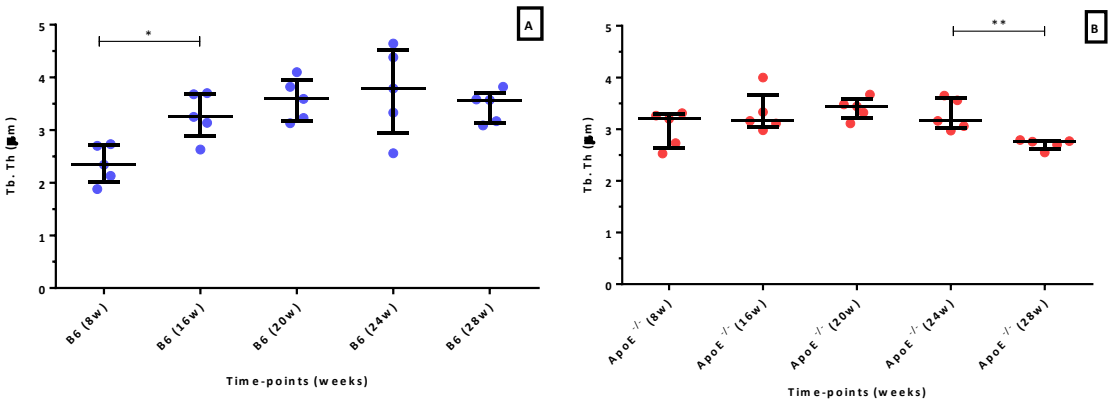

Figure 19 – Trabecular thickness for B6 (A) and ApoE $^{-/-}$ (B) groups at each time-point.

The results represented in micrometers and shown as dot plots displaying medians and IQR (interquartile range) [75-25%] in each time-point. (A) B6 group with * representing the statistical significant increase in trabecular thickness at 8 and 16 weeks old (*p*-value = 0.0317). (B) ApoE $^{-/-}$ group with ** representing the statistical significant decrease in trabecular thickness from 24 to 28 weeks old (*p*-value = 0.0079). Tb.Th – Trabecular Thickness.

In Table 9 are reported the results of trabecular separation (Tb.Sp), where is possible to see that both groups had an increased in trabecular separation along the time, with a decrease for the ApoE $^{-/-}$ group at the late stages of experiment.

Table 9 - Measurements of trabecular separation for B6 and ApoE $^{-/-}$ along the experimental time.

Groups	Time-points (age in weeks)	number of animals (N)	Tb. Sp (µm)	
			mean with SD	median with IQR
C57BL/6 (B6)	8	5	8,98 ± 0,86	9,34 [9,38 - 8,61]
	16	5	10,79 ± 2,12	11,02 [11,27 - 10,82]
	20	5	12,26 ± 0,79	12,48 [12,98 - 11,82]
	24	5	13,01 ± 2,53	13,13 [13,55 - 11,85]
	28	5	15,87 ± 0,94	15,65 [16,59 - 15,51]
ApoE $^{-/-}$	8	5	10,09 ± 1,01	10,07 [10,24 - 10,03]
	16	5	12,06 ± 1,23	11,61 [13,10 - 11,23]
	20	5	13,78 ± 1,28	13,90 [14,61 - 13,72]
	24	5	14,83 ± 2,01	13,68 [15,61 - 13,45]
	28	5	13,76 ± 1,54	12,86 [15,08 - 12,65]

Values are represented in micrometers and shown as means ± standard deviation (SD) and medians with IQR (Interquartile range) [75% - 25%]. Tb.Sp – Trabecular Separation.

In the representation of these values it is possible to see the increase in trabeculae separation along the time (Figure 20). Although after the 24 weeks' time-point the groups inverted their position, and B6 group appear to gain a rapid separation rate, although this was not significant when comparing between groups.

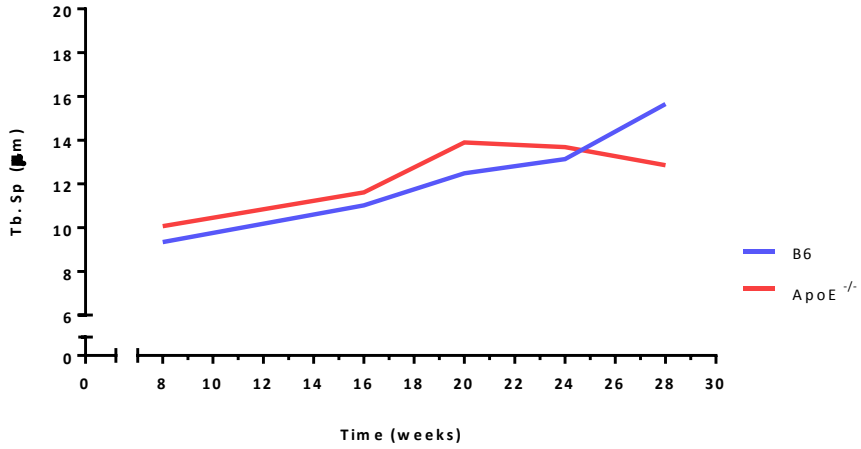

Figure 20 - Representation of trabecular separation for B6 and ApoE $^{-/-}$ groups along the experimental time.

The values used are medians, in micrometers. Tb.Sp – Trabecular Separation.

Comparing the values obtained at each time-point for each group (Figures 21A and 21B) it is possible to see that trabecular separation had increased over time in both groups, especially when compared with the first time-point (8 weeks) where the increase in separation was statistical significant.

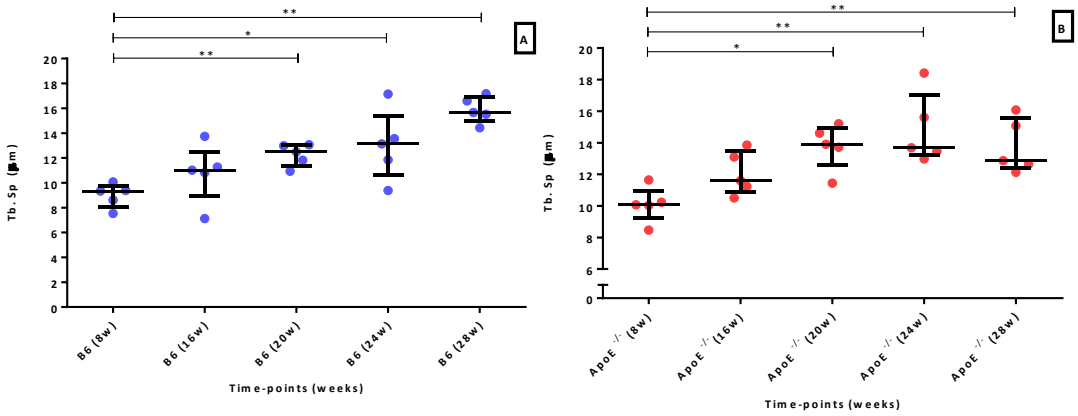

Figure 21 – Trabecular separation for B6 (A) and ApoE $^{-/-}$ (B) groups at each time-point.

The results are represented in micrometers and shown as dot plots displaying medians and IQR (interquartile range) [75-25%] in each time-point. (A) B6 group with * representing the statistical significant increase in trabecular separation at 8 and 24 weeks old (*p*-value = 0.0159); ** representing the statistical significant increase in trabecular separation between 8w and 20 w, and 8w *vs* 28 w (*p*-value = 0.0079). (B) ApoE $^{-/-}$ group with * representing the statistical significant increase in trabecular separation at 8 and 20 weeks old (*p*-value = 0.0159); ** represents the statistical significant increase in trabecular separation between 8 weeks with 24 and 28 weeks old (*p*-value = 0.0079, in both). Tb.Sp – Trabecular Separation.

Gene expression

In order to evaluate the effect of inflammation on bones and arteries, and the relation between cardiovascular and bone remodeling systems, the relative gene expression of proteins associated with both systems were evaluated in two types of mice tissues, the whole aorta and the femoral bone.

Inflammation related genes

In Table 10 are shown the mRNA expression levels of IL-1β gene in both tissues for the two experimental groups. Comparing the results, one thing that strikes the most is the discrepancy of values obtained in aorta and in bone.

Table 10 - IL-1β relative gene expression levels, in aorta and bone, for B6 and ApoE $^{-/-}$ groups along the time of experiment.

Groups	Time-points (age in weeks)	IL-1β					
		Aorta			Bone		
		number of animals (N)	mean with SD	median with IQR	number of animals (N)	mean with SD	median with IQR
C57BL/6 (B6)	8	4	9,69 ± 10,65	4,75 [11,93 - 2,52]	5	0,62 ± 0,33	0,49 [0,93 - 0,38]
	16	4	3,28 ± 0,97	3,21 [3,85 - 2,64]	5	0,72 ± 0,43	0,72 [0,72 - 0,44]
	20	4	2,81 ± 1,83	2,36 [3,82 - 1,35]	4	0,61 ± 0,33	0,54 [0,77 - 0,38]
	24	4	3,58 ± 0,61	3,60 [4,09 - 3,10]	5	0,91 ± 0,67	0,81 [1,52 - 0,22]
	28	5	28,25 ± 25,83	15,36 [55,22 - 4,74]	5	0,38 ± 0,22	0,46 [0,51 - 0,21]
ApoE $^{-/-}$	8	5	23,24 ± 29,41	9,68 [27,48 - 0,34]	5	0,53 ± 0,49	0,20 [0,89 - 0,15]
	16	4	28,33 ± 21,23	22,74 [35,94 - 15,13]	5	0,68 ± 0,42	0,56 [0,80 - 0,40]
	20	4	4,81 ± 5,06	2,64 [6,49 - 0,96]	5	0,68 ± 0,20	0,66 [0,67 - 0,62]
	24	4	1,22 ± 0,95	1,10 [1,94 - 0,38]	5	0,87 ± 0,86	0,22 [1,87 - 0,16]
	28	4	1,98 ± 1,28	1,27 [2,07 - 1,19]	5	0,92 ± 0,46	0,77 [0,97 - 0,63]

Data were normalized to 18S rRNA and are represented as means ± standard deviation (SD) and medians with IQR (Interquartile range) [75% - 25%]. IL- Interleukin.

In Figure 22 are represented the results of IL-1β relative expression levels in aortas throughout time, and we can see that the ApoE $^{-/-}$ group had a peak of expression at 16 weeks in the aorta tissue (*p*-value = 0.0286 comparing to B6 mice), although after week 20 presented a slight decrease. On contrary, for the B6 group the IL-1 β expression levels were lower in early evaluations and started to increase significantly after 20 weeks of age, (*p*-value = 0.0286 comparing to B6 at 24 weeks, and *p*-value = 0.0317 comparing to B6 at 28 weeks) presenting an inverted tendency between them.

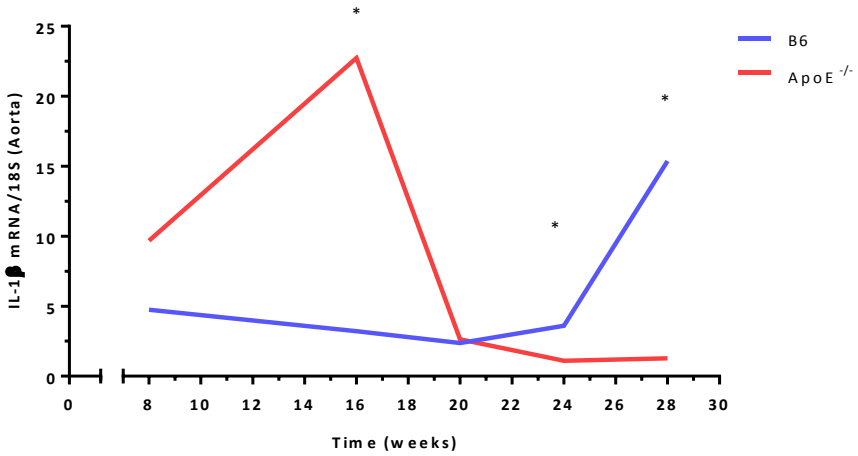

Figure 22 - IL-1β mRNA expression levels along the experimental time for B6 and ApoE $^{-/-}$ groups, in aorta tissue.

The values used were corrected to 18S rRNA and are presented as medians. * represents the statistical differences of increased mRNA expression levels of IL-1β in ApoE $^{-/-}$ group compared with B6 at 16 weeks (p-value = 0.0286), representing as well the difference of mRNA levels that are higher in B6 compared to ApoE $^{-/-}$ group at 24 weeks (p-value = 0.0286) and at 28 weeks (p-value = 0.0317). IL- Interleukin.

When we look more closely to the results obtained at each time-point, in a graphic representation for each group it is possible to see that at 8 and 16 weeks in the ApoE $^{-/-}$ group (Figure 23B) and 28 weeks in B6 group (Figure 23A) the results obtained are very dispersed, and no statistically significant differences were found along time in each group.

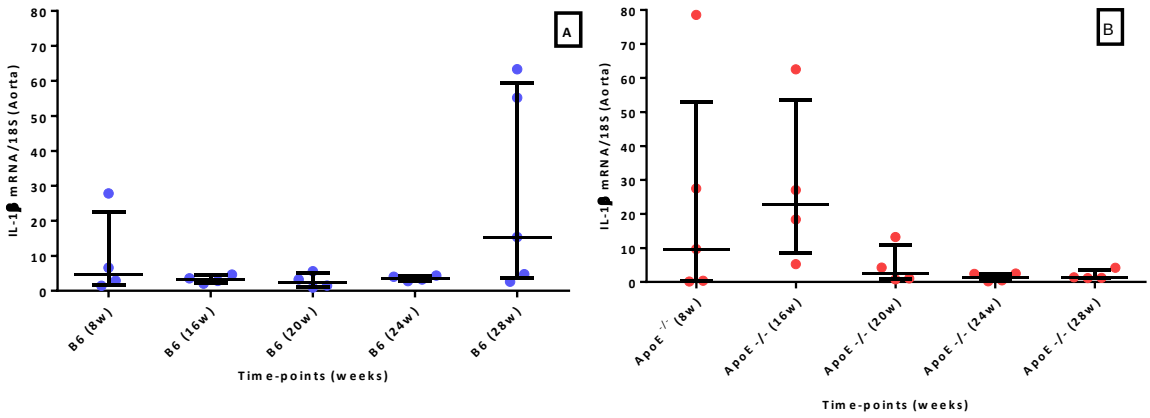

Figure 23 - IL-1β mRNA expression levels for B6 (A) and ApoE $^{-/-}$ (B) groups, in aorta tissue, at each time-point.

The results represented by relative expression levels were corrected to 18S rRNA and are shown as dot plots displaying medians and IQR (interquartile range) [75-25%] in each time-point. (A) mRNA levels of IL-1β in aorta at each time-point for B6 group. (B) Relative mRNA levels of IL-1β in aorta at each time-point for ApoE $^{-/-}$ group. IL- Interleukin.

In bone tissue (Figure 24), the IL-1 β mRNA expression presented a different trend comparing with aorta (Figure 22), i.e. along time it seems that this cytokine is more expressed in B6 mice rather than in ApoE $^{-/-}$, despite the inversions at 20 weeks and 28 weeks.

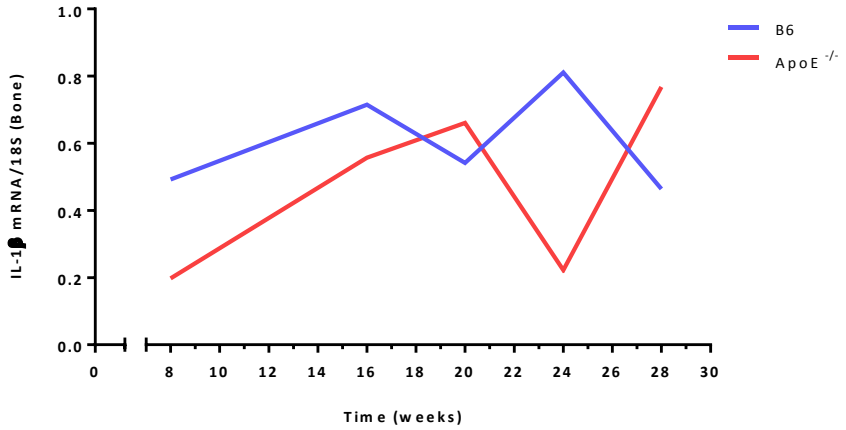

Figure 24 - IL-1β mRNA expression levels along the experimental time for B6 and ApoE $^{-/-}$ groups, in bone tissue.

The values were corrected to 18S rRNA and was used the medians. IL- Interleukin.

We found no significant differences between B6 and ApoE $^{-/-}$ groups for each time-point (Figure 24), neither were found differences between times-points for any of the groups (Figure 25).

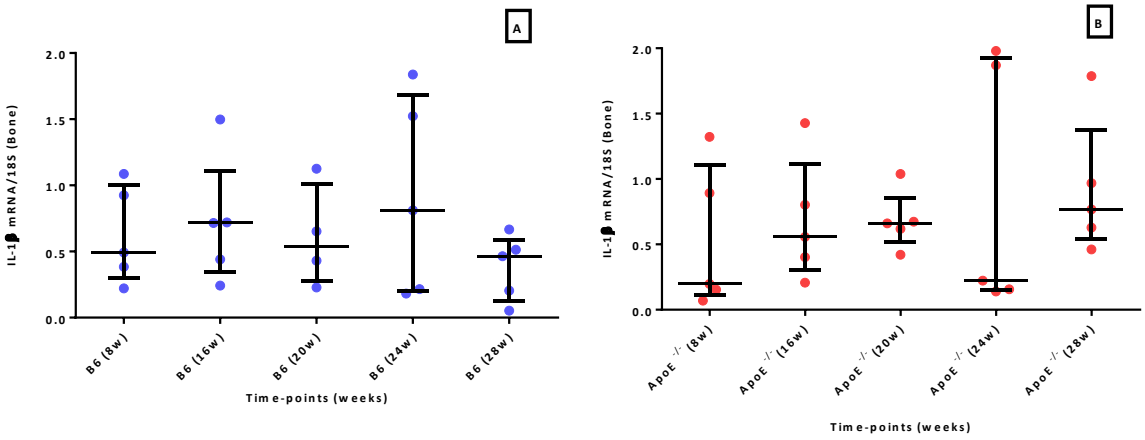

Figure 25 - IL-1β mRNA expression levels for B6 (A) and ApoE $^{-/-}$ (B) groups, in bone tissue, at each time-point.

The results are represented by expression levels corrected to 18S rRNA and are shown as dot plots displaying median and IQR (interquartile range) [75-25%] in each time-point. (A) Relative mRNA levels of IL-1β in bone at each time-point for B6 group. (B) Relative mRNA levels of IL-1β in bone at each time-point for ApoE $^{-/-}$ group. IL- Interleukin.

In Table 11 are displayed the results in aorta and bone tissues for IL-6 mRNA expression levels of the experimental groups.

Table 11 - IL-6 mRNA expression levels in aorta and bone tissues of B6 and ApoE $^{-/-}$ group at each time-point.

Groups	Time-points (age in weeks)	IL-6					
		Aorta			Bone		
		number of animals (N)	mean with SD	median with IQR	number of animals (N)	mean with SD	median with IQR
C57BL/6 (B6)	8	3	2,47 ± 1,37	2,95 [3,40 - 1,78]	5	0,40 ± 0,28	0,33 [0,45 - 0,18]
	16	5	6,52 ± 3,06	5,95 [9,57 - 3,89]	5	5,39 ± 5,39	2,69 [10,13 - 0,48]
	20	5	4,87 ± 1,98	3,96 [5,44 - 3,92]	5	0,46 ± 0,24	0,52 [0,63 - 0,33]
	24	4	4,18 ± 1,18	4,50 [4,76 - 3,91]	5	0,92 ± 0,54	0,92 [0,98 - 0,25]
	28	5	6,58 ± 4,10	8,23 [10,41 - 2,82]	5	1,64 ± 1,47	1,39 [1,45 - 0,11]
ApoE $^{-/-}$	8	5	11,05 ± 10,54	8,08 [14,49 - 1,46]	4	0,15 ± 0,07	0,15 [0,18 - 0,12]
	16	4	8,58 ± 4,81	6,93 [10,53 - 4,99]	5	1,00 ± 1,25	0,24 [1,23 - 0,10]
	20	5	2,52 ± 1,77	1,72 [2,85 - 1,58]	5	0,81 ± 0,60	0,55 [0,99 - 0,53]
	24	5	5,35 ± 3,35	4,19 [7,10 - 3,05]	4	0,33 ± 0,22	0,33 [0,42 - 0,24]
	28	5	2,69 ± 1,68	2,14 [3,47 - 1,51]	5	1,65 ± 1,09	1,11 [1,78 - 0,98]

Data were normalized to 18S rRNA and are represented as means ± standard deviation (SD) and medians with IQR (Interquartile range) [75% - 25%]. IL- Interleukin.

The graphical representation of relative mRNA IL-6 expression shows no significant differences between groups (Figure 26), but it was observable that for B6 group the levels of this cytokine seemed to increase throughout time (with a slight decrease at 20 weeks, although not significant; Figure 27A), rather ApoE $^{-/-}$ group that presented higher expression levels in the first evaluations, and then decreased over time, especially after 16 weeks, although it was not significant (see Figure 27B).

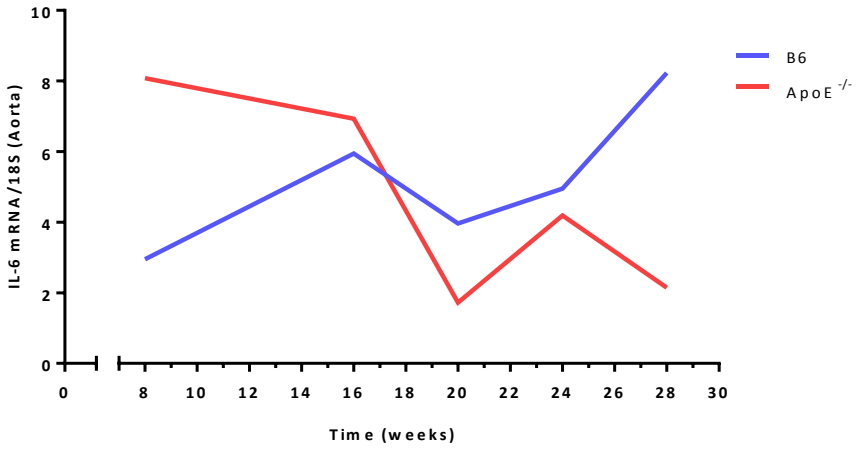

Figure 26 - Representation of IL-6 mRNA expression levels in aorta tissue, for B6 and ApoE $^{-/-}$ groups along experimental time.

The values used were corrected to 18S rRNA and are represented by medians. IL- Interleukin.

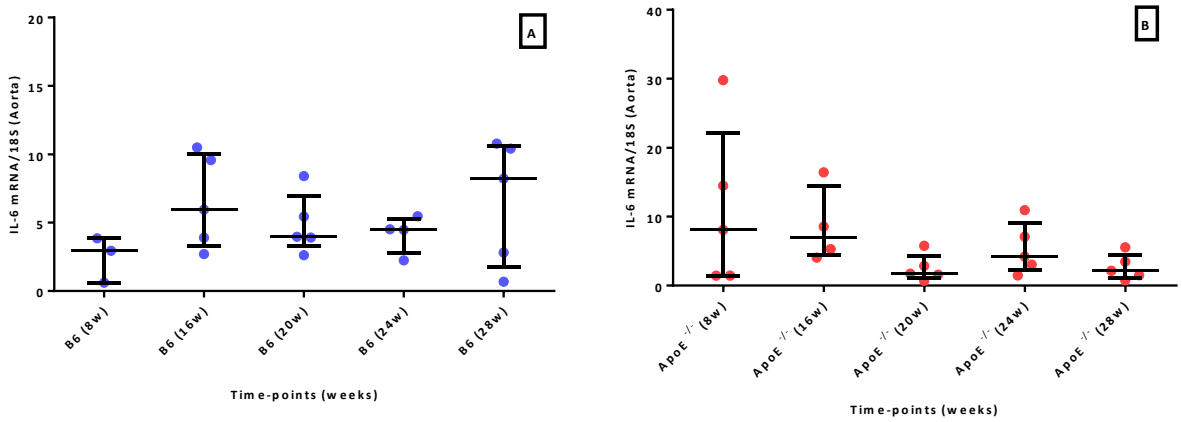

Figure 27 - IL-6 mRNA expression levels, in aorta tissue, for B6 (A) and ApoE $^{-/-}$ (B) groups at each time-point.

The values were corrected to 18S rRNA and are shown as dot plots displaying medians and IQR (interquartile range) [75-25%] in each time-point. (A) Relative mRNA IL-6 levels in aorta at each time-point for B6 group. (B) Relative mRNA IL-6 levels in aorta at each time-point for ApoE $^{-/-}$ group, with values slightly higher at 8 and 16 weeks (not significant). IL- Interleukin.

Although in aorta tissue the relative mRNA levels of IL-6 seemed somewhat variable, in bone tissue the levels of IL-6 seemed to present a more similar tendency in both groups, with increasing levels along time (Figure 28).

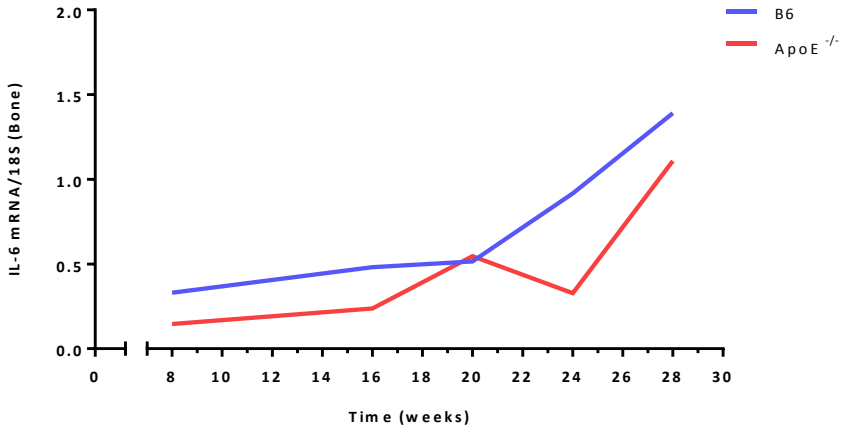

Figure 28 - Representation of IL-6 mRNA expression levels, in bone tissue, for B6 and ApoE $^{-/-}$ groups along experimental time.

The values used were corrected to 18S rRNA and represented by medians. IL- Interleukin.

Despite no significant differences were found between both groups, when we look at the distribution for each group, B6 had an increase in IL-6 mRNA expression levels at 16 weeks, but not significant (probably due to the values dispersion; Figure 29A).

On the other hand ApoE $^{-/-}$, that presented lower expression levels of IL-6 in bone throughout time compared with B6 group (Figure 28), have increased expression levels in the later time-point comparing to the first evaluation at 8 weeks (*p*-value = 0.0159 for 28 weeks) and when compared with 24 weeks (*p*-value = 0.0159) (Figure 29B).

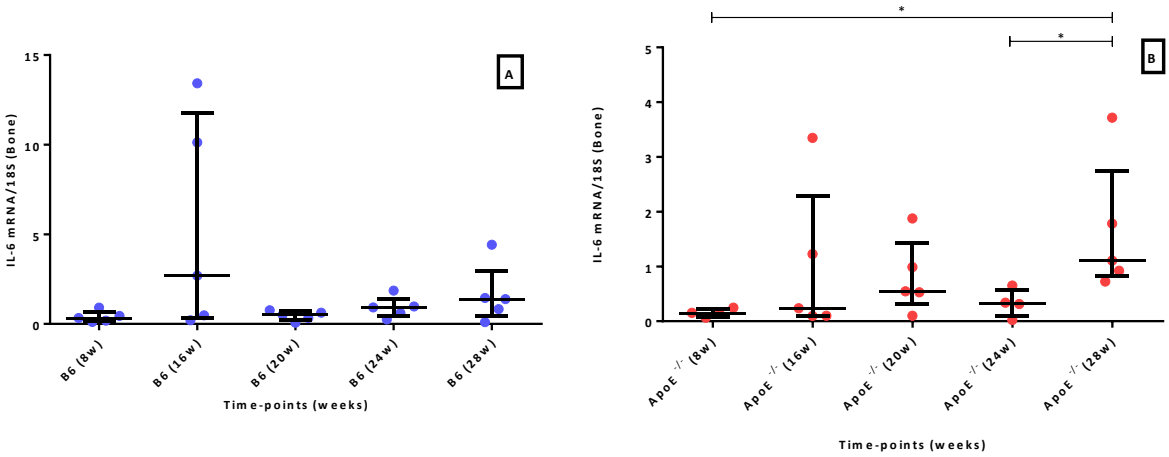

Figure 29 - IL-6 mRNA expression in bone tissue, for B6 and ApoE $^{-/-}$ groups at each time-point.

The values were corrected to 18S rRNA and are shown as dot plots displaying medians and IQR (interquartile range) [75-25%] in each time-point. (A) mRNA expression levels of IL-6 in bone at each time-point for B6 group, showing a slight increase in those levels, but not significant. (B) mRNA expression levels of IL-6 in bone at each time-point for ApoE $^{-/-}$ group showing an increase with slight variations (not significant). IL- Interleukin.

In Table 12 are shown the results of relative expression levels of IL-17A in aorta and bone, for both groups.

Table 12 - IL-17A mRNA expression levels in aorta and bone tissues of B6 and ApoE $^{-/-}$ group at each time-point.

Groups	Time-points (age in weeks)	IL-17A					
		Aorta			Bone		
		number of animals (N)	mean with SD	median with IQR	number of animals (N)	mean with SD	median with IQR
C57BL/6 (B6)	8	3	3,19 ± 0,21	3,08 [3,28 - 3,05]	5	0,62 ± 0,32	0,50 [0,65 - 0,39]
	16	5	2,67 ± 1,44	1,90 [2,72 - 1,72]	4	1,34 ± 0,43	1,45 [1,68 - 1,11]
	20	4	1,65 ± 0,87	1,32 [1,82 - 1,15]	5	1,11 ± 0,57	1,11 [1,22 - 0,80]
	24	4	2,01 ± 1,50	1,59 [2,91 - 0,69]	5	1,07 ± 0,87	0,76 [0,99 - 0,67]
	28	5	4,87 ± 2,42	5,53 [6,59 - 3,55]	5	0,77 ± 0,47	0,93 [1,06 - 0,32]
ApoE $^{-/-}$	8	5	2,96 ± 2,27	2,31 [3,32 - 1,05]	5	0,56 ± 0,24	0,55 [0,56 - 0,38]
	16	4	3,39 ± 3,13	2,21 [4,13 - 1,47]	5	0,42 ± 0,17	0,39 [0,41 - 0,37]
	20	3	1,95 ± 0,63	1,66 [2,24 - 1,51]	4	0,55 ± 0,07	0,56 [0,62 - 0,49]
	24	5	2,78 ± 2,14	2,18 [2,36 - 1,39]	5	1,70 ± 1,88	0,41 [2,84 - 0,19]
	28	5	1,97 ± 0,75	2,26 [2,32 - 1,48]	4	0,64 ± 0,15	0,60 [0,73 - 0,51]

Data were normalized to 18S rRNA and are represented as mean ± standard deviation (SD) and median with IQR (Interquartile range) [75% - 25%]. IL- Interleukin.

The IL-17A mRNA expression levels in aorta was fairly constant in ApoE $^{-/-}$ group, and although the B6 group shown a minor decrease followed by a striking increase at 24 weeks, no statistical significance was found neither between groups or throughout time (Figures 30 and 31).

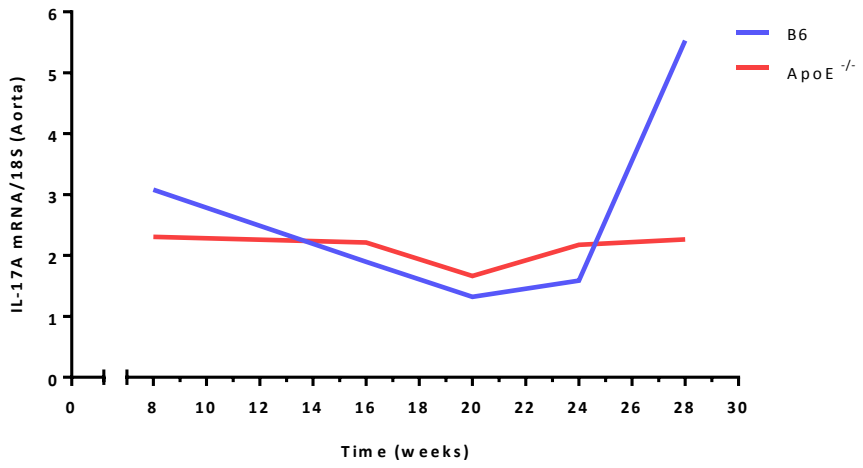

Figure 30 – Representation of IL-17A mRNA expression levels in aorta tissue, for B6 and ApoE $^{-/-}$ groups along experimental time.

The values used were corrected to 18S rRNA and represented by medians. IL- Interleukin.

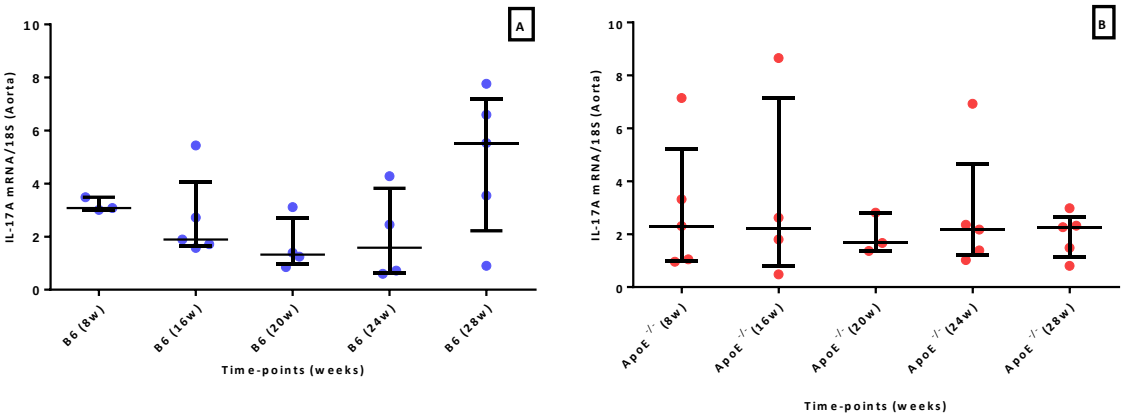

Figure 31 – IL-17A mRNA expression in aorta tissue, for B6 and ApoE $^{-/-}$ groups at each time-point.

The values were corrected to 18S rRNA and are shown as dot plots displaying medians and IQR (interquartile range) [75-25%] in each time-point. (A) Relative mRNA levels of IL-17A in aorta at each time-point for B6 group, showing an increase in IL-17A levels at 28 weeks, but not significant. (B) Relative mRNA levels of IL-17A in aorta at each time-point for ApoE $^{-/-}$ group showing a relatively constant IL-17A levels. IL- Interleukin.

In bone, the relative expression of IL-17A also seemed to be relatively constant along time for both groups, except at 16 weeks when the levels increased significantly in B6 group, comparing with ApoE $^{-/-}$ group (*p*-value = 0.0317) (Figure 32) and was also significantly increased compared with the levels obtained at baseline (p value =0.0317) (Figure 33A).

Regarding ApoE $^{-/-}$ group, the levels of IL-17A not only maintained relatively constant but were also lower when compared with B6 group (Figures 32 and 33B).

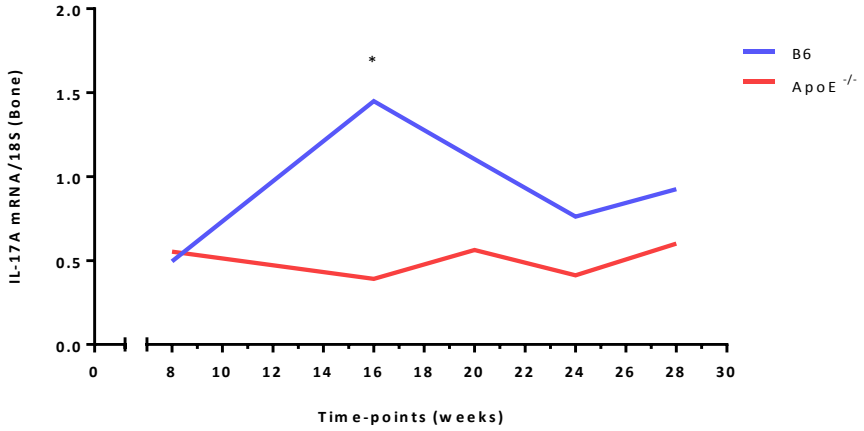

Figure 32 - Representation of IL-17A in bone tissue for B6 and ApoE $^{-/-}$ groups along experimental time.

The values were corrected to 18S rRNA and are represented by medians.

* represents the statistical significant differences between both groups, with the mRNA levels of IL-17A higher in B6 compared with ApoE $^{-/-}$ group, at 16 weeks of age (*p*-value = 0.0317). IL- Interleukin.

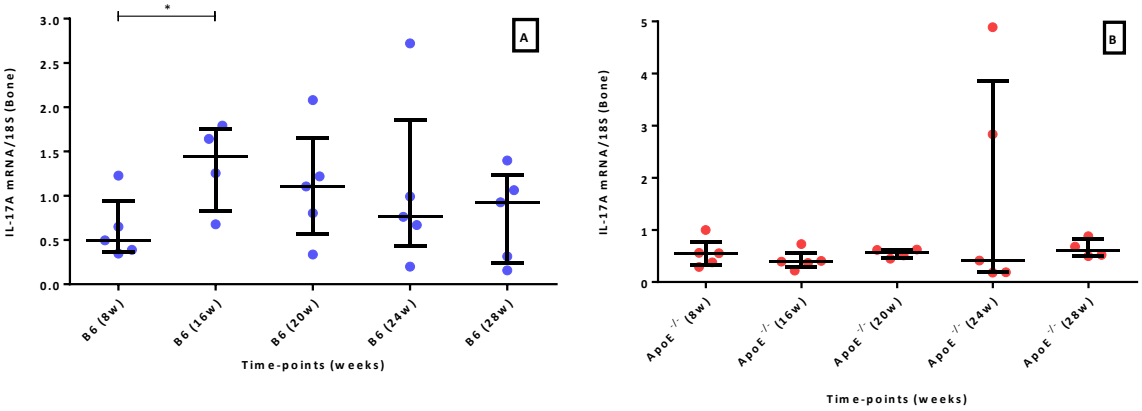

Figure 33 - IL-17A mRNA expression levels in bone tissue for B6 and ApoE $^{-/-}$ groups along experimental time.

The results were corrected to 18S rRNA and are shown as dot plots displaying medians and IQR (interquartile range) [75-25%] in each time-point. (A) Relative mRNA levels of IL-17A in bone at each time-point for B6 group, showing an increase in those levels at 16 weeks, with a * *p*-value = 0.0317. (B) Relative mRNA levels of IL-17A in bone at each time-point for ApoE $^{-/-}$ group showing a relatively constant levels of IL-17A. IL- Interleukin.

The last pro-inflammatory cytokine evaluated was the TNF and the results are stated in Table 13.

Table 13 - TNF mRNA expression levels in aorta and bone tissues for B6 and ApoE $^{-/-}$ groups at each time-point.

Groups	Time-points (age in weeks)	TNF					
		Aorta			Bone		
		number of animals (N)	mean with SD	median with IQR	number of animals (N)	mean with SD	median with IQR
C57BL/6 (B6)	8	4	8,33 ± 6,15	8,83 [13,70 - 3,46]	5	0,30 ± 0,18	0,23 [0,42 - 0,22]
	16	5	19,84 ± 8,09	19,27 [24,18 - 14,63]	4	0,43 ± 0,18	0,42 [0,57 - 0,28]
	20	4	25,26 ± 13,00	23,91 [36,20 - 12,97]	5	0,16 ± 0,10	0,20 [0,22 - 0,05]
	24	3	0,76 ± 0,43	0,53 [0,95 - 0,46	5	0,38 ± 0,35	0,25 [0,37 - 0,22]
	28	5	18,62 ± 21,13	9,97 [21,73 - 2,92]	5	0,50 ± 0,38	0,37 [0,88 - 0,11]
ApoE $^{-/-}$	8	3	0,12 ± 0,08	0,07 [0,15 - 0,06]	4	0,19 ± 0,07	0,15 [0,20 - 0,14]
	16	4	8,66 ± 9,26	5,35 [12,04 - 1,97]	5	0,33 ± 0,25	0,15 [0,55 - 0,15]
	20	5	3,63 ± 3,99	1,03 [4,97 - 0,85]	5	0,27 ± 0,15	0,28 [0,29 - 0,20]
	24	3	2,46 ± 2,45	0,88 [3,40 - 0,73]	4	0,62 ± 0,41	0,66 [1,01 - 0,27]
	28	5	10,10 ± 13,84	0,76 [13,38 - 0,40]	5	0,30 ± 0,19	0,31 [0,46 - 0,13]

Data were normalized to 18S rRNA and are represented as means ± standard deviation (SD) and medians with IQR (Interquartile range) [75% - 25%]. TNF – Tumor Necrosis Factor.

In the graphical representation of both groups (Figure 33) we can see that ApoE $^{-/-}$ also presents lower levels of this inflammatory cytokine compared with B6 group in aorta tissue, although it was only statistically different at 20 weeks of age (*p*-value = 0.0159).

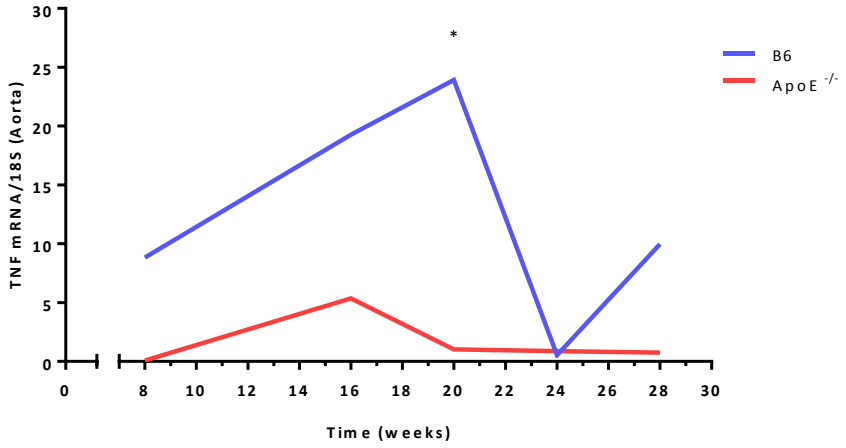

Figure 34 - Representation of TNF mRNA expression levels in aorta tissue for B6 and ApoE $^{-/-}$ groups along experimental time.

The values were corrected to 18S rRNA and are represented by medians.

* represents the statistical significant differences between both groups, with the levels of TNF higher in B6 compared with ApoE $^{-/-}$ group, at 20 weeks of age (*p*-value = 0.0159). TNF – Tumor Necrosis Factor.

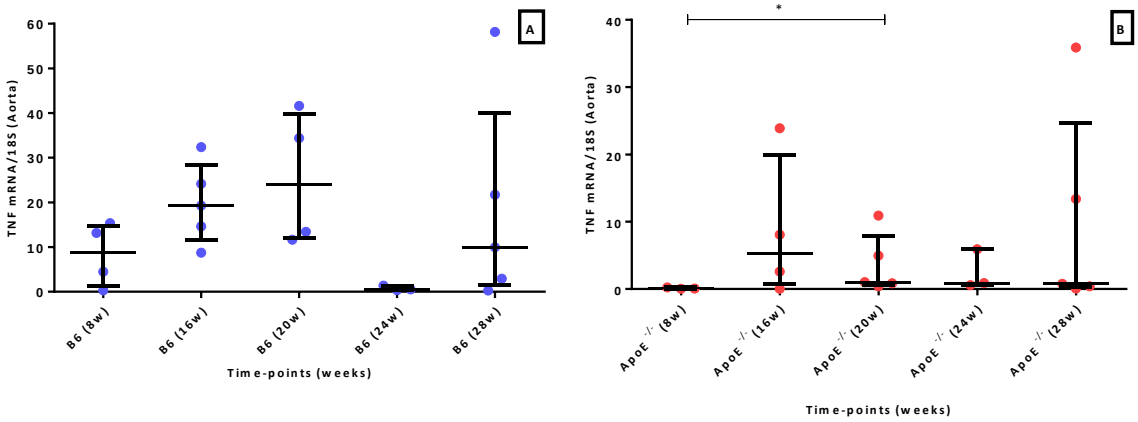

Figure 35 - TNF mRNA expression levels in aorta tissue for B6 (A) and ApoE $^{-/-}$ (B) groups at each time-point.

The results were corrected to 18S rRNA and are shown as dot plots displaying medians and IQR (interquartile range) [75-25%] in each time-point. (A) Relative mRNA levels of TNF in aorta at each time-point for B6 group, showing a slight increase until 20 weeks, followed by a drop although not significant. (B) Relative mRNA levels of TNF in aorta at each time-point for ApoE $^{-/-}$ group showing a relatively constant levels of TNF relative expression levels, although at 20 weeks the increase was significant compared at baseline (*p-value = 0.0357). TNF – Tumor Necrosis Factor.

Comparing the results in both tissues, what strike the most was the difference in relative expression levels between B6 and ApoE $^{-/-}$ groups, in which the last group presented lowers levels of TNF in aorta along time, but in bone, although it started with lower levels, it started to increase and reach higher expression levels compared to B6 mice, reaching a peak at 24 weeks, although not significant (Figure 36).

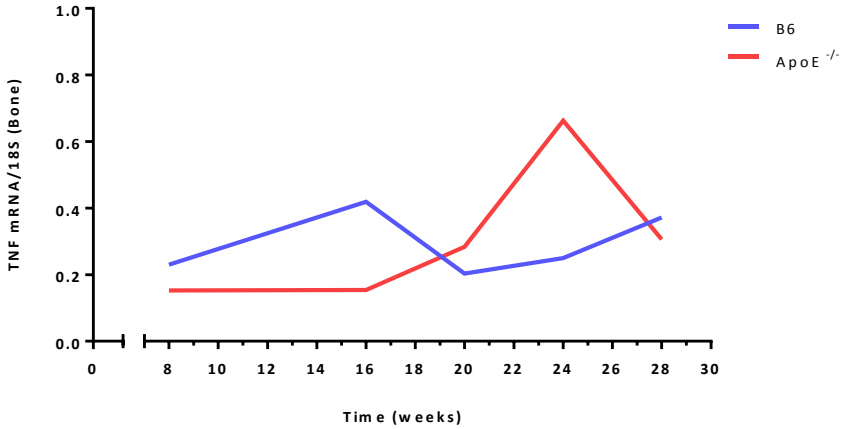

Figure 36 - Representation of TNF mRNA expression levels in bone tissue for B6 and ApoE $^{-/-}$ groups along experimental time.

The values used were corrected to 18S rRNA and represented by the median for each time-point. ApoE $^{-/-}$ group shown an increase in TNF levels throughout time until 24 weeks, time when those levels drop (not significantly). The B6 group had higher levels in the beginning than the ApoE $^{-/-}$ group, although they suffered a reduction at 16 weeks, increasing again after 24 weeks. TNF – Tumor Necrosis Factor.

Despite the changes observed in TNF expression in bones throughout evaluations, no statistical differences were found between each time-point (Figure 37).

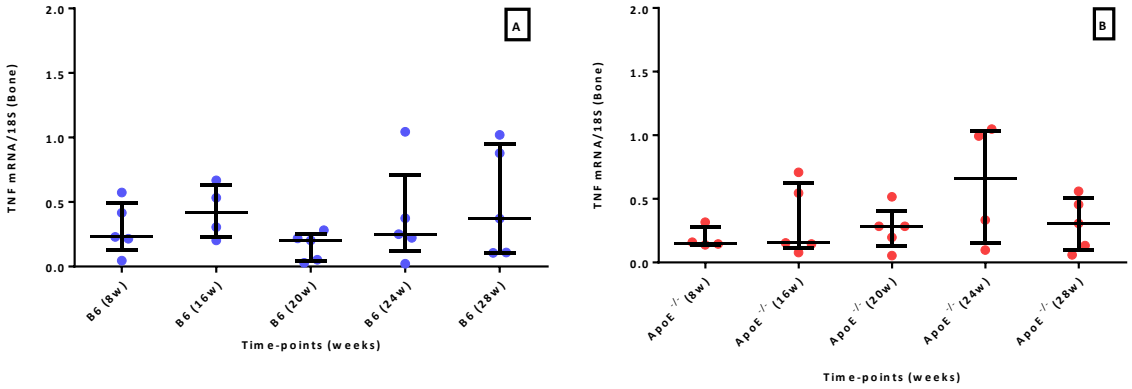

Figure 37 - TNF mRNA expression levels in bone tissue for B6 (A) and ApoE $^{-/-}$ (B) groups at each time-point.

The results are represented by expression levels corrected to 18S rRNA and are shown as dot plots displaying median and IQR (interquartile range) [75-25%] in each time-point. (A) Displays the mRNA levels of TNF in bone tissue at each time-point for B6 group, showing a slight decrease at 20 weeks but not significant. (B) Represents the ApoE $^{-/-}$ group showing a slight increase in TNF expression levels, although at 24 weeks the increase is much higher although not significant. TNF – Tumor Necrosis Factor.

Bone remodeling related genes

In order to evaluate the possible bone alterations in a mouse model affected by a cardiovascular disease, in this case atherosclerosis, we looked at the major genes associated with the bone remodeling process, RANKL and OPG, which are the key regulators of bone remodeling. We evaluated their expression in aortas and bones and alterations in their ratio (RANKL/OPG).

In Table 14 and Figure 38 are reported the results of RANKL mRNA expression levels and the variation over time comparing the two groups.

Table 14 - RANKL mRNA expression levels in aorta and bone tissues for B6 and ApoE $^{-/-}$ group at each time-point.

Groups	Time-points (age in weeks)	RANKL					
		Aorta			Bone		
		number of animals (N)	mean with SD	median with IQR	number of animals (N)	mean with SD	median with IQR
C57BL/6 (B6)	8	3	5,25 ± 1,02	4,97 [5,79 - 4,56]	4	0,28 ± 0,05	0,27 [0,30 - 0,25]
	16	5	2,85 ± 1,41	2,30 [3,13 - 2,17]	4	0,94 ± 0,22	0,89 [1,01 - 0,82]
	20	4	2,49 ± 0,83	2,37 [3,12 - 1,74]	5	0,60 ± 0,35	0,40 [0,89 - 0,37]
	24	5	2,74 ± 0,73	3,08 [3,12 - 1,96]	5	0,51 ± 0,41	0,37 [0,62 - 0,21]
	28	5	3,31 ± 1,33	2,99 [4,07 - 2,84]	5	0,82 ± 0,75	0,39 [1,16 - 0,37]
ApoE $^{-/-}$	8	4	4,36 ± 0,65	4,42 [4,78 - 4,00]	5	1,00 ± 0,87	0,32 [1,91 - 0,30]
	16	4	5,25 ± 1,25	5,32 [6,18 - 4,38]	5	0,36 ± 0,10	0,39 [0,44 - 0,25]
	20	3	1,12 ± 0,07	1,15 [1,17 - 1,09]	5	0,55 ± 0,39	0,46 [0,51 - 0,37]
	24	4	1,26 ± 0,69	1,24 [1,51 - 0,99]	4	0,24 ± 0,19	0,15 [0,29 - 0,10]
	28	5	1,77 ± 1,01	1,56 [1,74 - 1,08]	4	0,40 ± 0,12	0,40 [0,50 - 0,30]

Data were normalized to 18S rRNA and are represented as means ± standard deviation (SD) and medians with IQR (Interquartile range) [75% - 25%]. RANKL - Receptor Activator of Nuclear factor Kappa-B Ligand.

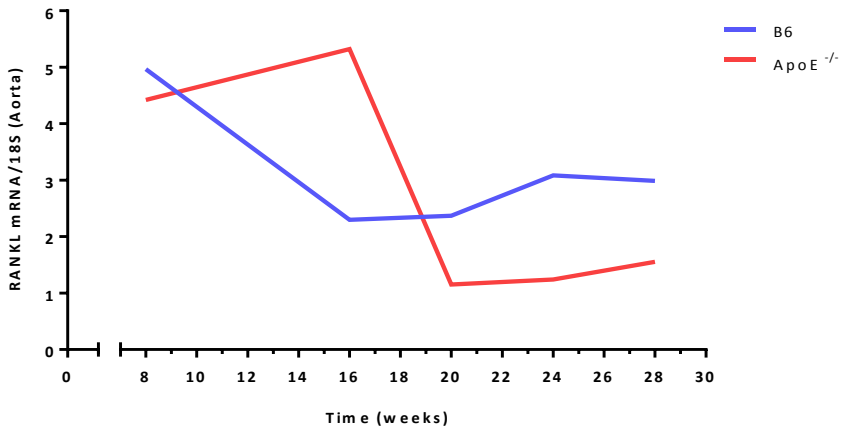

Figure 38 - Representation of RANKL mRNA expression levels in aorta tissue for B6 and ApoE $^{-/-}$ groups along experimental time.

The values were corrected to 18S rRNA and are represented by medians.

ApoE $^{-/-}$ group shown a slight increase in RANKL expression in the beginning, and after the 16 weeks' time-point the values dropped. The B6 had a reduction in levels since the beginning until the 16th weeks of age, time when the levels maintained relatively constant and higher than those for the ApoE $^{-/-}$ group. RANKL - Receptor Activator of Nuclear factor Kappa-B Ligand.

Although the expression levels in both groups did not differ significantly along experimental time (Figure 38), in ApoE $^{-/-}$ group the relative expression levels of RANKL were higher and reach a noticeable peak at 16 weeks (not significant), dropping considerably after, into levels lower than those at baseline (p-value < 0.05) (Figure 39B). B6 group on the other hand shown a more discreet variation (Figure 39A), with a reduction after 8 weeks' point but only significant at 24 weeks (p-value = 0.0357).

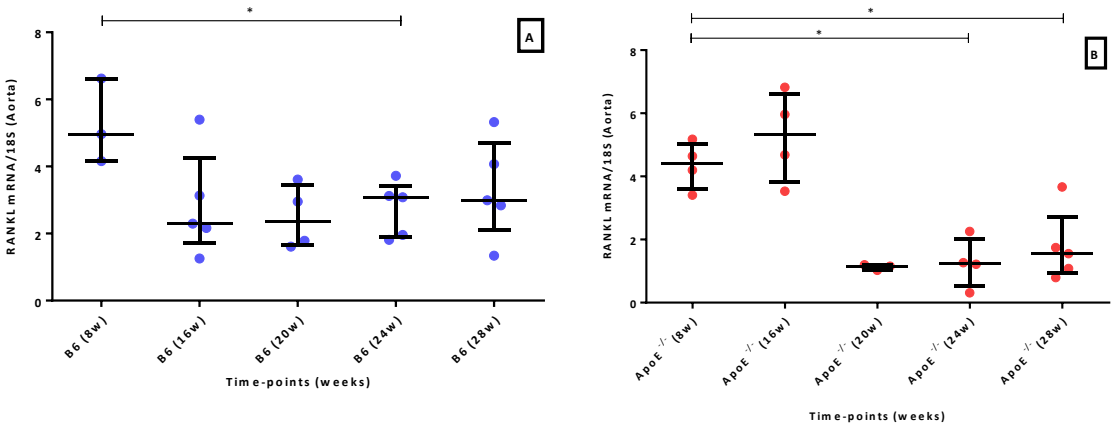

Figure 39 – RANKL mRNA expression levels in aorta tissue for B6 (A) and ApoE $^{-/-}$ (B) at each time-point.

The results were corrected to 18S rRNA and are shown as dot plots displaying medians and IQR (interquartile range) [75-25%] in each time-point. (A) Relative mRNA levels of RANKL in aorta at each time-point for B6 group, showing a decrease after 8 weeks but only significant when compared with levels at 24 weeks (*p value = 0.0357). (B) Relative mRNA levels of RANKL in aorta at each time-point for ApoE $^{-/-}$ group with * representing a statistically significant decrease in RANKL mRNA expression at 24 weeks (p-value = 0.0286) and 28 weeks (p-value = 0.0357) comparing with first point of evaluation. RANKL - Receptor Activator of Nuclear factor Kappa-B Ligand.

In bone tissue, the expression levels of RANKL had a different profile from the one in the aorta (Figure 40), i.e. in this case the ApoE $^{-/-}$ group seemed to had more constant expression levels (Figure 41B) unlike the B6 group witch presented an abruptly increase in RANKL levels at 16 weeks (p-value of 0.0286) (Figure 41A).

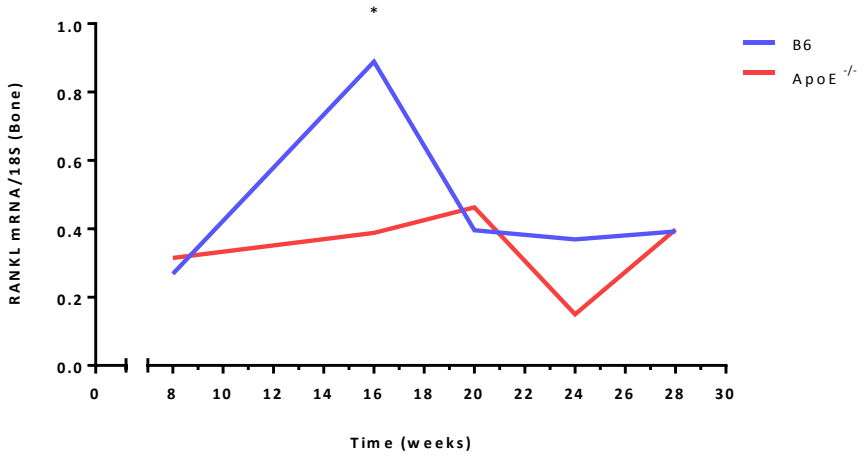

Figure 40 - Representation of RANKL mRNA expression levels in bone tissue for B6 and ApoE $^{-/-}$ groups along experimental time.

The values were corrected to 18S rRNA and represented by medians.

The B6 shows a striking increase in RANKL expression levels until 16 weeks with a significant difference compared with ApoE $^{-/-}$ group (*p-value = 0.0159) and the levels maintained relatively constant. The ApoE $^{-/-}$ group shown a minor increase in RANKL levels at baseline, and after the 20 weeks' time-point the values dropped, and increased again into levels similar to B6 group. RANKL - Receptor Activator of Nuclear factor Kappa-B Ligand.

The B6 group showned a striking increase in RANKL expression levels until 16 weeks with a significant difference compared with ApoE $^{-/-}$ group (p-value = 0.0159), and also when compared with the first evaluation for the same group (p-value = 0.0286) (Figure 41A). The ApoE $^{-/-}$ group shown a minor increase in RANKL levels at baseline, and after the 20 weeks' time-point the values dropped, although not significant (Figure 41B) and increased again into levels similar to B6 group.

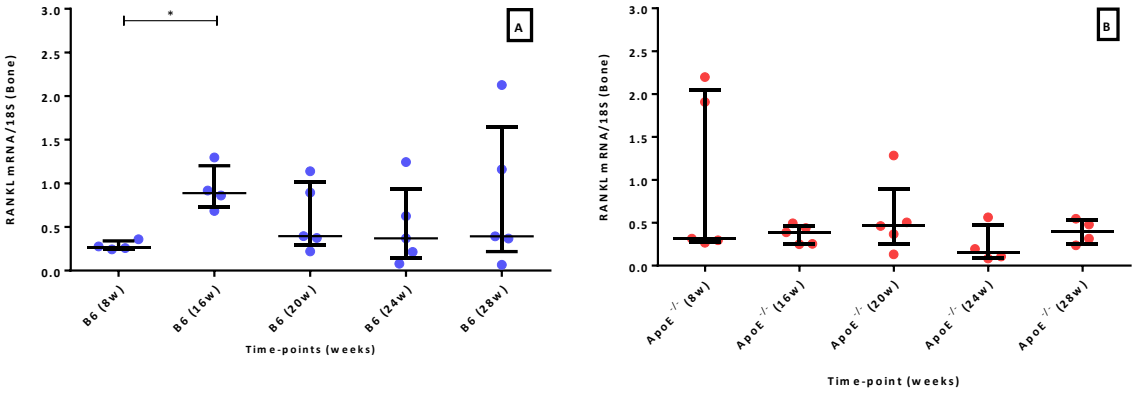

Figure 41 - RANKL mRNA expression levels in bone tissue for B6 and ApoE $^{-/-}$ groups at each time-point.

The results were corrected to 18S rRNA and are shown as dot plots displaying medians and IQR (interquartile range) [75-25%] in each time-point. (A) Relative mRNA expression levels of RANKL in bone at each time-point for B6 group, showing an increase at 16 weeks (*p value = 0.0286). (B) Relative mRNA expression levels of RANKL in bone at each time-point for ApoE $^{-/-}$ group showing relatively stable expression levels. RANKL - Receptor Activator of Nuclear factor Kappa-B Ligand.

For the relative expression of OPG, the results obtained are stated in Table 15 and Figure 42 shows the progression of OPG expression in the aorta, with no differences between groups throughout time.

Looking at each group individually (Figure 43), only ApoE $^{-/-}$ showed significant differences, when compared the levels at 16 weeks with the levels at baseline (*p*-value < 0.05) (Figure 43B).

Table 15 - OPG mRNA expression levels in aorta and bone tissues for B6 and ApoE $^{-/-}$ groups at each time-point.

Groups	Time-points (age in weeks)	OPG					
		Aorta			Bone		
		number of animals (N)	mean with SD	median with IQR	number of animals (N)	mean with SD	median with IQR
C57BL/6 (B6)	8	4	3,07 ± 1,12	3,31 [4,06 - 2,32]	4	0,37 ± 0,03	0,39 [0,39 - 0,37]
	16	5	2,28 ± 0,92	2,22 [2,74 - 1,91]	4	0,82 ± 0,27	0,71 [0,88 - 0,65
	20	5	2,67 ± 1,30	2,37 [2,78 - 2,12]	5	0,74 ± 0,45	0,87 [0,91 - 0,32]
	24	5	2,24 ± 1,25	2,05 [3,42 - 1,09]	5	0,71 ± 0,59	0,39 [0,12 - 0,33]
	28	4	2,44 ± 0,86	2,42 [3,28 - 1,59]	5	0,64 ± 0,42	0,65 [1,01 - 0,10]
ApoE $^{-/-}$	8	5	1,59 ± 0,59	1,92 [2,00 - 1,01]	5	0,34 ± 0,06	0,34 [0,39 - 0,29]
	16	4	2,66 ± 0,43	2,62 [3,03 - 2,25]	5	0,44 ± 0,15	0,43 [0,52 - 0,33]
	20	4	1,54 ± 0,76	1,46 [2,18 - 0,81]	5	0,58 ± 0,18	0,50 [0,74 - 0,35]
	24	5	1,94 ± 1,00	1,26 [2,86 - 1,19]	5	0,47 ± 0,31	0,27 [0,62 - 0,25]
	28	5	2,95 ± 1,51	2,81 [2,91 - 2,08]	5	1,16 ± 0,28	1,35 [1,36 - 0,84]

Data were normalized to 18S rRNA and are represented as means ± standard deviation (SD) and medians with IQR (Interquartile range) [75% - 25%]. OPG - Osteoprotegerin.

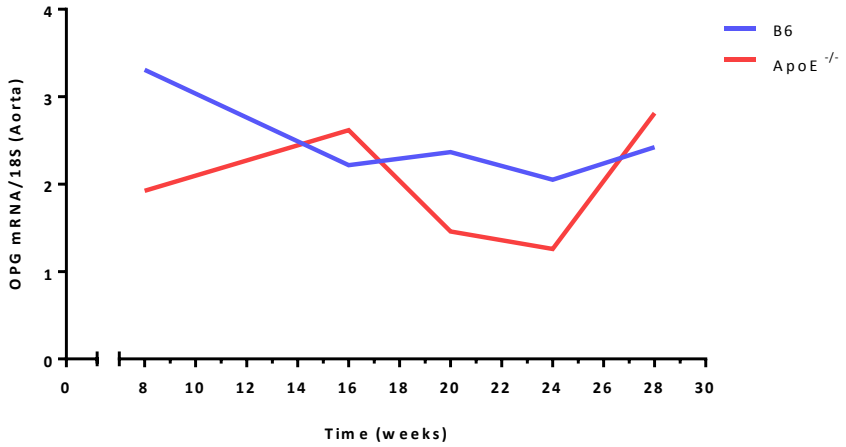

Figure 42 - Representation of OPG mRNA expression levels in aorta tissue for B6 and ApoE $^{-/-}$ groups along experimental time.

The values were corrected to 18S rRNA and represented by medians.

B6 group shows a slight decrease in mRNA expression of OPG at 16 weeks, followed by relatively constant levels. ApoE $^{-/-}$ group shows a slight increase at 16 weeks, and again at 24 weeks after a small decrease. OPG – Osteoprotegerin.

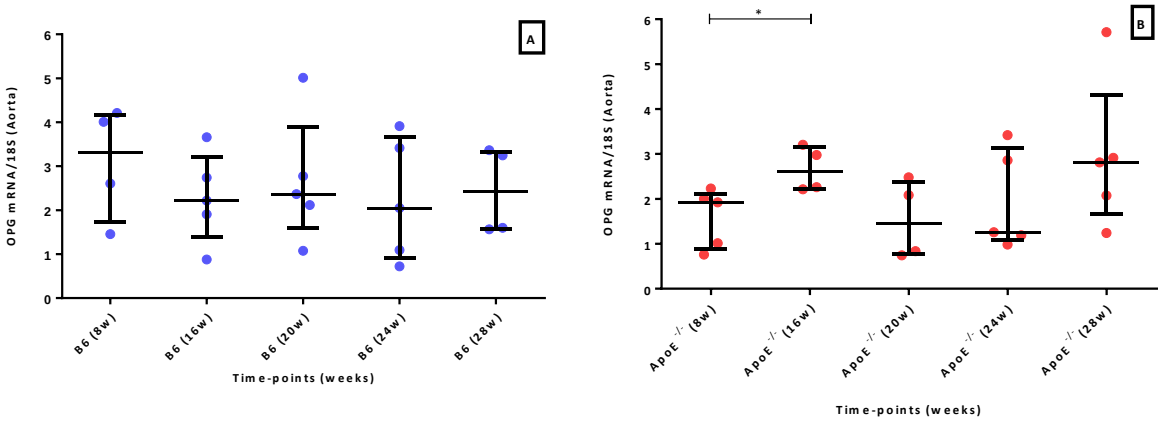

Figure 43 - OPG mRNA expression levels in aorta tissue for B6 (A) and ApoE $^{-/-}$ (B) groups at each time-point.

The results were corrected to 18S rRNA and are shown as dot plots displaying medians and IQR (interquartile range) [75-25%] in each time-point. (A) Relative mRNA expression levels of OPG in aorta at each time-point for B6 group, showing relatively constant levels throughout time. (B) Relative mRNA expression levels of OPG in aorta at each time-point for ApoE $^{-/-}$ group showing a statistical significant increase at 16 weeks (*p-value = 0.0317) compared to baseline. OPG - Osteoprotegerin.

In Figure 44 we can see the OPG expression levels progression along time in the two studied groups.

The levels increased until 20 weeks in a similar way in both groups, and increased again at 24 weeks more noticeably in ApoE $^{-/-}$ group, although not significant when compared to B6 group. Nevertheless, despite no differences were found comparing both groups, looking at each group individually, some statistical differences were found (Figure 45). Comparing with the levels at baseline, in the B6 there was an increase in OPG expression (p-value = 0.0286) (Figure 45A). In the ApoE $^{-/-}$ group we found an increase in OPG expression at 28 weeks when compared with baseline (p-value = 0.0159) and with 24 weeks evaluation (p-value = 0.0317) (Figure 45B).

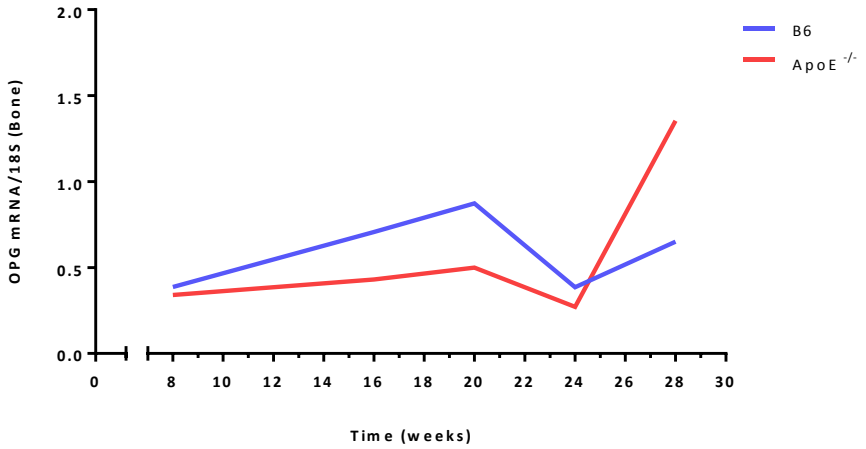

Figure 44 - Representation of OPG mRNA expression levels in bone tissue for B6 and ApoE $^{-/-}$ groups along experimental time.

The values were corrected to 18S rRNA and represented by medians.

B6 group shows an increase in mRNA expression of OPG until 20 weeks, followed by a slight reduction. ApoE $^{-/-}$ group shows a slight increase until 20 weeks, and again at 24 weeks after a small decrease. OPG – Osteoprotegerin.

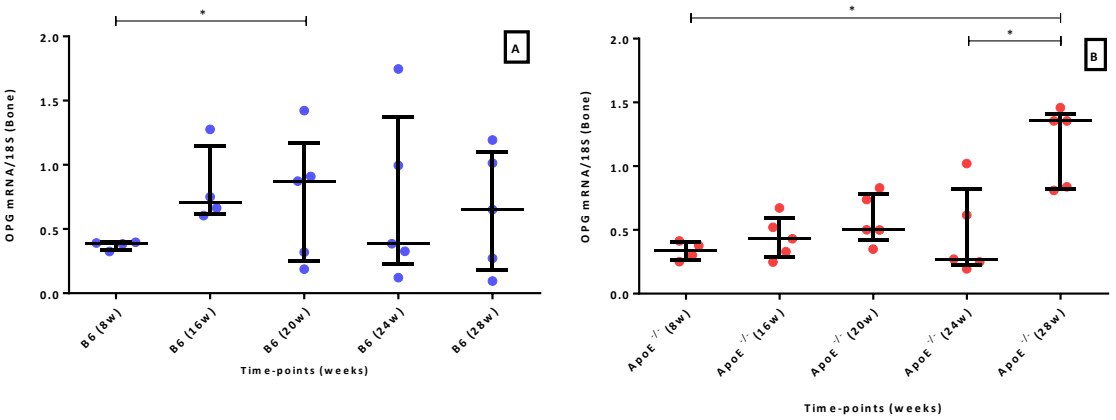

Figure 45 - OPG mRNA expression levels in bone tissue for B6 (A) and ApoE $^{-/-}$ (B) groups at each time-point.

The results were corrected to 18S rRNA and are shown as dot plots displaying medians and IQR (interquartile range) [75-25%] in each time-point. (A) Relative mRNA expression levels of OPG in bone at each time-point for B6 group with * representing a statistical significant increase in OPG levels at 20 weeks compared to the first evaluation (*p*-value = 0.0286). (B) Relative mRNA expression levels of OPG in aorta at each time-point for ApoE $^{-/-}$ group showing a statistical significant increase at 28 weeks when compared with baseline (**p*-value = 0.0317) and with 24 weeks (**p*-value = 0.0159). OPG - Osteoprotegerin.

To see if these proteins expression levels were altered, not only in vessel and bone, but also between them, we looked at their ratio (RANKL/OPG) in both tissues.

The results for the aorta are stated in Table 16 and represented in Figure 46 for both groups with no significant differences found between B6 and ApoE $^{-/-}$ groups.

Table 16 - RANKL/OPG ratio in aorta tissue for B6 and ApoE $^{-/-}$ groups at each time-point.

		RANKL/OPG ratio					
		Aorta			Bone		
Groups	Time-points (age in weeks)	number of animals (N)	mean with SD	median with IQR	number of animals (N)	mean with SD	median with IQR
C57BL/6 (B6)	8	3	2,21 ± 0,70	2,54 [2,70 - 1,89]	4	0,76 ± 0,10	0,75 [0,82 - 0,69]
	16	4	0,99 ± 0,31	0,91 [1,15 - 0,76]	4	1,19 ± 0,24	1,16 [1,35 - 0,99]
	20	5	1,31 ± 0,94	1,08 [1,83 - 0,56]	5	1,00 ± 0,58	0,80 [0,98 - 0,69]
	24	5	1,84 ± 1,32	1,79 [1,81 - 0,80]	4	0,63 ± 0,06	0,64 [0,66 - 0,61]
	28	4	1,21 ± 0,42	1,05 [1,41 - 0,85]	5	1,13 ± 0,45	1,15 [1,44 - 0,71]
ApoE $^{-/-}$	8	4	3,61 ± 1,92	2,77 [4,23 - 2,16]	3	0,98 ± 0,23	0,97 [1,12 - 0,84]
	16	4	1,95 ± 0,21	2,04 [2,09 - 1,90]	5	0,87 ± 0,20	0,84 [1,00 - 0,77]
	20	3	0,75 ± 0,34	0,57 [0,90 - 0,52]	5	0,86 ± 0,40	0,74 [1,01 - 0,63]
	24	4	0,93 ± 0,62	0,84 [1,37 - 0,40]	4	0,62 ± 0,21	0,57 [0,77 - 0,43]
	28	5	0,76 ± 0,55	0,60 [0,87 - 0,28]	4	0,35 ± 0,03	0,36 [0,38 - 0,34]

Data were normalized to 18S rRNA and are represented as means ± standard deviation (SD) and medians with IQR (Interquartile range) [75% - 25%]. RANKL - Receptor Activator of Nuclear factor Kappa-B Ligand; OPG - Osteoprotegerin.

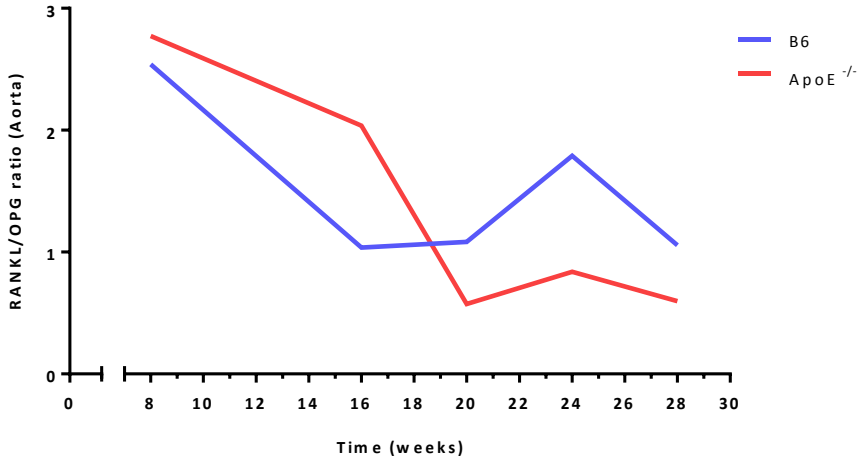

Figure 46 - Representation of the RANKL/OPG ratio in aorta tissue for B6 and ApoE $^{-/-}$ groups along experimental time.

The values were corrected to 18S rRNA and represented by medians.

B6 group shows a decrease in RANKL/ OPG ratio, only with a slight increase between 16 and 24 weeks of age and the ApoE $^{-/-}$ group decrease throughout time; No differences were found between groups. RANKL - Receptor Activator of Nuclear factor Kappa-B Ligand; OPG – Osteoprotegerin.

Individually, the ApoE $^{-/-}$ group shown a significant decrease of this ratio in the last stages of evaluation (24 and 28 weeks) compared to the first evaluation point (8 weeks) (*p*-value < 0.05 in both cases) (Figure 47B), while the B6 group, although showed a visible decrease at 16 weeks, the ratio increased at 24 weeks to levels higher when compared to ApoE $^{-/-}$, even though no statistical significances were found.

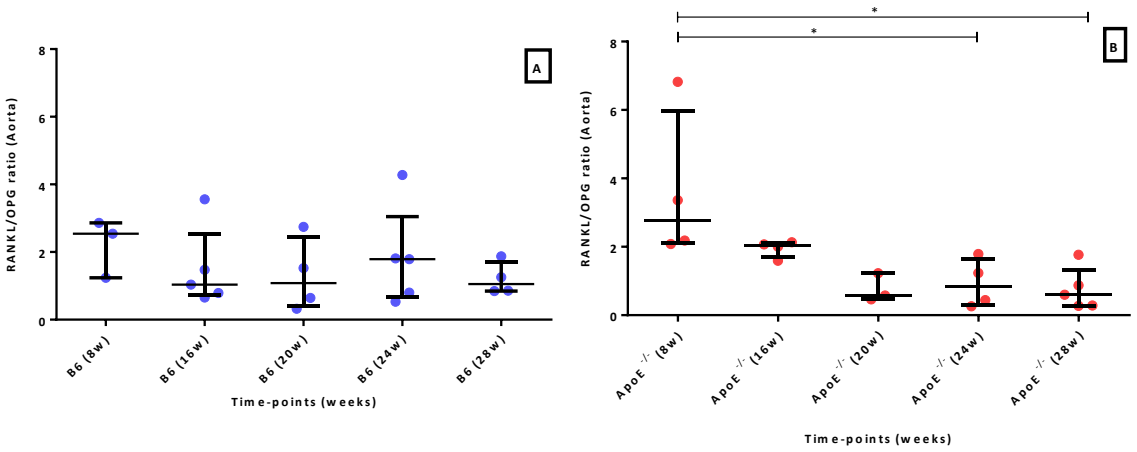

Figure 47 - RANKL/OPG mRNA expression levels in aorta tissue for B6 (A) and ApoE $^{-/-}$ (B) groups at each time-point.

The results were corrected to 18S rRNA and are shown as dot plots displaying medians and IQR (interquartile range) [75-25%] in each time-point. (A) RANKL/ OPG in aorta at each time-point for B6 group with * representing a statistical significant increase between 16 and 20 weeks (*p*-value = 0.0424). (B) RANKL/ OPG ratio in aorta at each time-point for ApoE $^{-/-}$ group showing a statistical significant decrease at 24 weeks (**p*-value = 0.0286) and 28 weeks (**p*-value = 0.0159) compared at baseline. RANKL - Receptor Activator of Nuclear factor Kappa-B Ligand; OPG - Osteoprotegerin.

In bone, the RANKL/OPG ratio, seemed to follow a similar tendency (Figure 48) compared to aorta, in both groups.

Comparing both groups, the ApoE $^{-/-}$ group seems to have presented a more continuous decrease in RANKL/OPG ratio, unlike B6 group had some increases, although the only statistical significant difference found with the ApoE $^{-/-}$ group was at 28 weeks when the groups seem to had opposite trends (the B6 group had increased the RANKL/OPG ratio unlike ApoE $^{-/-}$ that shown a decrease in this ratio) (*p*-value <0.05).

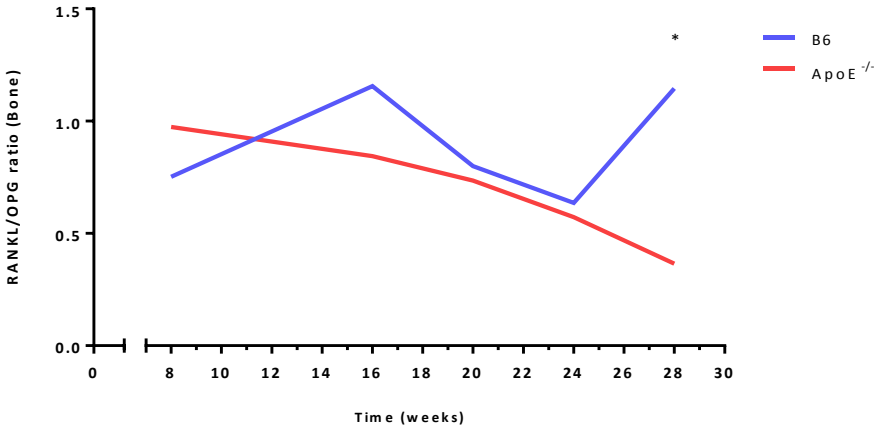

Figure 48 - Representation of RANKL/OPG ratio in bone tissue for B6 and ApoE $^{-/-}$ groups along experimental time.

The values were corrected to 18S rRNA and represented by medians.

B6 group shows increased in RANKL/ OPG ratio until 16weeks and again after 24 weeks of age (not significant). ApoE $^{-/-}$ group decrease continuously throughout time. * represents the statistical difference between B6 and ApoE $^{-/-}$ groups at 28 weeks (*p*-value = 0.0159). RANKL - Receptor Activator of Nuclear factor Kappa-B Ligand; OPG – Osteoprotegerin.

Looking more closely to each group individually, the variations in B6 group was only statistically significant regarding the increase in RANKL/OPG ratio until 16 weeks (*p*-value = 0.0286) (Figure 49A), while in ApoE $^{-/-}$ group, although it shown a more continuous trend, the decrease in the last stage (from 24 to 28 weeks) was the only statistical significance reported (*p*-value = 0.0286) (Figure 49B).

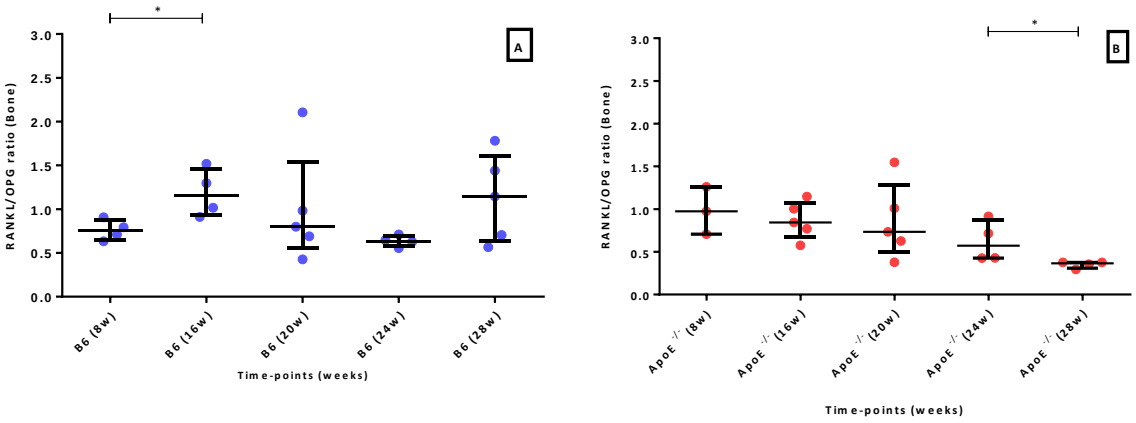

Figure 49 - RANKL/OPG mRNA expression levels in bone tissue for B6 and ApoE $^{-/-}$ groups at each time-point.

The results were corrected to 18S rRNA and are shown as dot plots displaying medians and IQR (interquartile range) [75-25%] in each time-point. (A) RANKL/ OPG in bone at each time-point for B6 group with * representing a statistical significant increase until 16 weeks (*p*-value = 0.0286). (B) RANKL/ OPG ratio in bone at each time-point for ApoE $^{-/-}$ group showing a statistical significant decrease between 24 and 28 weeks (**p*-value = 0.0286). RANKL - Receptor Activator of Nuclear factor Kappa-B Ligand; OPG - Osteoprotegerin.

In order to see if the parameters analyzed had any associations when comparing the two types of tissues (aorta and bone), we did Spermann's correlations for each group.

Although no correlations were found comparing the expression of each gene in aorta and bone for both groups (data not shown), we have evaluated possible relations between the expression of different genes in the same tissue and with the other analysis previously described (serum turnover markers and histomorphometry), but the results obtained were punctual, limited to just one point of evaluation in either ApoE $^{-/-}$ or B6 mice with no tendency throughout the next time-points. We tried to see if possible associations would appear if we did not count for the age of the animals, and so we tested all animals of each group regardless of their age, but no correlations were found (data not shown).

Regarding the cytokines relative gene expression, we found a positive association between IL-1β and IL-6 in bone, in ApoE $^{-/-}$ group at 16 weeks (Figure 50), and also between TNF and OPG in bone for the same group and time-point (Figure 51), showing the increased levels of one cytokine seem to be correlated with the increase levels of the other (*p*-value = 0.0167).

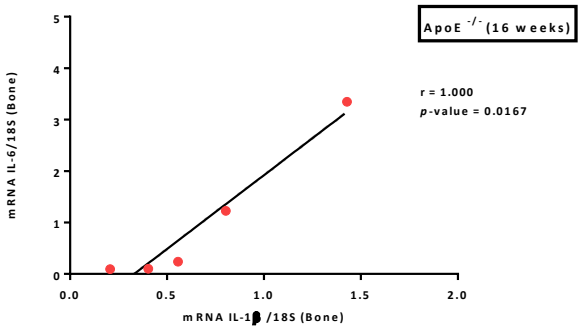

Figure 50 - Association between IL-1β and IL-6 in bone of the ApoE $^{-/-}$ group at 16 weeks.

The results were corrected to 18S rRNA and are shown as dots, with the regression line. The correlation was made using the Spermann's rank comparing the IL-1β relative gene expression levels with IL-6 levels in bone, giving a positive association with an r = 1.000 and a *p*-value = 0.0167. IL- Interleukin.

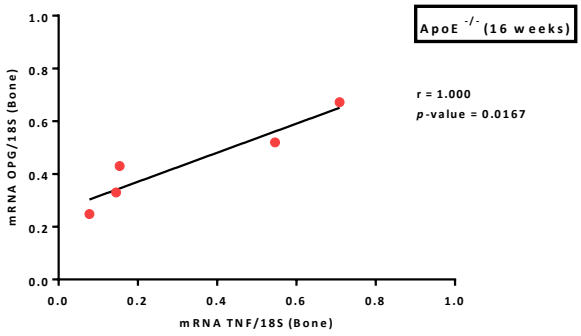

Figure 51 - Association between TNF and OPG in bone of the ApoE $^{-/-}$ group at 16 weeks.

The results were corrected to 18S rRNA and are shown as dots, with the regression line. The correlation was made using the Spermann's rank comparing TNF relative expression levels and OPG levels in bone, giving a positive association with an r = 1.000 and a *p*-value = 0.0167. TNF – Tumor Necrosis Factor; OPG – Osteoprotegerin.

For the B6 group the correlations found were also between TNF and OPG in bone, but in a later stage (28 weeks) (Figure 52), and between IL-17A and RANKL in bone as well (Figure 53), both correlations showing a positive association between the two cytokines (*p*-value = 0.0167).

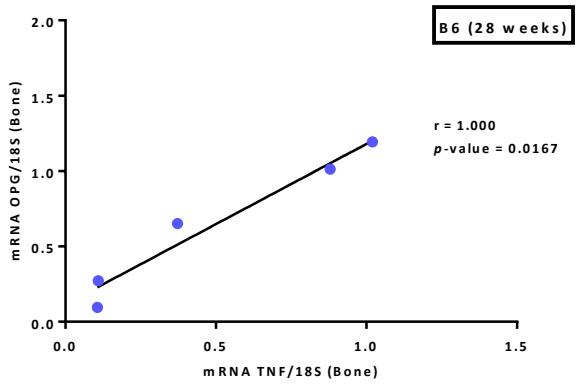

Figure 52 - Association between TNF and OPG in bone of B6 group at 28 weeks.

The results were corrected to 18S rRNA and are shown as dots, with the regression line. The correlation was made using the Spermann's rank comparing TNF relative expression levels and OPG levels in bone, giving a positive association with an r = 1.000 and a *p*-value = 0.0167. TNF – Tumor Necrosis Factor; OPG – Osteoprotegerin.

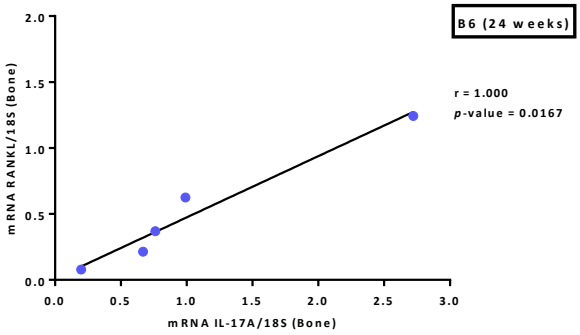

Figure 53 - Association between IL-17A and RANKL in bone of B6 group at 24 weeks.

The results were corrected to 18S rRNA and are shown as dots, with the regression line. The correlation was made using the Spermann's rank comparing IL-17A relative expression levels and RANKL levels in bone, giving a positive association with an r = 1.000 and a *p*-value = 0.0167. IL – Interleukin; RANKL - Receptor Activator of Nuclear factor Kappa-B Ligand.

Comparing the relative expression of cytokines and the parameters associated with bone structure (bone volume, trabecular thickness and trabecular separation), the only correlations found was for ApoE $^{-/-}$ group and only at 24 weeks regarding trabecular thickness (Tb.Th) and OPG expression levels in bone (Figure 54), and between bone volume (BV/TV) and trabecular separation (Tb.Sp) in B6 group at 28 weeks (Figure 55).

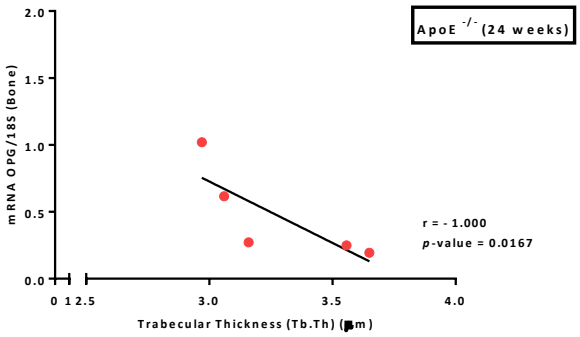

Figure 54 - Association between trabecular thickness and OPG levels in bone of ApoE $^{-/-}$ at 24 weeks.

The results are shown as dots, with the regression line. mRNA OPG expression values were corrected to 18S rRNA. The correlation was made using the Spermann's rank comparing trabecular thickness and the relative expression levels of OPG in bone, giving a negative association with an r = - 1.000 and a *p*-value = 0.0167. Tb.Th – Trabecular Thickness; OPG – Osteoprotegerin.

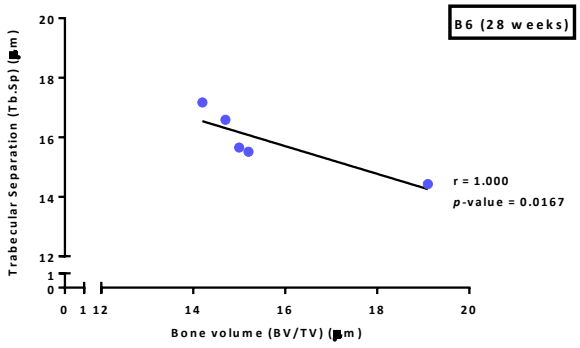

Figure 55 - Association between bone volume and trabecular separation in B6 group at 28 weeks.

The results are shown as dots, with the regression line. The correlation was made using the Spermann's rank comparing bone volume and trabecular separation, giving a negative association with an r = - 1.000 and a *p*-value = 0.0167. BV/TV – Bone Volume/Tissue Volume; Tb.Sp – Trabecular Separation.

Mouse model of inflammation

Body weight evaluation

For the secondary objective, twenty nine K/BxA^{g7} mice were used (nineteen with normal diet and ten with fat diet since 10 weeks old) to evaluate body weight and clinical score evolutions. These parameters were measured weekly during the time of the experiment, although the comparisons between groups, and among the same group, were only made at the points of evaluation defined previously. The serum was collected for bone turnover markers assessment and the left femur and aorta were collected for gene expression analysis.

To analyze gene expression and serum levels was chosen only the last time-point (24 weeks for these mice, due to a human endpoint defined according to the animal facility rules) and at this stage, eleven female mice were sacrificed in total (seven had been fed a normal diet and the other four fed a fat diet since 10 weeks old).

Table 17 - Body weight measurements in arthritic mice (K/BxA^{g7}) with normal diet and under a fat diet at each time-point.

Groups	Time-points (age in weeks)	number of animals (N)	Body weight (grams) mean with SD	Body weight (grams) median with IQR
K/BxA^{g7}	8	16	16,83 ± 2,40	16,65 [18,28 - 15,60]
	16	19	21,10 ± 2,63	20,15 [21,94 - 19,23]
	20	19	21,88 ± 2,97	21,08 [22,64 - 20,08]
	24	12	22,99 ± 2,50	22,23 [23,78 - 21,35]
	28	2	20,70 ± 0,57	20,70 [20,90 - 20,50]
K/BxA^{g7} FD	8	8	16,37 ± 1,69	16,60 [17,40 - 14,95]
	16	14	20,62 ± 1,96	20,30 [22,21 - 19,51]
	20	13	21,84 ± 1,94	21,90 [22,53 - 21,18]
	24	11	21,94 ± 3,17	22,30 [23,00 - 20,95]
	28	2	20,45 ± 4,45	20,45 [22,03 - 18,88]

Values are represented as means ± standard deviation (SD) and medians with IQR (Interquartile range) [75% - 25%].

The body weight variation throughout time was compared not only between both arthritic groups but also with the B6 group, used as healthy control (Figures 56 and 57) and although all groups gained weight along time, differences between the arthritic groups were only significant compared to the B6 group, especially for the arthritic group under a fat diet in which those differences were significant since the first point of evaluation.

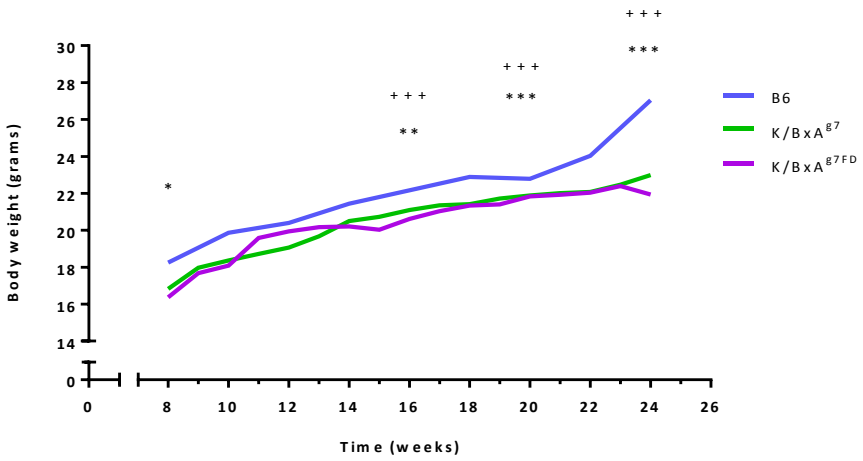

Figure 56 - Representation of body weight for K/BxA^{g7}, with normal and fat diet, compared with B6 group along experimental time.

The values used were medians and are represented in grams. * represents the statistical significant difference between body weight of B6 and K/BxA^{g7} FD at 8 weeks (*p*-value = 0.0417); ** represents the statistical significant difference between body weight of B6 and K/BxA^{g7} FD at 16 weeks (*p*-value = 0.0020); *** represents the statistical significant differences between body weight of B6 and K/BxA^{g7} FD at 20 weeks (*p*-value = 0.0010) and at 24 weeks (*p*-value = 0.0003). The +++ represents the statistical significant differences between body weight of B6 and K/BxA^{g7} at 16 weeks (*p*-value =0.0005), 20 weeks (*p*-value =0.0002) and at 24 weeks (*p*-value =0.0006). FD – Fat Diet.

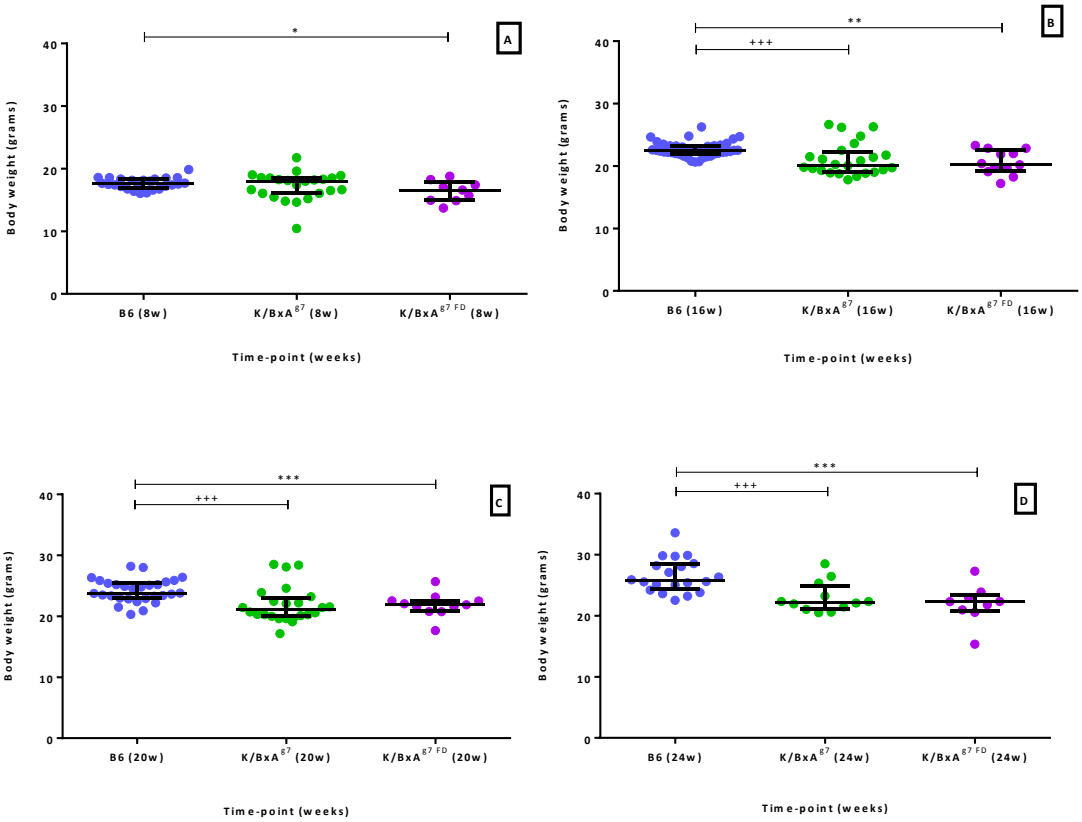

Figure 57 - Body weight for K/BxA^{g7}, with normal and fat diet, compared with B6 group, at (A) 8 weeks, (B) 16 weeks, (C) 20 weeks and (D) 24 weeks.

The results are represented in grams and shown as dot plots displaying medians and IQR (interquartile range) [75%-25%]. (A) * represents a statistical significant increase in body weight comparing B6 group and K/BxA^{g7} FD (*p*-value = 0.0417) at 8 weeks. (B) ** represents a statistical significant increase in body weight comparing B6 group and K/BxA^{g7} FD (*p*-value = 0.0020) and +++ representing a statistical significant increase in body weight comparing B6 group and K/BxA^{g7} (*p*-value = 0.0005) at 16 weeks. (C) *** represents a statistical significant increase in body weight comparing B6 group and K/BxA^{g7} FD (*p*-value = 0.0010) and +++ representing a statistical significant increase in body weight comparing B6 group and K/BxA^{g7} (*p*-value = 0.0002) at 20 weeks. (D) *** represents a statistical significant increase in body weight comparing B6 group and K/BxA^{g7} FD (*p*-value = 0.0003) and +++ representing a statistical significant increase in body weight comparing B6 group and K/BxA^{g7} (*p*-value = 0.0006) at 24 weeks. FD – Fat Diet.

Clinical Score

To evaluate the progression of the arthritis a clinical score was applied throughout the experiment, although the comparisons between groups, and among the same group, were only made at the defined time-points.
The first signs of the disease were visible at 4 weeks, but the score was only applied starting at 8 weeks.

In Table 18 are reported the clinical scores at each time-point for the arthritic groups and in Figure 58 are represented these groups as well as the B6 group for comparison, as a healthy control, and we can see that the only statistically difference between both arthritic group was at 8 weeks (*p*-value = 0.0010). Comparing to the B6 group, the difference between the arthritic score was significant at every time-point (*p*-value < 0.0001) since the B6 group did not shown any signs of arthritis (blue line in Figure 58).

Table 18 - Clinical score evaluation in K/BxA^{g7} mice, with normal and fat diet, at each time-point.

Groups	Time-points (age in weeks)	number of animals (N)	Clinical score (0-12) mean with SD	Clinical score (0-12) median with IQR
K/BxA^{g7}	8	16	5 ± 2	5 [7 - 4]
	16	19	8 ± 1	8 [8 - 8]
	20	19	9 ± 2	9 [10 - 8]
	24	12	9 ± 1	10 [10 - 8]
	28	2	12 ± 0	12 [12 - 12]
K/BxA^{g7} FD	8	8	8 ± 2	8 [10 - 8]
	16	14	8 ± 1	8 [8 - 7]
	20	13	9 ± 1	8 [9 - 8]
	24	11	10 ± 2	9 [11 - 8]
	28	2	10 ± 3	10 [11 - 9]

Values are represented as means ± standard deviation (SD) and medians with IQR (Interquartile range) [75% - 25%].

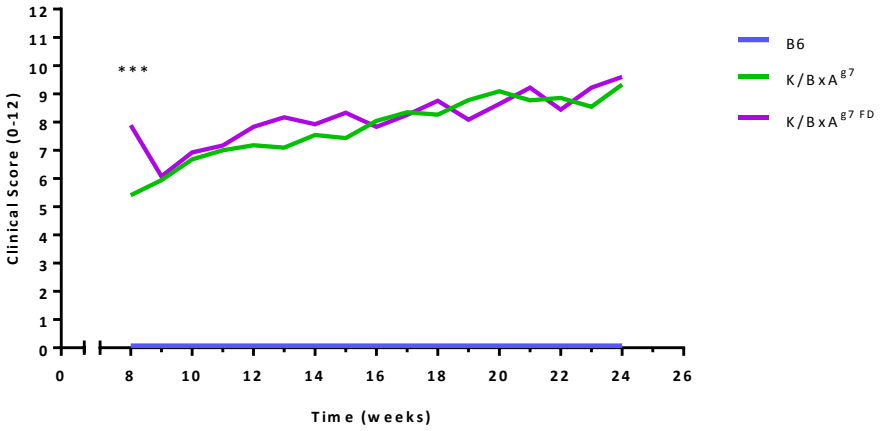

Figure 58 - Representation of clinical Score for K/BxA^{g7}, with normal and fat diet, compared with B6 group, along experimental time.

The values used were medians and are represented by a number resulted from a scoring system of arthritis of each paw (0-12). *** represents the statistical significant difference between K/BxA^{g7} and K/BxA^{g7} FD at 8 weeks (*p*-value = 0.0010). The B6 group presented no signs of arthritis reporting a score of zero throughout time (flat blue line at zero), and is statistically different from the other groups at each time-point (*p*-value < 0.001; not represented in the figure). FD – Fat Diet.

Looking for the arthritis development in each group isolated (Figure 59), we can see that the K/BxA^{g7} with a normal diet was the only group with a statistically significant increase in the arthritic score (Figure 59A), especially at 16 and 20 weeks, when this increase was substantially superior compared with the previous time-point (*p*-value < 0.0001 and *p*-value = 0.0034, respectively) but also in the later time-points (20 and 24 weeks) compared to baseline (*p*-value < 0.0001).

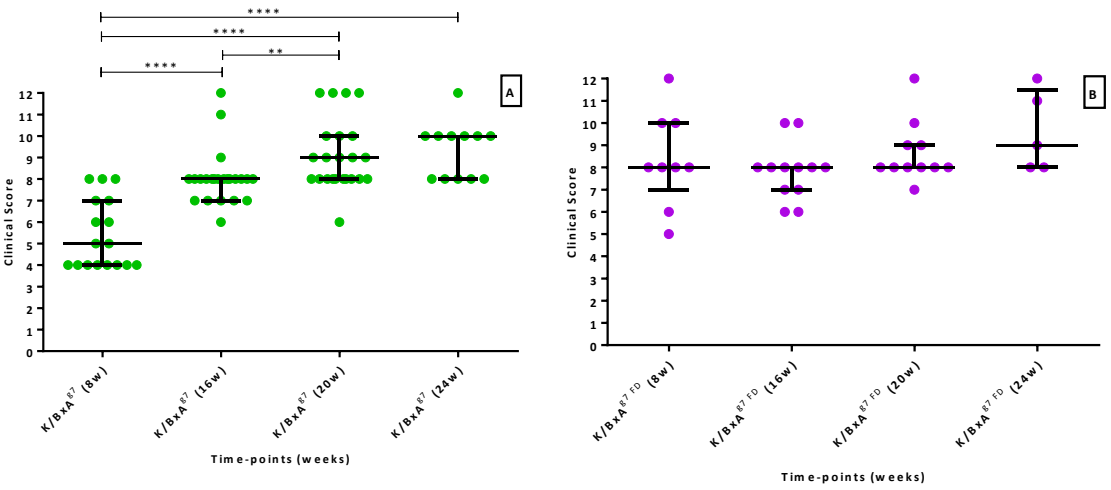

Figure 59 - Clinical score of K/BxAg7, with normal and fat diet, at each time point.

The results are represented in number resulted from a scoring system of arthritis of each paw (0-12), and are shown as dot plots displaying medians and IQR (interquartile range) [75%-25%]. (A) **** represents a statistical significant increase in clinical score of K/BxA^{g7} at 16, 20 and 24 weeks compared to baseline (p-value < 0.0001) and ** represents a statistical significant increase in clinical score of K/BxA^{g7} between 16 and 20 weeks. (B) Minor increase of clinical score of K/BxA^{g7} FD throughout time (not significant). FD – Fat Diet.

Atherosclerotic lesions

Regarding the evaluation of atherosclerotic lesions progression, no visible evidence of lesions was found in whole aorta of these mice (data not shown).

Posteriorly, two mice from each arthritic group were put in a different animal facility, and other four (two from each group) were brought until 28 weeks of age, resorting to an anesthetic (Buprernorphine), to evaluate the lesions at that time, but in these two situations, no changes were found, meaning, neither one of the mice in each group developed any visible signs of atherosclerotic lesions.

Bone turnover markers

To assess bone turnover, the levels of CTX-I and P1NP in serum samples were determined at 24 weeks.

Serum levels of CTX-I are presented in Table 19, and compared to B6 group in Figure 60, where we can see that the levels of CTX-I were higher in both arthritic groups, although those differences were not significant.

Table 19 - Measurement of CTX-I in serum of K/BxA^{g7}, with normal and fat diet, at 24 weeks.

Groups	Time-points (age in weeks)	number of animals (N)	CTX-I (ng/mL) mean with SD	CTX-I (ng/mL) median with IQR
K/BxA^{g7}	24	4	22,23 ± 3,79	21,20 [23,59 - 19,29]
K/BxA^{g7} FD	24	4	27,049 ± 7,70	28,51 [33,79 - 21,77]

Values are represented in nanograms per mL and are shown as means ± standard deviation (SD) and medians with IQR (Interquartile range) [75% - 25%]. CTX-I - C-terminal cross-link telopeptide of type I collagen.

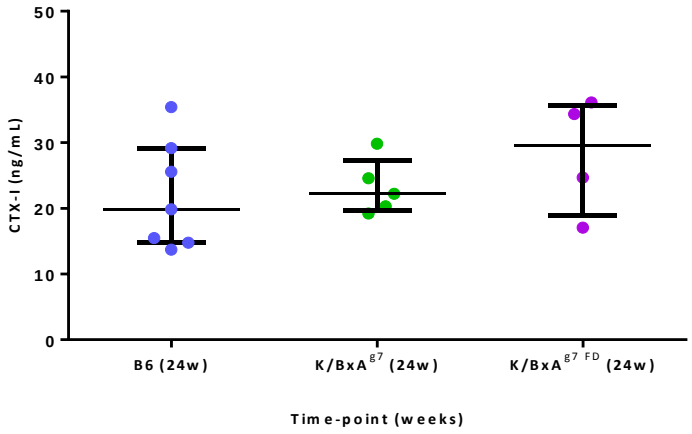

Figure 60 - CTX-I serum levels of K/BxA^{g7}, with normal and fat diet, compared with B6 group at 24 weeks.

The results are represented in nanograms per mL and are shown as dot plots displaying medians and IQR (interquartile range) [75-25%] at 24 weeks. Both arthritic groups shown higher serum levels of CTX-I compared to B6 group (not significant). CTX-I - C-terminal cross-link telopeptide of type I collagen; FD – Fat Diet.

For The P1NP protein, the serum levels are reported in Table 20.

Table 20 – Measurements of P1NP in serum in K/BxAg7, with normal and fat diet, at 24 weeks.

Groups	Time-points (age in weeks)	number of animals (N)	P1NP (ng/mL) mean with SD	P1NP (ng/mL) median with IQR
K/BxA^{g7}	24	4	78,86 ± 11,87	78,32 [86,39 - 70,78]
K/BxA^{g7} FD	24	4	83,33 ± 22,05	79,65 [89,92 - 73,06]

Values are represented in nanograms per mL and are shown as means ± standard deviation (SD) and medians with IQR (Interquartile range) [75% - 25%]. P1NP - N-propeptide of type I collagen; FD – Fat Diet.

Differences between arthritic and control groups were found, with statistical significance in both groups showing higher levels of this protein compared to B6 group (Figure 61).

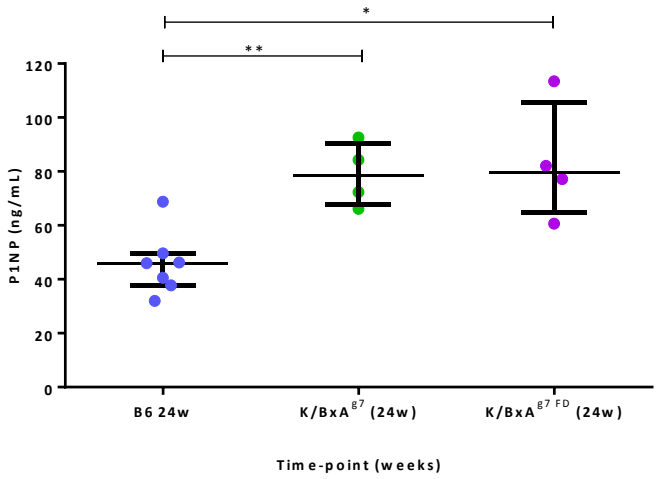

Figure 61 - P1NP serum levels of K/BxA^{g7}, with normal and fat diet, compared with B6 group at 24 weeks.

The results are represented in nanograms per mL and are shown as dot plots displaying medians and IQR (interquartile range) [75-25%] at 24 weeks. The arthritic groups show higher serum levels of P1NP compared to B6 group with * representing the statistical difference between B6 and K/BxA^{g7} FD (p-value = 0.0121), and ** representing a statistically significant difference between B6 and K/BxA^{g7} (p-value = 0.0051). P1NP - N-propeptide of type I collagen; FD – Fat Diet.

Looking at CTX-I/P1NP ratio results (Table 21), and the comparison with the B6 group (Figure 62), we can see that the ratio in both arthritic groups were lower compared to B6 group, but was only statistically significant between B6 and K/BxA^{g7} with normal diet (*p*-value = 0.0381).

Table 21 - CTX-I/P1NP ratio assessment for K/BxAg7, with normal and fat diet, at 24 weeks.

Groups	Time-points (age in weeks)	number of animals (N)	CTX-I/P1NP ratio	
			mean with SD	median with IQR
K/BxA^{g7}	24	4	0,28 ± 0,06	0,29 [0,33 - 0,25]
K/BxA^{g7} FD	24	4	0,33 ± 0,09	0,34 [0,40 - 0,27]

Values are represented in nanograms per mL and are shown as means ± standard deviation (SD) and medians with IQR (Interquartile range) [75% - 25%]. CTX-I - C-terminal cross-link telopeptide of type I collagen; P1NP - N-propeptide of type I collagen; FD – Fat Diet.

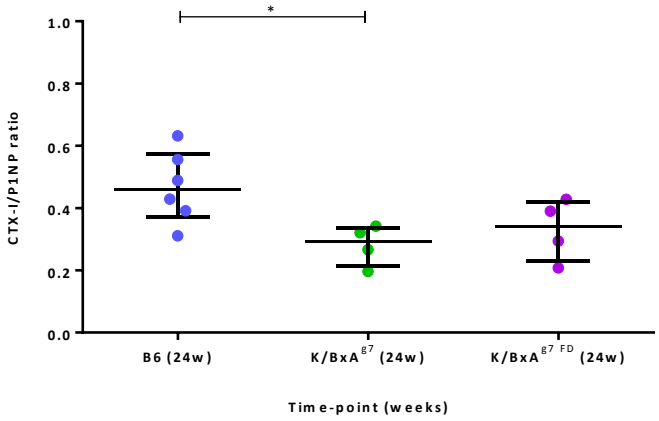

Figure 62 - CTX-I/P1NP ratio of K/BxA^{g7}, with normal and fat diet, compared with B6 group at 24 weeks.

The results are shown as dot plots displaying medians and IQR (interquartile range) [75-25%] at 24 weeks. The arthritic groups show lower levels in the CTX-I/P1NP ratio compared to B6 group with * representing the statistical difference between B6 and K/BxA^{g7} (p-value = 0.0381). CTX-I - C-terminal cross-link telopeptide of type I collagen; P1NP - N-propeptide of type I collagen; FD – Fat Diet.

Gene expression

Although no atherosclerotic lesions were found in this model of inflammation in the course of this work, was still important to see if there were any alteration in expression levels of genes associated with inflammation, especially on the cardiovascular system of these mice. The relative gene expression of proteins associated with inflammation and bone remodeling were evaluated in two types of mice tissues, the whole aorta and the femoral bone.

Inflammation related genes

In Table 22 is shown the panel of pro-inflammatory cytokines and their mRNA expression levels in aorta and bone, for both arthritic groups.
Comparing the results, one thing that strikes the most is the discrepancy of values obtained in aorta and in bone, just like what happened for the other experimental groups.

Regarding the comparison between the K/BxA^{g7} groups and B6 group (Figure 63), in general, both arthritic groups shown higher expression levels of these cytokines comparing to B6 group (with exception for IL-17A in bone, in which the values obtained for these groups were lower compared to the B6 group; Figure 63C2), although any statistical significant differences were found for any cytokine. Note that the results for the arthritic groups are composed by a small number of samples, which could explain the lack of statistical significance.

Table 22 - Relative gene expression levels of (A) IL-1β, (B) IL-6, (C) IL-17A and (D) TNF for K/BxA^{g7}, with normal and fat diet, at 24 weeks, in bone and aorta.

(A)

		IL-1β					
		Aorta			Bone		
Groups	Time-points (age in weeks	number of animals (N)	mean with SD	median with IQR	number of animals (N)	mean with SD	median with IQR
K/BxA^{g7}	24	2	317,54 ± 182,60	317,54 [408,84 - 226,25]	3	1,39 ± 0,73	1,15 [1,76 - 0,89]
K/BxA^{g7} FD	24	2	34,15 ± 29,13	34,15 [48,72 - 19,59]	2	1,85 ± 1,01	1,85 [2,35 - 1,35]

(B)

		IL-6					
		Aorta			Bone		
Groups	Time-points (age in weeks	number of animals (N)	mean with SD	median with IQR	number of animals (N)	mean with SD	median with IQR
K/BxA^{g7}	24	2	2,39 ± 2,09	2,39 [3,43 - 1,34]	3	1,03 ± 0,46	1,15 [1,34 - 0,78]
K/BxA^{g7} FD	24	2	6,76 ± 6,43	6,76 [9,98 - 3,54]	2	1,13 ± 0,56]	1,13 [1,41 - 0,85]

(C)

		IL-17A					
		Aorta			Bone		
Groups	Time-points (age in weeks	number of animals (N)	mean with SD	median with IQR	number of animals (N)	mean with SD	median with IQR
K/BxA^{g7}	24	2	2,35 ± 0,71	2,35 [2,70 - 2,00]	3	0,25 ± 0,11	0,23 [0,31 - 0,17]
K/BxA^{g7} FD	24	2	3,26 ± 1,12	3,26 [3,82 - 2,70]	2	0,21 ± 0,11	0,21 [0,26 - 0,15]

(D)

		TNF					
		Aorta			Bone		
Groups	Time-points (age in weeks	number of animals (N)	mean with SD	median with IQR	number of animals (N)	mean with SD	median with IQR
K/BxA^{g7}	24	2	21,88 ± 6,19	21,88 [24,97 - 18,78]	3	0,83 ± 0,75	0,44 [1,16 - 0,31]
K/BxA^{g7} FD	24	2	16,01 ± 9,36	16,01 [20,68 - 6,65]	2	0,31 ± 0,07	0,31 [0,35 - 0,28]

Data were normalized to 18S rRNA and are represented as means ± standard deviation (SD) and medians with IQR (Interquartile range) [75% - 25%]. (A) mRNA expression levels of IL-1β for K/BxA^{g7} with normal and fat diet, at 24 weeks. (B) mRNA expression levels of IL-6 for K/BxA^{g7} with normal and fat diet, at 24 weeks. (C) mRNA expression levels of IL-17A for K/BxA^{g7} with normal and fat diet, at 24 weeks. (D) mRNA expression levels of TNF for K/BxA^{g7} with normal and fat diet, at 24 weeks. IL- Interleukin; TNF – Tumor Necrosis Factor; FD – Fat Diet.

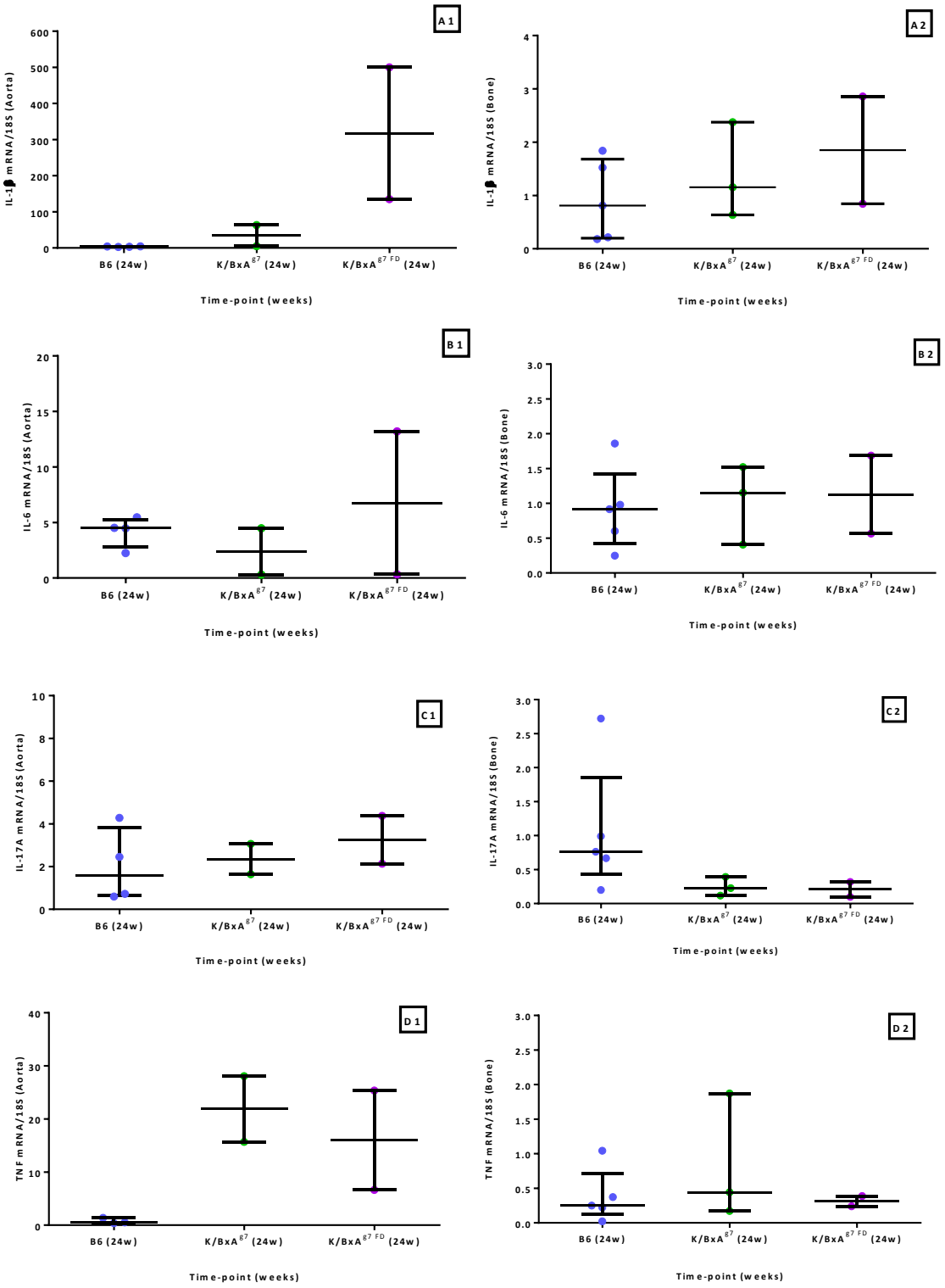

Figure 63 - Relative gene expression levels of (A1) IL-1β in aorta, (A2) IL-1β in bone, (B1) IL-6 in aorta, (B2) IL-6 in bone, (C1) IL-17A in aorta, (C2) IL-17A in bone, (D1) TNF in aorta and (D2) TNF in bone, for K/BxA^{g7}, with normal and fat diet, and B6 group, at 24 weeks.

The results represented the relative expression levels corrected to 18S rRNA and are shown as dot plots displaying medians and IQR (interquartile range) [75-25%]. (A1) mRNA levels of IL-1β in aorta at 24 weeks for B6 group and K/BxA^{g7}, with normal and fat diet, showing an increase, especially the K/BxA^{g7} FD (not significant). (A2) mRNA levels

of IL-1β in bone at 24 weeks for B6 group and K/BxA^{g7}, with normal and fat diet, showing an increase of these levels especially for K/BxA^{g7} FD. (B1) mRNA levels of IL-6 in aorta at 24 weeks for B6 group and K/BxA^{g7}, with normal and fat diet, showing increase levels in K/BxA^{g7} FD, but decrease levels in K/BxA^{g7}. (B2) mRNA levels of IL-6 in bone at 24 weeks for B6 group and K/BxA^{g7}, with normal and fat diet, showing similar levels. (C1) mRNA levels of IL-17A in aorta at 24 weeks for B6 group and K/BxA^{g7}, with normal and fat diet, showing increased levels of K/BxA^{g7} and higher for K/BxA^{g7} FD. (C2) mRNA levels of IL-17A in bone at 24 weeks for B6 group and K/BxA^{g7}, with normal and fat diet, showing a decrease in both arthritic groups. (D1) mRNA levels of TNF in aorta at 24 weeks for B6 group and K/BxA^{g7}, with normal and fat diet, showing higher levels for the arthritic groups, especially for K/BxA^{g7} with normal diet. (D2) mRNA levels of TNF in bone at 24 weeks for B6 group and K/BxA^{g7}, with normal and fat diet, showing a slight increase in K/BxAg7 with normal diet. No statistical differences were found in any of the analysis. IL- Interleukin; TNF – Tumor Necrosis Factor; FD – Fat Diet.

Bone remodeling related genes

To evaluate the bone remodeling process we looked at the major genes associated with this process, RANKL and OPG, and also the variations in their ratio (RANKL/OPG), not only in bone but also in the whole aorta.

In table 23 are stated the relative expression levels of RANKL, OPG and also the RANKL/OPG ratio, in aorta and bone of both arthritic groups. The comparison arthritic groups and B6 group are shown in Figure 64.

Although no statistical significant differences were found, it is noticeable that the levels are more similar between all groups (K/BxA^{g7}, K/BxA^{g7} under a fat diet and B6) in bone tissue compared to aortas (Figures 64-A2, B2 and C2). Note, once again, that the results for the arthritic groups are composed by a small number samples which could explain the lack of statistical significance.

Table 23 - Relative gene expression levels of (A) RANKL, (B) OPG and the (C) RANKL/OPG ratio for K/BxA^{g7}, with normal and fat diet, at 24 weeks, in bone and aorta.

(A)

		RANKL					
		Aorta			Bone		
Groups	Time-points (age in weeks	number of animals (N)	mean with SD	median with IQR	number of animals (N)	mean with SD	median with IQR
K/BxA^{g7}	24	2	4,89 ± 1,26	4,89 [5,52 - 4,26]	3	0,41 ± 0,20	0,32 [0,51 - 0,27]
K/BxA^{g7} FD	24	2	5,15 ± 0,65	5,15 [5,48 - 4,83]	2	0,35 ± 0,14	0,35 [0,42 - 0,28]

(B)

		OPG					
		Aorta			Bone		
Groups	Time-points (age in weeks	number of animals (N)	mean with SD	median with IQR	number of animals (N)	mean with SD	median with IQR
K/BxA^{g7}	24	2	1,45 ± 0,80	1,45 [1,85 - 1,05]	2	0,34 ± 0,00	0,34 [0,34 - 0,34]
K/BxA^{g7} FD	24	2	3,23 ± 2,00	3,23 [4,23 - 2,23]	2	0,42 ± 0,16	0,42 [0,50 - 0,35]

(C)

		RANKL/OPG ratio					
		Aorta			Bone		
Groups	Time-points (age in weeks	number of animals (N)	mean with SD	median with IQR	number of animals (N)	mean with SD	median with IQR
K/BxA^{g7}	24	2	5,52 ± 3,91	5,52 [7,47 - 3,57]	2	0,81 ± 0,14	0,81 [0,88 - 0,74]
K/BxA^{g7} FD	24	2	2,39 ± 1,28	2,39 [3,03 - 1,75]	2	0,81 ± 0,02	0,81 [0,83 - 0,80]

Data were normalized to 18S rRNA and are represented as means ± standard deviation (SD) and medians with IQR (Interquartile range) [75% - 25%]. (A) mRNA expression levels of RANKL for K/BxA^{g7} with normal and fat diet, at 24 weeks. (B) mRNA expression levels of OPG for K/BxA^{g7} with normal and fat diet, at 24 weeks. (C) RANKL/OPG ratio for K/BxA^{g7} with normal and fat diet, at 24 weeks. RANKL - Receptor Activator of Nuclear factor Kappa-B Ligand; OPG - Osteoprotegerin; FD – Fat Diet.

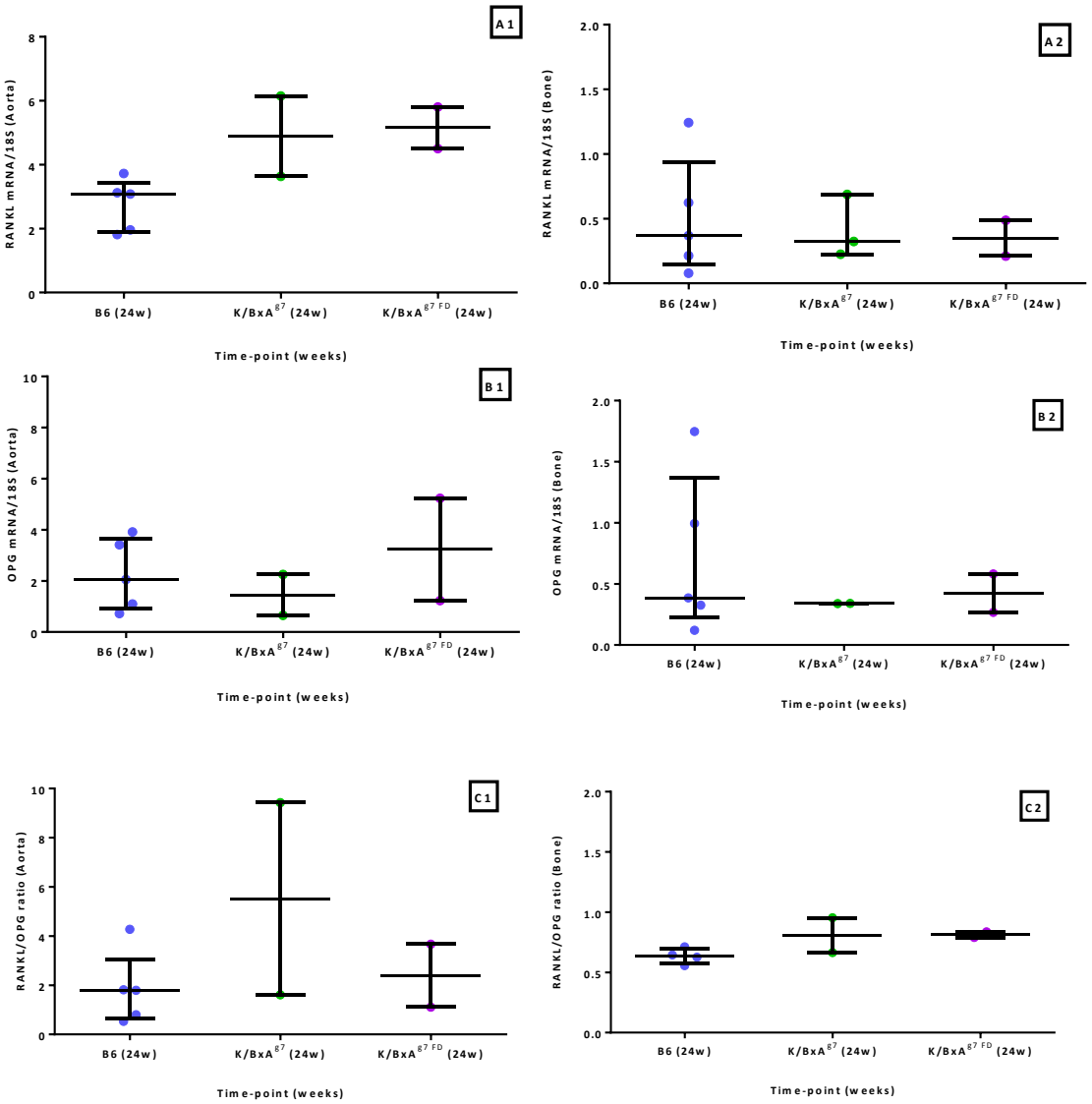

Figure 64 - Relative gene expression levels of (A1) RANKL in aorta, (A2) RANKL in bone, (B1) OPG in aorta, (B2) OPG in bone, the (C1) RANKL/OPG ratio in aorta and (C2) RANKL/OPG ratio in bone for K/BxA^{g7}, with normal and fat diet, and B6 group, at 24 weeks.

The results represent the relative expression levels corrected to 18S rRNA and are shown as dot plots displaying medians and IQR (interquartile range) [75-25%] at 24 weeks. (A1) mRNA levels of RANKL in aorta at 24 weeks for B6 group and K/BxA^{g7}, with normal and fat diet, showing an increase (not significant). (A2) mRNA levels of RANKL in bone at 24 weeks for B6 group and K/BxA^{g7}, with normal and fat diet, showing similar levels. (B1) mRNA levels of OPG in aorta at 24 weeks for B6 group and K/BxA^{g7}, with normal and fat diet, showing increase levels in K/BxA^{g7} FD, but decrease levels in K/BxA^{g7}. (B2) mRNA levels of OPG in bone at 24 weeks for B6 group and K/BxA^{g7}, with normal and fat diet, showing similar levels. (C1) RANKL/OPG ratio in aorta at 24 weeks for B6 group and K/BxA^{g7}, with normal and fat diet, showing higher levels of K/BxA^{g7}, and a slight increase of K/BxA^{g7} FD. (C2) RANKL/OPG ratio in bone at 24 weeks for B6 group and K/BxA^{g7}, with normal and fat diet, showing a slight increase in both arthritic groups. No statistical differences were found in any of the analysis. RANKL - Receptor Activator of Nuclear factor Kappa-B Ligand; OPG - Osteoprotegerin; FD – Fat Diet.

Discussion

The aim for this study was to understand if there were common mechanisms playing a role in the development and progression of atherosclerosis and bone disorders, and to evaluate the impact of inflammation in bone metabolism and remodeling process. It has been well established that certain inflammatory conditions can act in the bone remodeling process disturbing its balance and leading to development of bone pathologies like osteoporosis.

Because these diseases are not only multifactorial but a long-lasting processes in humans, an animal model is the best option as gives us the possibility to evaluate changes occurring in a short time. Despite all the limitations associated with the use of animal models to study human diseases, it is the only way to evaluate and understand the relation between both diseases and their progression over time.

Regarding our results, the evaluation of body weight changes throughout time showed a significant increase in both groups, and when comparing between them we saw ApoE $^{-/-}$ mice gaining more weight comparing to B6 mice. Since the ApoE $^{-/-}$ mice have a tendency to hyperlipidemia, even more after the introduction of a fat diet, this result was expected. Concerning the progression of atherosclerotic lesions, we seen a noticeable progression of these lesions in ApoE $^{-/-}$ mice (B6 mice did not shown visible lesions), especially after the introduction of the fat diet, which is in accordance with a previous report by Jawien *et al.* [83] where they show a 3-4 times increase in lesion sizes when animals were fed with a high fat content diet.

For the evaluation of bone remodeling we measured bone turnover markers and performed histomorphometric analysis of mice vertebras in each time-point. Concerning the bone turnover markers, the ApoE $^{-/-}$ group shown a more striking tendency of increase in CTX-I/P1NP ratio, resulted of the increase in CTX-I levels at later stages and also by the general decrease in P1NP serum levels. These alterations in the levels of both proteins seem to state that ApoE $^{-/-}$ mice had a more active bone turnover, and this was leading towards bone destruction. This data was accordant, with the results obtained by histomorphometry, i.e. along experimental time it seemed that remodeling

processes tends towards bone resorption (diminished bone volume and trabecular thickness, and an increase in trabecular separation, especially in the ApoE $^{-/-}$ mice). The trabecular thickness was the only parameter showing statistical significance (at 28 weeks) but it shown an continuous increase in B6 mice rather in ApoE $^{-/-}$ mice, where this increase was only observable in the initial phase and solely decreases after the peak of bone remodeling (that occurs around 16-20 weeks). Although the decrease in trabecular thickness could be explained by the decline in bone remodeling processes in adult life, with the statistical difference between the two groups, it appears that ApoE $^{-/-}$ had a more pronounced decay in this process that B6 mice. Regarding trabecular separation, it seemed that B6 mice had a higher separation rate, and although it was not significant, these results let to appear that B6 mice suffer bigger changes in bone throughout time, which was not completely expected. One thing that could help explain some of these results is this type of bone analysis (histomorphometry) that requires an operator-dependent analysis, in which the operator has to decide which bone is trabecular bone and delimit the area. Moreover, in this technique the samples can suffer some destruction, especially in the cutting step which could led, in the end, to a more altered bone that it was originally. Nevertheless, in our work the entire procedure and analyses were executed by the same operator to unify the results and minimize any errors.

Taking into account the epidemiological data linking these diseases, we could expected that the animal model of atherosclerosis (ApoE $^{-/-}$ mice), although this disease starts to develop in this model due to a metabolic disorder (caused by the lack of apolipropotein E) affecting lipids metabolism, an inflammatory condition should develop (especially with the hyperlipidemia induced by the fat diet that was shown to be responsible for inflammatory processes in atherosclerosis and vascular calcification) [101].

An inflammatory milieu might have repercussions in the expression of pro-inflammatory genes in the tissues, probably leading to an elevation of their levels when compared with a healthy control group. However our results did not follow this tendency, especially revealed by the fact that the majority of the inflammatory cytokines (IL-1β, IL-6, IL-17A

and TNF) expression levels were lower in ApoE $^{-/-}$ compared with B6 group, suggesting that the atherosclerotic model expresses lower levels of pro-inflammatory cytokines in the studied tissues compared with a healthy group, especially in the aorta.

Regarding the variation of pro-inflammatory cytokines expression along time, it shown no apparent changes, without significant variations over time and without any relation in the expression between the two tissues (aorta and bone). Even though, we tried to correlate the expression levels between both tissues regardless the time-points (ages), since previous work from our lab demonstrated the existence of correlations between some of the same pro-inflammatory cytokines in human samples independently of age (data not published), but still we did not find any significant correlations (data not shown). One thing that could explain the lack of correlations regarding the relative gene expression could be the fact that aorta tissue is more sensitive, especially because is made out of soft tissue, and so the RNA degradation in tissue processing is a real possibility, and that could probably affected the quantitative PCR reading, explaining the discrepancy in the results gotten in aorta versus bone tissues.

Even though our results pointed to a reduction in bone volume along time when looking at structural behavior, when we look at gene expression levels the results obtained were variable and did not allow to see if the deletion of ApoE gene had any effect on bone. Nevertheless the tendency shown in bone somehow guide us to an opposite conclusion, with the increased levels of OPG and higher expression levels compared with RANKL (with a subsequent decrease in RANKL/OPG ratio along time), especially in ApoE $^{-/-}$ group, which seems to indicate a shifting towards bone formation (since OPG acts as decoy for RANKL inhibiting osteoclasts maturation and action in osteoclastogenesis).

It is important to bear in mind that, although ApoE $^{-/-}$ mice are an animal model of excellence to study atherosclerosis, in these mice the disease starts due to a gene deletion that affects a metabolic pathway, and to achieve the goals of our study we encounter some limitations, one of them being the fact that it is not an inflammatory model, as already discussed above. Additionally there are the controversial results regarding bone alterations in this animal model. Some studies have reported an increase in bone mass, as well as increased bone formation rate [100,103,104], contrary to others that

stated an increased bone resorption in this animal model [102]. Even though there is no consensus regarding the effect over bone on this model, one thing that is important to consider is the fact that all these studies take into account only advanced stages of disease development and not their progression, unlike our work where that was the primary focus in order to try to understand how disease progression affects the tissues. Nevertheless, the lack of correlations and unexpected results could be somehow explained by the fact that in each time-point we had only five animals, and even though this has been considered as a sufficient number for statistical comparison and validity [86], this work would benefit from an increase in the number of animals, although always taking into account the 3R's policy applicable to animal work[†]. It is also important to remember that the control group (B6 mice) were under a fat diet, since it potentiates and accelerates the development of atherosclerotic lesions in ApoE $^{-/-}$ mice, but as it was reported by Hirasawa *et al.* [102], a fat diet leads to a reduction in bone mineralization, which reinforce the importance for the experimental design to introduce the fat diet in both experimental group (not only in ApoE $^{-/-}$ group, but also in B6 group) in order to unify any alterations caused by the diet. However, given the results, this project would benefit of another control group (B6) without the fat diet.

Regarding the second objective of this project, we were expecting to observe a development of atherosclerotic lesions in the aorta of these mouse model of inflammatory arthritis (K/BxA^{g7}), especially in the ones subjected to a fat diet, as it has been described by Rose *et al.* [85]. With this we wanted to study the progression of both diseases in the same organism and try to understand which mechanisms could be behind the development of atherosclerosis and osteoporosis, in mice that have a described active inflammation. However, these mice did not developed any observable lesions in

[†] 3R's policy for ethics in animal use for research is based on three principles of Replacement, Reduction and Refinement, in witch is expected that in an experiment using animals, is preferred an non-animal model as must as possible; reduce the number of animals used and choose methods that alleviate or minimize the animal pain and enhancing the animal welfare [108].

the aortas, although the arthritis development and progression was notoriously present and occurred as described earlier [86,91].

A possible explanation to the lack of visible lesions in the vessels of these mice, even though it has been previously published [85], might be due to housing conditions of the animals facility where the experience took place. It is under debate how environmental factors such as housing conditions of research animals influence the composition of their commensal intestinal microbiota. This is especially important since they are crucial to host immunity, and also they can initiate and perpetuate acute and chronic diseases [105], therefore alterations in animals microbiota can influence the development and progression of a certain diseases. Throughout this study all animals were housed in a SPF animal facility, which provides a very protective and sterile environment, essential for instant, for studies in immuno-compromised animals. Nevertheless, the absence of stimuli from pathogens has a known impact in the microbiota of the animals, affecting the organism in several ways.

In order to try to unveil some possible causes for the absence of lesions in the aortas of these mice, we extend the experience time using four animals (two fed normal diet and two fed a high fat diet) until 28 weeks of age with the help of an anesthetic (Buprenorphine). With this test we tried to understand if the 24 weeks evaluation was not enough for the lesions development, but no visible lesions were found in any of these mice with 28 weeks of age.

Another possible cause for the absence of lesions in the aortas of these mice was the influence of the housing conditions, as stated above. To tests this hypothesis, two animals from each diet group were placed in a different room of the IMM animal facility, which has the presence of some pathogens e.g. *Helicobacter pylori*, that has been associated with the development of atherosclerosis in mice [106]. Although the environment in this facility is more challenging, the mice are housed in IVC racks, like the ones used in the room where the previously described mice were housed, and we did not find any visible lesions in this four animals. Nevertheless, it is still important to test different housing conditions, and especially less protective of the mice surrounding

environment (e.g. a conventional animal facility), and if possible using a larger number of animals.

The preliminary data regarding the animals from this model comparing with the healthy control (B6 group) shown no statistical significant differences between groups concerning gene expression levels, although in general both arthritic groups shown higher levels of the inflammatory cytokines comparing to B6 group, which could be a good indication that, even thought was not reported visible lesions, it appears that there are some kind of inflammatory processes already in development in those tissues. It is however important take into account that only few animals used for each group, which could "weakened" the statistical strength of these groups for comparisons, reinforcing the importance to increase the animal number in future studies.

On the other hand comparing the bone turnover markers we found statistical differences between P1NP levels and CTX-I/P1NP ratio but not with CTX-I levels, although these results were against what was expected. Since this inflammatory arthritis model had a marked disease outcome (shown by clinical score elevated at this age: 24 weeks), it was expected that the remodeling process was deflected towards increased bone resorption (osteoclastogenesis), with an increase in CTX-I levels (marker of bone resorption) relatively to P1NP (marker of bone formation). Nevertheless, it is important to remember that these results were a result in only one time-point, so we do not have information on the progression, to see how these proteins levels alter through time, reinforcing the importance to study different time-points to see the tendency.

Conclusions

As a conclusion of this work we shown that ApoE $^{-/-}$ mice develops atherosclerotic lesions since an early stage, as reported before, and also they experience some alterations in the bones throughout time, although our results were somewhat contradictory and with no considerable differences compared to the healthy group, and so, it seemed that our results did not support our hypothesis.

Bone histomorphometric analysis shown a tendency in which seemed to lead into the idea of alterations in bone towards bone loss (with decrease in bone volume and trabecular thickness, and with the increase in trabecular separation), concomitantly with the serum levels of CTX-I and P1NP (the levels of CTX-I were higher and the P1NP levels were lower). On the other hand the relative expression of the genes associated with bone remodeling as well as the genes associated with inflammation shown an opposite trend, suggesting a shifting in the bone remodeling process towards bone formation.

To complement this project it would be interesting to increase the number of animals in the study in order to strengthen the statistical power of the results and also to see if any tendency would be maintained.

Regarding the secondary objective, the K/BxAg7 mice did not shown visible signs of atherosclerotic lesions in the aorta, contrary to what has been previously described. This result could be caused by the animal housing conditions, since they were in a SPF-facility, and it has been shown that housing conditions play a fundamental role in inflammatory diseases development. The preliminary results shown no significant differences compared to a healthy control (B6 group), although in general all inflammation related genes shown a tendency to be augmented in these mice, possibly indicating that some inflammatory process was already ongoing in the tissues.

Additionally, we should perform histomorphometric analysis of the K/BxA^{g7} bones to evaluate their bone micro-arquitecture, as well as the other parameters evaluated in the same time-points as the other experimental groups. To verify if the housing conditions had some cause in the lack of visible lesion in the vessels, would be important to house a group of these mice in a conventional animal facility, with a more challenging environment, to see if visible lesions are developed.

References

1. WHO. *Global status report on noncommunicable diseases 2010*. *World Health Organization* (World Health Organization, 2011). at <http://www.who.int/mediacentre/factsheets/fs317/en/>
2. Frostegård, J. Atherosclerosis and cardiovascular disease in rheumatoid arthritis. *J. Rheumatol.* **39,** 2233–4 (2012).
3. Becker, C. Pathophysiology and Clinical Manifestations of Osteoporosis. *Clin. Cornerstone* **9,** 42–50 (2008).
4. Ralston, S. H. & Uitterlinden, A. G. Genetics of osteoporosis. *Endocr. Rev.* **31,** 629–662 (2010).
5. Den Uyl, D., Nurmohamed, M. T., van Tuyl, L. H., Raterman, H. G. & Lems, W. F. (Sub)clinical cardiovascular disease is associated with increased bone loss and fracture risk; a systematic review of the association between cardiovascular disease and osteoporosis. *Arthritis Res. Ther.* **13,** R5 (2011).
6. Tankó, L. B. *et al.* Relationship between osteoporosis and cardiovascular disease in postmenopausal women. *J. Bone Miner. Res.* **20,** 1912–20 (2005).
7. Montalcini, T. *et al.* Relation of low bone mineral density and carotid atherosclerosis in postmenopausal women. *Am. J. Cardiol.* **94,** 266–9 (2004).
8. Gravani, F. *et al.* Subclinical atherosclerosis and impaired bone health in patients with primary Sjogren's syndrome: prevalence, clinical and laboratory associations. *Arthritis Res. Ther.* **17,** (2015).
9. Santos, Maria José; Vinagre, Filipe; Silva, José; Gil, Victor; Fonseca, J. E. Cardiovascular Risk Profile in Sytemic Lupus Erythematosus and Rheumatoid Arthritis: A Comparative Study of Female Patients. *Acta Reumatol. Port.* **35,** 325–332 (2010).
10. Galkina, E. & Ley, K. Immune and Inflammatory Mechanisms of Atherosclerosis. *Annu. Rev. Immunol.* **27,** 165–197 (2009).
11. Wang, X. *et al.* Adiponectin abates atherosclerosis by reducing oxidative stress. *Med. Sci. Monit.* **20,** 1792–800 (2014).
12. Wang, J. C. & Bennett, M. Aging and atherosclerosis: Mechanisms, functional consequences, and potential therapeutics for cellular senescence. *Circ. Res.* **111,** 245–259 (2012).
13. Hansson, G. K. & Hermansson, A. The immune system in atherosclerosis. *Nat. Immunol.* **12,** 204–12 (2011).
14. Libby, P., Ridker, P. M. & Hansson, G. K. Progress and challenges in translating the biology of atherosclerosis. *Nature* **473,** 317–25 (2011).
15. Hofbauer, L. C., Brueck, C. C., Shanahan, C. M., Schoppet, M. & Dobnig, H. Vascular calcification and osteoporosis--from clinical observation towards molecular understanding. *Osteoporos. Int.* **18,** 251–9 (2007).

16. Sherer, Y. & Shoenfeld, Y. Mechanisms of disease: atherosclerosis in autoimmune diseases. *Nat. Clin. Pract. Rheumatol.* **2,** 99–106 (2006).

17. Tilg, H. & Moschen, A. R. Adipocytokines: mediators linking adipose tissue, inflammation and immunity. *Nat. Rev. Immunol.* **6,** 772–83 (2006).

18. Fantuzzi, G. Adiponectin and inflammation: consensus and controversy. *J. Allergy Clin. Immunol.* **121,** 326–30 (2008).

19. Heymann, M.-F. *et al.* Role of the OPG/RANK/RANKL triad in calcifications of the atheromatous plaques: comparison between carotid and femoral beds. *Cytokine* **58,** 300–6 (2012).

20. Yan, J. *et al.* Dual effects of IL-1 overactivity on the immune system in a mouse model of arthritis due to deficiency of IL-1 receptor antagonist. *J. Genet. Genomics* **40,** 83–91 (2013).

21. Usui, F. *et al.* Critical role of caspase-1 in vascular inflammation and development of atherosclerosis in Western diet-fed apolipoprotein E-deficient mice. *Biochem. Biophys. Res. Commun.* **425,** 162–8 (2012).

22. Van den Oever, I. a M., Sattar, N. & Nurmohamed, M. T. Thromboembolic and cardiovascular risk in rheumatoid arthritis: role of the haemostatic system. *Ann. Rheum. Dis.* **73,** 954–7 (2014).

23. Ditzel, H. J. The K/BxN mouse: a model of human inflammatory arthritis. *Trends Mol. Med.* **10,** 40–45 (2004).

24. Smith, B. J. *et al.* Induction of cardiovascular pathology in a novel model of low-grade chronic inflammation. *Cardiovasc. Pathol.* **18,** 1–10 (2009).

25. Barbour, K. E. *et al.* Inflammatory Markers and Risk of Hip Fracture in Older White Women: The Study of Osteoporotic Fractures. *J. Bone Miner. Res.* (2014). doi:10.1002/jbmr.2245

26. Yun, a J. & Lee, P. Y. Maldaptation of the link between inflammation and bone turnover may be a key determinant of osteoporosis. *Med. Hypotheses* **63,** 532–7 (2004).

27. Lane, N. E. Epidemiology, etiology, and diagnosis of osteoporosis. *Am. J. Obstet. Gynecol.* **194,** S3–11 (2006).

28. Emkey, G. R. & Epstein, S. Secondary osteoporosis: pathophysiology & diagnosis. *Best Pract. Res. Clin. Endocrinol. Metab.* **28,** 911–35 (2014).

29. Ji, M.-X. & Yu, Q. Primary osteoporosis in postmenopausal women. *Chronic Dis. Transl. Med.* **1,** 9–13 (2015).

30. Sandhu, S. K. & Hampson, G. The pathogenesis, diagnosis, investigation and management of osteoporosis. *J. Clin. Pathol.* **64,** 1042–50 (2011).

31. Pathak, J. L. *et al.* Inflammatory factors in the circulation of patients with active rheumatoid arthritis stimulate osteoclastogenesis via endogenous cytokine production by osteoblasts. *Osteoporos. Int.* (2014). doi:10.1007/s00198-014-2779-1

32. Bultink, I. E. M., Lems, W. F., Kostense, P. J., Dijkmans, B. a C. & Voskuyl, A. E. Prevalence of and risk factors for low bone mineral density and vertebral

fractures in patients with systemic lupus erythematosus. *Arthritis Rheum.* **52,** 2044–2050 (2005).

33. Fatemi, G., Gensler, L. S., Learch, T. J. & Weisman, M. H. Spine fractures in ankylosing spondylitis: A case report and review of imaging as well as predisposing factors to falls and fractures. *Semin. Arthritis Rheum.* **44,** 20–4 (2014).

34. Soriano, R., Herrera, S., Nogués, X. & Diez-Perez, A. Current and future treatments of secondary osteoporosis. *Best Pract. Res. Clin. Endocrinol. Metab.* **28,** 885–94 (2014).

35. Adamopoulos, I. E. & Mellins, E. D. Alternative pathways of osteoclastogenesis in inflammatory arthritis. *Nat. Rev. Rheumatol.* 1–6 (2014). doi:10.1038/nrrheum.2014.198

36. Boyce, B. F. & Xing, L. Functions of RANKL/RANK/OPG in bone modeling and remodeling. *Arch. Biochem. Biophys.* **473,** 139–46 (2008).

37. Aido, M. *et al.* Relationship between nanoscale mineral properties and calcein labeling in mineralizing bone surfaces. *Connect. Tissue Res.* **55 Suppl 1,** 15–7 (2014).

38. Bonnick, S. Lou. *Bone Densitometry in Clinical Practice: Application and Interpretation*. (Springer Science & Business Media, 2009). at <https://books.google.com/books?id=8TbyQqyHhCYC&pgis=1>

39. Baron, R. & Kneissel, M. WNT signaling in bone homeostasis and disease: from human mutations to treatments. *Nat. Med.* **19,** 179–92 (2013).

40. Steeve, K. T., Marc, P., Sandrine, T., Dominique, H. & Yannick, F. IL-6, RANKL, TNF-alpha/IL-1: interrelations in bone resorption pathophysiology. *Cytokine Growth Factor Rev.* **15,** 49–60 (2004).

41. Zaidi, M. Skeletal remodeling in health and disease. *Nat. Med.* **13,** 791–801 (2007).

42. Min, H. *et al.* Osteoprotegerin Reverses Osteoporosis by Inhibiting Endosteal Osteoclasts and Prevents Vascular Calcification by Blocking a Process Resembling Osteoclastogenesis. *J. Exp. Med.* **192,** 463–474 (2000).

43. Okamura, H., Yang, D., Yoshida, K. & Haneji, T. Protein phosphatase 2A Cα is involved in osteoclastogenesis by regulating RANKL and OPG expression in osteoblasts. *FEBS Lett.* **587,** 48–53 (2013).

44. Pérez-Sayáns, M., Somoza-Martín, J. M., Barros-Angueira, F., Rey Gándara, J. M. & Gracía-García, A. RANK/RANKL/OPG role in distraction osteogenesis. *Oral Surgery, Oral Med. Oral Pathol. Oral Radiol. Endodontology* **109,** 679–686 (2010).

45. Kang, J. H. *et al.* Osteoprotegerin expressed by osteoclasts: an autoregulator of osteoclastogenesis. *J. Dent. Res.* **93,** 1116–23 (2014).

46. Smith, B. *et al.* Systemic bone loss and induction of coronary vessel disease in a rat model of chronic inflammation. *Bone* **38,** 378–86 (2006).

47. Baud'huin, M. *et al.* Osteoprotegerin: multiple partners for multiple functions. *Cytokine Growth Factor Rev.* **24,** 401–9 (2013).

48. Herman, S., Krönke, G. & Schett, G. Molecular mechanisms of inflammatory bone damage: emerging targets for therapy. *Trends Mol. Med.* **14,** 245–53 (2008).

49. Zhang, Y. *et al.* Synergistic effects of interleukin-1βand interleukin-17A antibodies on collagen-induced arthritis mouse model. *Int. Immunopharmacol.* **15,** 199–205 (2013).

50. Doherty, T. M. *et al.* Calcification in atherosclerosis: bone biology and chronic inflammation at the arterial crossroads. *Proc. Natl. Acad. Sci. U. S. A.* **100,** 11201–6 (2003).

51. Charles, J. F. & Nakamura, M. C. Bone and the innate immune system. *Curr. Osteoporos. Rep.* **12,** 1–8 (2014).

52. Walsh, N. C. & Gravallese, E. M. Bone remodeling in rheumatic disease: a question of balance. *Immunol. Rev.* **233,** 301–12 (2010).

53. Caetano-Lopes, J. *et al.* Chronic arthritis leads to disturbances in the bone collagen network. *Arthritis Res. Ther.* **12,** R9 (2010).

54. Silva, I. & Branco, J. C. RANK/RANKL/OPG: Literature review. *Acta Reumatol. Port.* 209–218 (2011).

55. Bucay, N. *et al.* osteoprotegerin-deficient mice develop early onset osteoporosis and arterial calcification. *Genes Dev.* **12,** 1260–8 (1998).

56. Simonet, W. . *et al.* Osteoprotegerin: A Novel Secreted Protein Involved in the Regulation of Bone Density. *Cell* **89,** 309–319 (1997).

57. Sapir-Koren, R. & Livshits, G. Osteocyte control of bone remodeling: is sclerostin a key molecular coordinator of the balanced bone resorption-formation cycles? *Osteoporos. Int.* (2014). doi:10.1007/s00198-014-2808-0

58. Rachner, T. D., Khosla, S. & Hofbauer, L. C. Osteoporosis: Now and the future. *Lancet* **377,** 1276–1287 (2011).

59. Bonewald, L. F. & Johnson, M. L. Osteocytes, mechanosensing and Wnt signaling. *Bone* **42,** 606–15 (2008).

60. Weilbaecher, K. N., Guise, T. a & McCauley, L. K. Cancer to bone: a fatal attraction. *Nat. Rev. Cancer* **11,** 411–425 (2011).

61. Liu, Y. & Shanahan, C. M. Signalling pathways and vascular calcification. *Front. Biosci.* **16,** 1302–1314 (2011).

62. Leopold, J. a. MicroRNAs Regulate Vascular Medial Calcification. *Cells* **3,** 963–80 (2014).

63. Persy, V. & D'Haese, P. Vascular calcification and bone disease: the calcification paradox. *Trends Mol. Med.* **15,** 405–16 (2009).

64. Demer, L. L. Vascular calcification and osteoporosis: inflammatory responses to oxidized lipids. *Int. J. Epidemiol.* **31,** 737–741 (2002).

65. Bennett, B. J. *et al.* Osteoprotegerin inactivation accelerates advanced atherosclerotic lesion progression and calcification in older ApoE-/- mice. *Arterioscler. Thromb. Vasc. Biol.* **26,** 2117–24 (2006).

66. Collin-Osdoby, P. Regulation of vascular calcification by osteoclast regulatory factors RANKL and osteoprotegerin. *Circ. Res.* **95,** 1046–57 (2004).

67. D'Amelio, P., Isaia, G. & Isaia, G. The osteoprotegeriniRANKIRANKL system : A bone key to vascular disease. *J. Endocrinol. Invest.* **32,** 6–9 (2009).

68. Vik, a *et al.* Serum osteoprotegerin, sRANKL and carotid plaque formation and growth in a general population--the Tromsø study. *J. Thromb. Haemost.* **8,** 898–905 (2010).

69. Osako, M. K. *et al.* Estrogen inhibits vascular calcification via vascular RANKL system: common mechanism of osteoporosis and vascular calcification. *Circ. Res.* **107,** 466–75 (2010).

70. Van Campenhout, A. & Golledge, J. Osteoprotegerin, vascular calcification and atherosclerosis. *Atherosclerosis* **204,** 321–9 (2009).

71. Hak, A. E., Pols, H. A. P., van Hemert, A. M., Hofman, A. & Witteman, J. C. M. Progression of Aortic Calcification Is Associated With Metacarpal Bone Loss During Menopause : A Population-Based Longitudinal Study. *Arterioscler. Thromb. Vasc. Biol.* **20,** 1926–1931 (2000).

72. Hyder, J. A. *et al.* Bone mineral density and atherosclerosis: the Multi-Ethnic Study of Atherosclerosis, Abdominal Aortic Calcium Study. *Atherosclerosis* **209,** 283–9 (2010).

73. Yesil, Y. *et al.* Coexistence of osteoporosis (OP) and coronary artery disease (CAD) in the elderly: it is not just a by chance event. *Arch. Gerontol. Geriatr.* **54,** 473–6 (2012).

74. Fischer, J. A. A. *et al.* Combined inhibition of TNFα and IL-17 as therapeutic opportunity for treatment in rheumatoid arthritis: Development and characterization of a novel bispecific antibody. *Arthritis Rheumatol. (Hoboken, N.J.)* **67,** 51–62 (2014).

75. Lee, Y. The role of interleukin-17 in bone metabolism and inflammatory skeletal diseases. *BMB Rep.* **46,** 479–83 (2013).

76. Burmester, G. R., Feist, E. & Dörner, T. Emerging cell and cytokine targets in rheumatoid arthritis. *Nat. Rev. Rheumatol.* **10,** 77–88 (2014).

77. Van Baarsen, L. *et al.* Heterogeneous expression pattern of interleukin-17A (IL-17A), IL-17F and their receptors in synovium of rheumatoid arthritis, psoriatic arthritis and osteoarthritis: possible explanation for non-response to anti-IL-17 therapy? *Arthritis Res. Ther.* **16,** 426 (2014).

78. Taylor, P. C. & Williams, R. O. Combination cytokine blockade: the way forward in therapy for rheumatoid arthritis? *Arthritis Rheumatol.* 1–7 (2014). doi:10.1002/art.

79. Moghadasian, M. H. *et al.* Pathophysiology of apolipoprotein E deficiency in mice: relevance to apo E-related disorders in humans. *FASEB J.* **15,** 2623–30 (2001).

80. Kolovou, G., Anagnostopoulou, K., Mikhailidis, D. P. & Cokkinos, D. V. Apolipoprotein E knockout models. *Curr. Pharm. Des.* **14,** 338–51 (2008).

81. Nakashima, Y., Plump, A. S., Raines, E. W., Breslow, J. L. & Ross, R. ApoE-deficient mice develop lesions of all phases of atherosclerosis throughout the arterial tree. *Arterioscler. Thromb.* **14,** 133–40 (1994).

82. Rose, S. & Perlman, H. Spontaneous arthritis is protective for the development of aortic atherosclerosis in ApoE-/- mice. *Ann. Rheum. Dis.* **70,** A94–A94 (2011).

83. Jawien, J., Nastalek, P. & Korbut, R. Mouse model of experimental atherosclerosis. *J. Physiol. Pharmacol.* **55,** 503–517 (2004).

84. Ma, Y. D. *et al.* Defects in osteoblast function but no changes in long-term repopulating potential of hematopoietic stem cells in a mouse chronic inflammatory arthritis model. *Blood* **114,** 4402–10 (2009).

85. Rose, S. *et al.* A novel mouse model that develops spontaneous arthritis and is predisposed towards atherosclerosis. *Ann. Rheum. Dis.* **72,** 89–95 (2013).

86. Monach, P. *et al.* in *Arthritis Research: Methods in Molecular Medicine ,Volume 2* (ed. Cope, A. P.) **136,** 269–282 (2007).

87. Matsumoto, I., Staub, A., Benoist, C. & Mathis, D. Arthritis provoked by linked T and B cell recognition of a glycolytic enzyme. *Science* **286,** 1732–1735 (1999).

88. Monach, P. a, Mathis, D. & Benoist, C. The K/BxN arthritis model. *Curr. Protoc. Immunol.* **Chapter 15,** Unit 15.22 (2008).

89. Maccioni, M. Arthritogenic Monoclonal Antibodies from K/BxN Mice. *J. Exp. Med.* **195,** 1071–1077 (2002).

90. Korganow, a S. *et al.* From systemic T cell self-reactivity to organ-specific autoimmune disease via immunoglobulins. *Immunity* **10,** 451–61 (1999).

91. Kyburz, D. & Corr, M. The KRN mouse model of inflammatory arthritis. *Springer Semin. Immunopathol.* **25,** 79–90 (2003).

92. C57 Mice | Charles River. *Charles River* at <http://www.criver.com/products-services/basic-research/find-a-model/c57bl-6n-mouse>

93. B6.NOD-(D17Mit21-D17Mit10)/LtJ - 003300. *The Jackson Laboratory* at <https://www.jax.org/strain/003300>

94. Hughes, A., Stewart, T. L. & Mann, V. in *Bone Research Protocols* (eds. Helfrich, M. H. & Ralston, S. H.) 249–260 (Humana Press, 2009). doi:10.1007/978-1-62703-239-1_1

95. Egyházi, S. *et al.* Proteinase K Added to the Extraction Procedure Markedly Increases RNA Yield from Primary Breast Tumors for Use in Microarray Studies. *Clin. Chem.* **50,** 974–975 (2004).

96. 26/280 and 260/230 ratios. *T009-Technical Bulletin. Nanodrop 1000 & 8000* 1–2 doi:http://www.nanodrop.com/Library/T009-NanoDrop 1000-&-NanoDrop 8000-Nucleic-Acid-Purity-Ratios.pdf

97. Logan, J. M. J., Edwards, K. J. & Saunders, N. A. *Real-time PCR: Current Technology and Applications*. (Horizon Scientific Press, 2009). at <https://books.google.com/books?id=YxGKpOg8TuQC&pgis=1>

98. Wong, M. L. & Medrano, J. F. Real-time PCR for mRNA quantification. *Biotechniques* **39,** 75–85 (2005).

99. Vidal, B. *et al.* Bone histomorphometry revisited. *Acta Reum. Port.* **37,** 294–300 (2012).

100. Schilling, A. F. *et al.* Increased bone formation in mice lacking apolipoprotein E. *J Bone Min. Res* **20,** 274–282 (2005).

101. Parhami, F. *et al.* Atherogenic high-fat diet reduces bone mineralization in mice. *J. Bone Miner. Res.* **16,** 182–8 (2001).

102. Hirasawa, H. *et al.* ApoE gene deficiency enhances the reduction of bone formation induced by a high-fat diet through the stimulation of p53-mediated apoptosis in osteoblastic cells. *J. Bone Miner. Res.* **22,** 1020–30 (2007).

103. Niemeier, A., Schinke, T., Heeren, J. & Amling, M. The role of apolipoprotein E in bone metabolism. *Bone* **50,** 518–24 (2012).

104. Bartelt, A. *et al.* Apolipoprotein E-dependent inverse regulation of vertebral bone and adipose tissue mass in C57Bl/6 mice: modulation by diet-induced obesity. *Bone* **47,** 736–45 (2010).

105. Thoene-Reineke, C. *et al.* Composition of intestinal microbiota in immune-deficient mice kept in three different housing conditions. *PLoS One* **9,** e113406 (2014).

106. Ayada, K. *et al.* Chronic infections and atherosclerosis. *Ann. N. Y. Acad. Sci.* **1108,** 594–602 (2007).

107. 'Germ-free' Versus 'Specific-pathogen-free' Mice...What's the Difference? | MouseClique. *The Jackson Laboratory* (2013). at <http://mouseclique.jax.org/dear-jaxy-germ-free-versus-specific-pathogen-free-mice-whats-the-difference/>

108. Three Rs | Animal Ethics Infolink. at <http://www.animalethics.org.au/three-rs>

Annexes

Annex I

ssniff® SM R/M High Fat (standard)

Experimental diet for rats and mice, with 15 % fat

Description

This experimental diet contains besides purified feed ingredients also conventional feedingstuffs. When fed to satiation (ad libitum) the diet supports, at least in certain rat and mouse strains, the incidence of obesity and the development of atherosclerotic lesions due to the addtion of fat with mainly saturated fatty acids and cholesterol.

Crude Nutrients	[%]
Dry matter	90.6
Crude protein (N x 6.25)	19.0
Crude fat	**15.2**
Crude fibre	3.4
Crude ash	6.3
N free extracts	46.8
Starch	25.6
Sugar	11.2

Energy	[MJ/kg]
Gross Energy (GE)	19.5
Metabolizable Energy (ME)	

16.1 [1)]

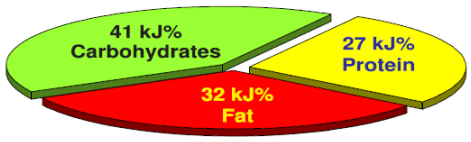

16.8 [2)]

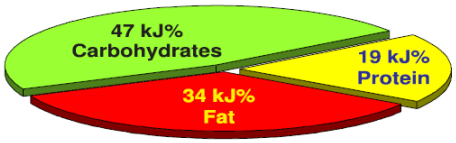

[1)] *ME calculated according to the pig formula, Annex 4 of the German feed regulation*

[2)] *ME calculated with the Atwater factors*

Minerals	[%]
Calcium	1.00
Phosphorus	0.70
Sodium	0.21
Magnesium	0.17
Potassium	0.65

Fatty acids	[%]
C 4:0	0.08
C 6:0	0.05
C 8:0	0.76
C 10:0	0.61
C 12:0	4.38
C 14:0	1.87
C 16:0	1.69
C 16:1	0.05
C 17:0	0.01
C 18:0	0.50
C 18:1	1.52
C 18:2	1.45
C 18:3	0.17
C 20:0	0.01
C 20:1	0.01
C 20:4	—
C 20:5	—
C 22:6	—
Cholesterol (orig./add.) [mg/kg]	**12,500**

Amino acids	[%]
Lysine	1.17
Methionine	0.53
Cystine	0.27
Met+Cys	0.80
Threonine	0.72
Tryptophan	0.25
Arginine	1.00
Histidine	0.49
Valine	1.00
Isoleucine	0.83
Leucine	1.47
Phenylalanine	0.90
Phe+Tyr	1.61
Glycine	0.68
Glutamic acid	4.00
Aspartic acid	1.55
Proline	1.52
Alanine	0.74
Serine	0.96

Vitamins	per kg
Vitamin A	15,000 IU
Vitamin D_3	1,000 IU
Vitamin E	110 mg
Vitamin K (as menadione)	5 mg
Vitamin C	---- mg
Thiamin (B_1)	16 mg
Riboflavin (B_2)	21 mg
Pyridoxine (B_6)	19 mg
Cobalamin (B_{12})	100 µg
Nicotinic acid	110 mg
Pantothenic acid	39 mg
Folic acid	7 mg
Biotin	465 µg
Choline-Chloride	2,610 mg
Inositol	100 mg

Trace elements	per kg
Iron	155 mg
Manganese	58 mg
Zinc	83 mg
Copper	13 mg
Iodine	2.1 mg
Selenium	0.3 mg
Cobalt	2.1 mg

Feed composition
On request

Main products
E15103-30 Meal / Powder
E15103-34 10 mm pellets

Production and sale
ssniff Spezialdiäten GmbH
Phone:+49-(0)2921-9658-0
Fax: +49-(0)2921-9658-40
E-Mail mail@ssniff.de
www.ssniff.de / www.ssniff.com

Annex II

Protocol of extraction of RNA from frozen bone

1- Samples that have been stored at -80ºC, ground into a fine powder, using a mortar and pestle, previously autoclaved.

2- Transfer the powder into a clean 2-ml microtube, and add 1 ml of TRIzol® (Invitrogen), mix well by shaking the tube vigorously. Incubate at room temperature for 5 minutes.

3- Add 300 µl of chloroform (VWR) and shake vigorously for 15 seconds. Place the tubes on ice for 5 minutes.

4- Centrifuge at 6000 x *g* for 30 minutes at 4ºC.

5- Carefully aspirate the supernatant into a 1.5-ml microtube, taking care not to disturb the interface.

6- Add 13 µl of proteinase k (Sigma-Aldrich) at 1mg/ml and let incubate at 55ºC during 15 minutes.

7- Add 750 µl of ice-cold isopropyl alcohol (VWR) and mix gently by inverting the tube 5-6 times.

8- Incubate the samples on ice for 15 minutes to precipitate the RNA.

9- Centrifuge at 6000 x *g* for 30 minutes at 4ºC. Discard the supernatant.

10- Wash the pellet with 750 µl ice-cold 75% ethanol (VWR) and centrifuge at 6000 x *g* for 10 minutes at 4ºC. Discard the supernatant.

11- Repeat the step 10, two times more.

12- Allow the pellet to air-dry for 3-5 minutes. Careful not to over-dry the pellet.

13- Dissolve the RNA pellet in 30 µl of DNase/Rnase-free water (Gibco) and let incubate at 55ºC for 10-15 minutes, mixing occasionally.

14- Quantitative and assess purity of the eluted RNA by spectrophotometry. Store the RNA at -80ºC until further use.

Annex III

Protocol for cDNA synthesis

1- Calculate the RNA quantity necessary to obtain a concentration of cDNA of 3 ng/ µl in 20 µl volume of reaction.

2- The volume of RNA is added to each well and filled up with Gibco® DNase/RNase-free water (Invitrogen. Life Technologies, Paisley, UK) until 3 µl of volume.

3- Add 17 µl of Mix reaction to each well to account to a final volume of 20 µl, using the amounts followed below:

Reagents	**Concentration in the reaction**	**Volume (µl) per sample**
MilliQ H_2O	-	10
RT Buffer (5X)	1X	4
Random Hexamers	300 ng/ µl	1
M-Mulv RNase H^+	-	2
Total		**17 l**

4 - Seal the plate and put it in the Thermocycler with the following program:

37ºC, 30 minutes

●----------● 85ºC, 5 minutes

1X ●----------●

35X

Annex IV

Protocol for bone processing for histomorphometric analysis

The L3-L4 lumbar vertebras are cleaned from soft tissue and placed in 10-ml glass flasks.

1- *Fixation step:* Fix the samples at 70% ethanol (VWR, Leicestershire, UK) and store in 4ºC for 6-7 days.

2- *Dehydration step:* Replace the ethanol for 96% ethanol (Proclínica, Lisboa, Portugal) for 24h at 4ºC, and then replace this solution for absolute ethanol (VWR, Leicestershire, UK) for 12h at 4ºC.

3- Clearing step: Remove the solution and embed the sample in Xylene (Klinipath, Duiven, Holland) for 1h at 4ºC. Then replace the solution for Methyl methacrylate (MMA) (Sigma-Aldrich, St. Lois, MO, USA) solution (A):

   Solution (A):

   5,5 g of Benzoyl Peroxidase (previously dehydrated) (Merck, Kenilworth, NJ, USA)

   500 ml of Methyl methacrylate (MMA) solution (Sigma-Aldrich, St. Lois, MO, USA)

   56,1 ml of Poly(ethylene) glycol 400 (Fluka, Sigma-Aldrich, St. Lois, MO, USA)

4- *Inclusion step*: Remove the previous solution and replace with a mix solution of Solution (A) + Solution (B):

   Solution (B):

   1 ml of Dimethylaniline 2% (Merck, Kenilworth, NJ, USA)

   19 ml of isopropyl alcohol (VWR, Leicestershire, UK)

5- Leave to polymerize at 4ºC until the resin is solidified.

6- After polymerization, the mold is broken and the block is cut in a parallelepiped shape using a plaster cutter.

7- *Cutting step:* Cut the blocks in 5µm thickness sections using a microtome (Leica, Wetzlar, Germany) with a tungsten blade (Leica, Wetzlar, Germany). Place each cut in a glass slide, previously coated with gelatin chrome alum (Panreac AppliChem, Barcelona, Spain), add 1 drop of 70% ethanol to the slide and stretch the cut in the slide with the help of a brush. Press the slides (using a clamp) for 1-2 days at 55ºC.

8- *Staining:* Incubate the slides in Fucsina/Ponceau for 2 minutes, and then wash the slides with acetic water 1%. Wash with distilled water and then incubate the slides in 0.2% aniline blue solution for 15 minutes. Wash with distilled water and after proceed to dehydration step, deeping the slides rapidly in a series of alcohols: 70%, 95% and last 100% alcohol. Clarify the slides with Xylene and mount the slides using a Slide Mounting solution.